

**P-07-180**

## **Oskarshamn site investigation**

### **Groundwater flow measurements and SWIW tests in borehole KLX11A**

Pernilla Thur, Rune Nordqvist, Erik Gustafsson  
Geosigma AB

October 2007

**Svensk Kärnbränslehantering AB**

Swedish Nuclear Fuel  
and Waste Management Co  
Box 250, SE-101 24 Stockholm  
Tel +46 8 459 84 00



## **Oskarshamn site investigation**

# **Groundwater flow measurements and SWIW tests in borehole KLX11A**

Pernilla Thur, Rune Nordqvist, Erik Gustafsson  
Geosigma AB

October 2007

*Keywords:* AP PS 400-07-026, Oskarshamn, Hydrogeology, Borehole, Groundwater, Flow, Tracer tests, Dilution probe, SWIW test.

This report concerns a study which was conducted for SKB. The conclusions and viewpoints presented in the report are those of the authors and do not necessarily coincide with those of the client.

Data in SKB's database can be changed for different reasons. Minor changes in SKB's database will not necessarily result in a revised report. Data revisions may also be presented as supplements, available at [www.skb.se](http://www.skb.se).

A pdf version of this document can be downloaded from [www.skb.se](http://www.skb.se).

## Abstract

This report describes the performance, evaluation and interpretation of in situ groundwater flow measurements and single well injection withdrawal tracer tests (SWIW tests) at Laxemar area at the Oskarshamn site. The objectives of the activity were to determine the natural groundwater flow in selected fractures/fracture zones intersecting the core drilled borehole KLX11A, as well as to determine transport properties of fractures by means of SWIW tests in the borehole.

Groundwater flow measurements were carried out in six local fracture zones at borehole lengths ranging from c. 168 to c. 598 m (148 to 514 m vertical depth). The hydraulic transmissivity ranged within  $T = 6.2 \cdot 10^{-8} - 1.8 \cdot 10^{-5} \text{ m}^2/\text{s}$ . The results of the dilution measurements in borehole KLX11A show that the groundwater flow varies in fracture zones during natural, i.e. undisturbed, conditions. There is no obvious correlation between borehole depth and flow rates or Darcy velocities. The flow rate ranged from 0.017 to 2.9 ml/min and the Darcy velocity from  $1.9 \cdot 10^{-9}$  to  $6.3 \cdot 10^{-8} \text{ m/s}$  ( $1.6 \cdot 10^{-4} - 5.4 \cdot 10^{-3} \text{ m/d}$ ), values that are similar to results from previously performed dilution measurements under natural gradient conditions at the Oskarshamn site. Both the highest and the lowest flow rate were measured in the deepest sections of the borehole. Hydraulic gradients, calculated according to the Darcy concept, are within the expected range (0.001–0.05) in five out of six measured sections. The determined groundwater flow rates are fairly proportional to the hydraulic transmissivity although the statistical basis is weak.

Measurements were also attempted in two 1-metre sections at c. 107 m and c. 265 m borehole length. Unfortunately, these measurements could not be completed due to delays in the measurement programme, caused by problems with the probe getting jammed in the borehole.

One SWIW test was carried out at borehole length c. 516 m (447 m vertical depth) with a hydraulic transmissivity of  $T = 3.4 \cdot 10^{-6} \text{ m}^2/\text{s}$ . The other SWIW test was performed in the deformation zone DZ14 at c. 598 m (514 m vertical depth) with a hydraulic transmissivity of  $T = 1.3 \cdot 10^{-7} \text{ m}^2/\text{s}$ .

# Sammanfattning

Denna rapport beskriver genomförandet, utvärderingen samt tolkningen av in situ grundvattenflödesmätningar och enhålsspår försök (SWIW test) i Laxemar, Oskarshamn. Syftet med aktiviteten var dels att bestämma det naturliga grundvattenflödet i enskilda sprickor och sprickzoner som skär borrhålet KLX11A, dels att karaktärisera transportegenskaperna i potentiella flödesvägar genom att utföra och utvärdera SWIW test i borrhålet.

Grundvattenflödesmätningar genomfördes i sex lokala sprickzoner på nivåer från ca 168 till ca 598 m borrhålsdjup (148 till 514 m vertikalt djup). Den hydrauliska transmissiviteten varierade inom intervallet  $T = 6,2 \cdot 10^{-8} - 1,8 \cdot 10^{-5} \text{ m}^2/\text{s}$ . Resultaten från utspädningsmätningarna i borrhålet KLX11A visar att grundvattenflödet varierar under naturliga, dvs. ostörda, hydrauliska förhållanden. Ingen märkbar koppling syns mellan borrhålsdjup och flödet eller Darcy hastighet. Beräknade grundvattenflöden låg inom intervallet 0,017–2,9 ml/min och Darcy hastigheterna varierade mellan  $1,9 \cdot 10^{-9}$  och  $6,3 \cdot 10^{-8} \text{ m/s}$  ( $1,6 \cdot 10^{-4} - 5,4 \cdot 10^{-3} \text{ m/d}$ ), resultat vilka överensstämmer med resultat från motsvarande djup i tidigare utspädningsmätningar vid ostörda, hydrauliska förhållanden i Laxemarsområdet.

Både det högsta och det lägsta flödet respektive Darcy hastighet uppmättes i de djupaste sektionerna. Hydrauliska gradienter, beräknade enligt Darcy konceptet, ligger inom det förväntade området (0,001–0,05) i fem av sex testade sprickor/zoner. Grundvattenflödet är tämligen proportionellt mot den hydrauliska transmissiviteten, dock är det statistiska underlaget litet.

Det var även tänkt att utföra mätningar i två 1-meters sektioner på ca 107 m och ca 265 m borrhålsdjup. Dessvärre kunde dessa mätningar inte genomföras på grund av försening i mätprogrammet orsakad av att sonden fastnade i borrhålet.

Ett SWIW test genomfördes på ca 516 m borrhålsdjup (447 m vertikalt djup) med  $T = 3,4 \cdot 10^{-6} \text{ m}^2/\text{s}$ . Det andra SWIW testet utfördes i deformationszonen DZ14 på ca 598 m djup (514 m vertikalt djup) med  $T = 1,3 \cdot 10^{-7} \text{ m}^2/\text{s}$ .

# Contents

<b>1</b>	<b>Introduction</b>	7
<b>2</b>	<b>Objectives and scope</b>	9
<b>3</b>	<b>Equipment</b>	11
3.1	Borehole dilution probe	11
3.1.1	Measurement range and accuracy	11
3.2	SWIW test equipment	13
3.2.1	Measurement range and accuracy	14
<b>4</b>	<b>Execution</b>	15
4.1	Preparations	15
4.2	Procedure	15
4.2.1	Groundwater flow measurement	15
4.2.2	SWIW tests	16
4.3	Data handling	16
4.4	Analyses and interpretation	16
4.4.1	The dilution method – general principles	16
4.4.2	The dilution method – evaluation and analysis	18
4.4.3	SWIW test – basic outline	19
4.4.4	SWIW test – evaluation and analysis	20
4.5	Nonconformities	21
<b>5</b>	<b>Results</b>	23
5.1	Dilution measurements	23
5.1.1	KLX11A, section 167.8–170.8 m	25
5.1.2	KLX11A, section 306.0–309.0 m	26
5.1.3	KLX11A, section 439.0–442.0 m	26
5.1.4	KLX11A, section 516.5–519.5 m	29
5.1.5	KLX11A, section 579.0–584.0 m	29
5.1.6	KLX11A, section 598.0–599.0 m	31
5.1.7	Summary of dilution results	33
5.2	SWIW tests	36
5.2.1	Treatment of experimental data	36
5.2.2	Tracer recovery breakthrough in KLX11A, 516.5–519.5 m	36
5.2.3	Model evaluation KLX11A, 516.5–519.5 m	39
5.2.4	Tracer recovery breakthrough in KLX11A, 598.0–599.0 m	41
5.2.5	Model evaluation KLX11A, 598.0–599.0 m	44
<b>6</b>	<b>Discussion and conclusions</b>	47
<b>7</b>	<b>References</b>	49
<b>Appendix A</b>	<b>Borehole data KLX11A</b>	51
<b>Appendix B1</b>	<b>Dilution measurement KLX11A 167.8–170.8 m</b>	53
<b>Appendix B2</b>	<b>Dilution measurement KLX11A 306.0–309.0 m</b>	56
<b>Appendix B3</b>	<b>Dilution measurement KLX11A 439.0–442.0 m</b>	59
<b>Appendix B4</b>	<b>Dilution measurement KLX11A 516.5–519.5 m</b>	62
<b>Appendix B5</b>	<b>Dilution measurement KLX11A 579.0–584.0 m</b>	65
<b>Appendix B6</b>	<b>Dilution measurement KLX11A 598.0–599.0 m</b>	68
<b>Appendix C</b>	<b>BIPS logging KLX11A</b>	71

# 1 Introduction

SKB is currently conducting a site investigation for a deep repository in Oskarshamn, according to general and site specific programmes /SKB 2001ab/. Two, among several methods for site characterisation are in situ groundwater flow measurements and single well injection withdrawal tests (SWIW tests).

This document reports the results gained by two SWIW tests and six groundwater flow measurements with the borehole dilution probe in borehole KLX11A. The work was conducted by Geosigma AB and carried out between March and July 2007 in borehole KLX11A according to activity plan AP PS 400-07-026. In Table 1-1 controlling documents for performing this activity are listed. The activity plans and method descriptions/instructions are SKB's internal controlling documents. Data and results were delivered to the SKB site characterization database Sicada.

Borehole KLX11A is located in the south-west part of the investigation area, see Figure 1-1. KLX11A is a telescopic borehole where the part below 100 m borehole length is core drilled. KLX11A is inclined  $-76.43^\circ$  from the horizontal plane at the collaring. The borehole is 992 m long and cased down to 101 m. From 101 m down to 992 m the diameter is 76 mm.

Detailed information about borehole KLX11A is listed in Appendix A (excerpt from the SKB database Sicada).

**Table 1-1. Controlling documents for performance of the activity.**

<b>Activity Plan</b>	<b>Number</b>	<b>Version</b>
Grundvattenflödesmätningar, vattenprovtagningar och SWIW-tester i kärnborrhål KLX11A	AP PS 400-07-026	1.0
<b>Method Documents</b>	<b>Number</b>	<b>Version</b>
Metodbeskrivning för grundvattenflödesmätning	SKB MD 350.001	1.0
Kalibrering av tryckgivare, temperaturgivare och flödesmätare	SKB MD 353.014	2.0
Kalibrering av fluorescensmätning	SKB MD 353.015	2.0
Kalibrering Elektrisk konduktivitet	SKB MD 353.017	2.0
Utspädningsmätning	SKB MD 353.025	2.0
Löpande och avhjälpande underhåll av Utspädningssond	SKB MD 353.065	1.0
Systemöversikt – SWIW-test utrustning	SKB MD 353.069	1.0
Löpande och avhjälpande underhåll av SWIW-test utrustning	SKB MD 353.070	1.0
Kalibrering av flödesmätare i SWIW-test utrustning	SKB MD 353.090	1.0
Instruktion för rengöring av borrhålsutrustning och viss markbaserad utrustning	SKB MD 600.004	1.0
Instruktion för längdkalibrering vid undersökningar i kärnborrhål	SKB MD 620.010	1.0

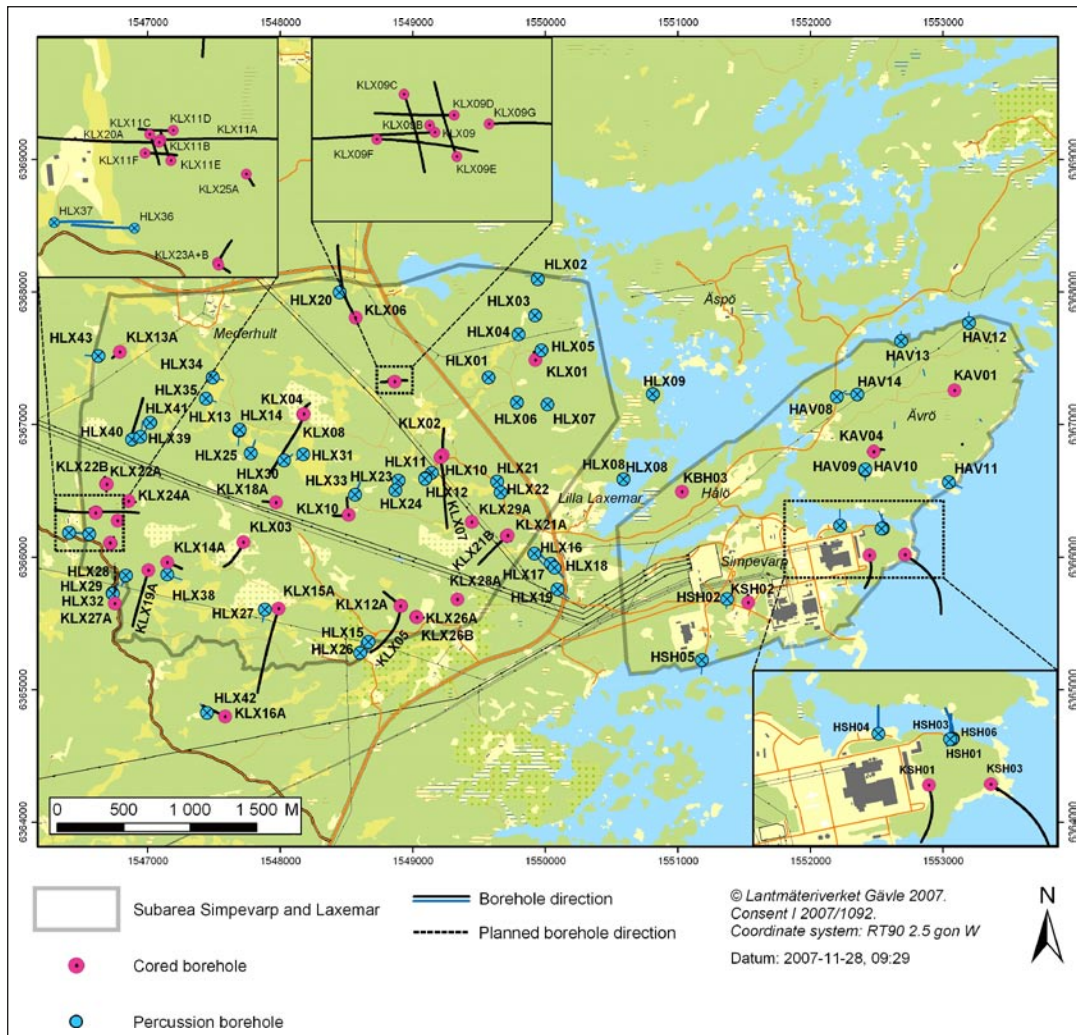


Figure 1-1. Overview of the Oskarshamn site investigation area, showing core boreholes (purple) and percussion boreholes (blue). KLX11A at coordinates 6366340 north and 1546608 east.

## 2 Objectives and scope

One objective of the activity was to determine groundwater flow under natural gradient in the Oskarshamn area.

The objective of the SWIW tests in the area were to determine transport properties of groundwater flow paths in fractures/fracture zones in a depth range of 300–700 m and a hydraulic transmissivity of  $1 \cdot 10^{-8}$ – $1 \cdot 10^{-6}$  m<sup>2</sup>/s in the test section. In KLX11A the SWIW tests were executed at a borehole length of 516.5–519.5 m with hydraulic transmissivity  $3.4 \cdot 10^{-6}$  m<sup>2</sup>/s and at 598.0–599.0 m with  $T = 1.4 \cdot 10^{-7}$  m<sup>2</sup>/s.

The groundwater flow measurements were performed in fractures and fracture zones at a borehole length range of 168–598 m (148–514 m vertical depth) using the SKB borehole dilution probe. The hydraulic transmissivity in the test sections ranged between  $6.2 \cdot 10^{-8}$ – $1.8 \cdot 10^{-5}$  m<sup>2</sup>/s. Groundwater flow measurements were carried out in totally six test sections. In two of these sections SWIW tests were also conducted using both sorbing and non-sorbing tracers, simultaneously.



## 3 Equipment

### 3.1 Borehole dilution probe

The borehole dilution probe is a mobile system for groundwater flow measurements, Figure 3-1. Measurements can be made in boreholes with 56 mm or 76–77 mm diameter and the test section length can be arranged for 1, 2, 3, 4 or 5 m with an optimised special packer/dummy system and section lengths between 1 and 10 m with standard packers. The maximum measurement depth is at 1,030 borehole length. The vital part of the equipment is the probe which measures the tracer concentration in the test section down hole and in situ. The probe is equipped with two different measurement devices. One is the optic device, which is a combined fluorometer and light-transmission meter. Several fluorescent and light-absorbing tracers can be used with this device. The other device is the electrical conductivity device, which measures the electrical conductivity of the water and is used for detection/analysis of saline tracers. The probe and the packers that straddle the test section are lowered down the borehole with an umbilical hose. The hose contains a tube for hydraulic inflation/deflation of the packers and electrical wires for power supply and communication/data transfer. Besides tracer dilution detection, the absolute pressure and temperature are measured. The absolute pressure is measured during the process of dilution because a change in pressure indicates that the hydraulic gradient, and thus the groundwater flow, may have changed. The pressure gauge and the temperature gauge are both positioned in the dilution probe, about seven metres from top of test section. This bias is not corrected for as only changes and trends relative to the start value are of great importance for the dilution measurement. Since the dilution method requires homogenous distribution of the tracer in the test section, a circulation pump is also installed and circulation flow rate measured.

A caliper log, attached to the dilution probe, is used to position the probe and test section at the pre-selected borehole length. The caliper detects reference marks previously made by a drill bit at exact length along the borehole, approximately every 50 m. This method makes it possible to position the test section with an accuracy of  $c. \pm 0.10$  m.

#### 3.1.1 Measurement range and accuracy

The lower limit of groundwater flow measurements is set by the dilution caused by molecular diffusion of the tracer into the fractured/porous aquifer, relative to the dilution of the tracer due to advective groundwater flow through the test section. In a normally fractured granite, the lower limit of a groundwater flow measurements is approximately at a hydraulic conductivity, (K), between  $6 \cdot 10^{-9}$  and  $4 \cdot 10^{-8}$  m/s, if the hydraulic gradient, (I), is 0.01. This corresponds to a groundwater flux (Darcy velocity), in the range of  $6 \cdot 10^{-11}$  to  $4 \cdot 10^{-10}$  m/s, which in turn may be transformed into groundwater flow rates,  $Q_w$ , corresponding to 0.03–0.2 ml/hour through a one m test section in a 76 mm diameter borehole. In a fracture zone with high porosity, and thus a higher effective rate of molecular diffusion from the test section into the fractures, the lower limit is about  $K = 4 \cdot 10^{-7}$  m/s if  $I = 0.01$ . The corresponding flux value is in this case  $v = 4 \cdot 10^{-9}$  m/s and flow rate  $Q_w = 2.2$  ml/hour. The lower limit of flow measurements is, however, in most cases constrained by the time available for the dilution test. The required time frame for an accurate flow determination from a dilution test is within 7–60 hours at hydraulic conductivity values greater than about  $1 \cdot 10^{-7}$  m/s. At conductivity values below  $1 \cdot 10^{-8}$  m/s, measurement times should be at least 70 hours for natural (undisturbed) hydraulic gradient conditions.

The upper limit of groundwater flow measurements is determined by the capability of maintaining a homogeneous mix of tracer in the borehole test section. This limit is determined by several factors, such as length of the test section, volume, distribution of the water conducting fractures and how the circulation pump inlet and outlet are designed. The practical upper measurement limit is about 2,000 ml/hour for the equipment developed by SKB.

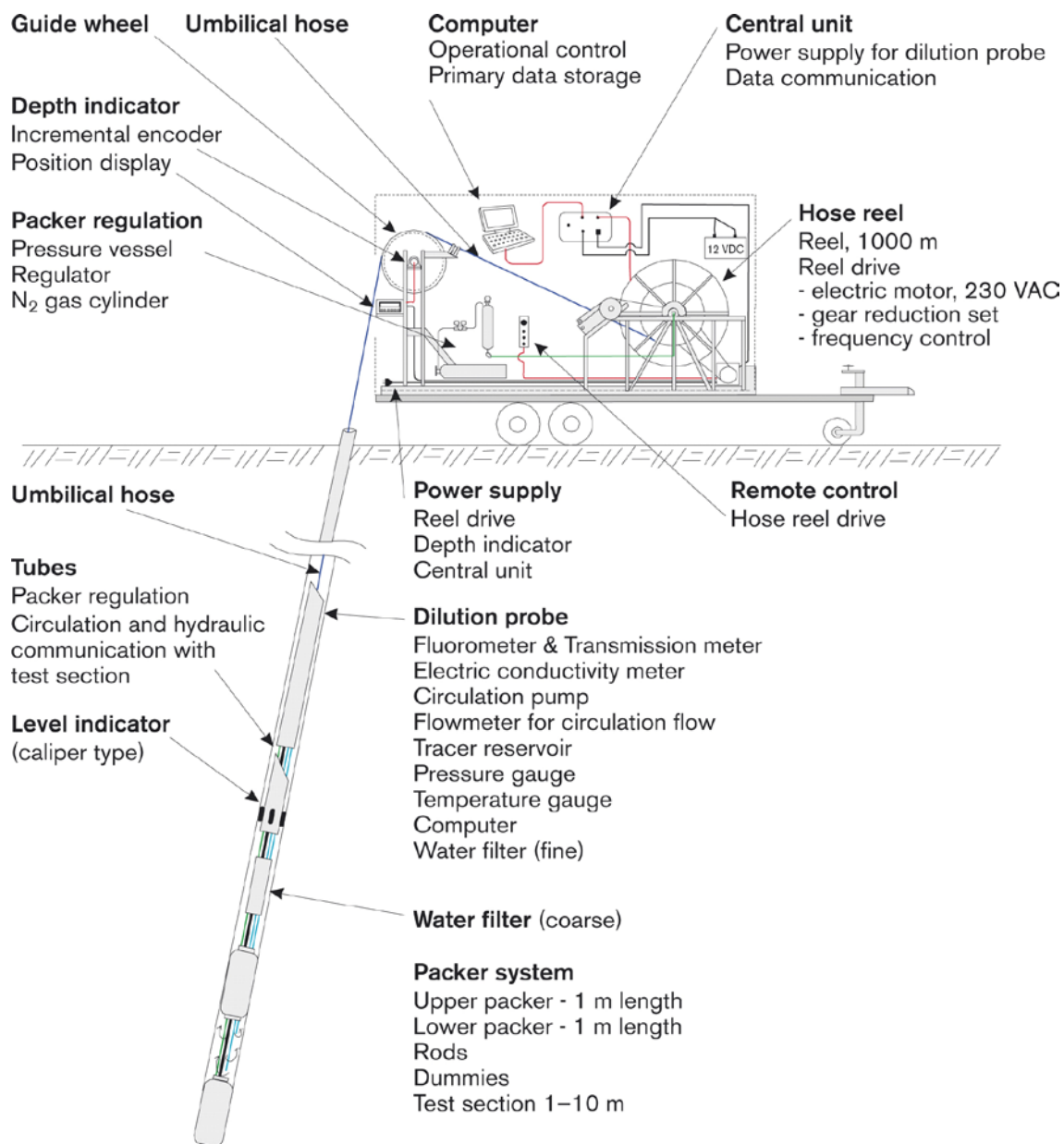


**Figure 3-1.** The SKB borehole dilution probe.

The accuracy of determined flow rates through the borehole test section is affected by various measurement errors related to, for example, the accuracy of the calculated test section volume and determination of tracer concentration. The overall accuracy when determining flow rates through the borehole test section is better than  $\pm 30\%$ , based on laboratory measurements in artificial borehole test sections.

The groundwater flow rates in the rock formation are determined from the calculated groundwater flow rates through the borehole test section and by using some assumption about the flow field around the borehole test section. This flow field depends on the hydraulic properties close to the borehole and is given by the correction factor  $\alpha$ , as discussed below in Section 4.4.1. The value of  $\alpha$  will, at least, vary within  $\alpha = 2 \pm 1.5$  in fractured rock /Gustafsson 2002/. Hence, the groundwater flow in the rock formation is calculated with an accuracy of about  $\pm 75\%$ , depending on the flow-field distortion.

### 3.2 SWIW test equipment

The SWIW (Single Well Injection Withdrawal) test equipment constitutes a complement to the borehole dilution probe making it possible to carry out a SWIW test in the same test section as the dilution measurement, Figure 3-2. Measurements can be made in boreholes with 56 mm or 76–77 mm diameter and the test section length can be arranged for 1, 2, 3, 4 or 5 m with an optimised special packer/dummy system for 76–77 mm boreholes. The equipment is primarily designed for measurements in the depth interval 300–700 m borehole length. However, measurements can be carried out at shallower depths as well at depths larger than 700 m. The possibility to carry out a SWIW test much depends on the hydraulic transmissivity in the investigated test section and frictional loss in the tubing at tracer withdrawal pumping. Besides the dilution probe, the main parts of the SWIW test equipment are:

- Polyamide tubing constituting the hydraulic connection between SWIW test equipment at ground surface and the dilution probe in the borehole.
- Air tight vessel for storage of groundwater under anoxic conditions, i.e. N<sub>2</sub>-atmosphere.
- Control system for injection of tracer solution and groundwater (chaser fluid).
- Injection pumps for tracer solution and groundwater.

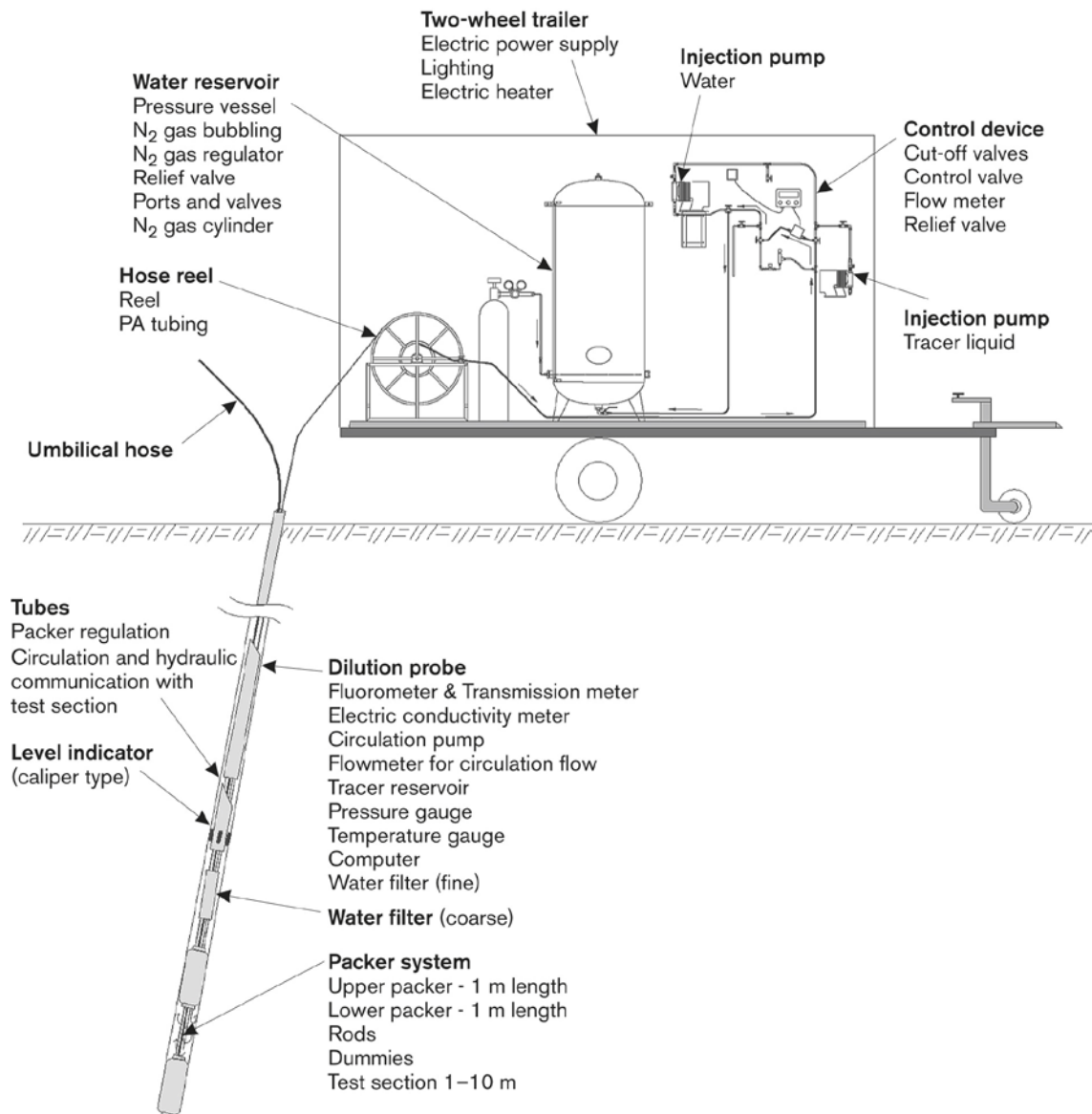


Figure 3-2. SWIW test equipment, connected to the borehole dilution probe.

### **3.2.1 Measurement range and accuracy**

The result of a SWIW test depends on the accuracy of the determined tracer concentration in injection solutions and withdrawn water. The result also depends on the accuracy in the volume of injection solution and volumes of injected and withdrawn water. For non-sorbing dye tracers (e.g. Uranine) the tracer concentration in collected water samples can be analysed with a resolution of 10 µg/l in the range 0.0–4.0 mg/l. The accuracy is within  $\pm 5\%$ . The volume of injected tracer solution can be determined within  $\pm 0.1\%$  and the volume of injected and withdrawn water can be determined within 5%.

The evaluation of a SWIW test and determination of transport parameters is done with model simulations, fitting the model to the measured data (concentration as a function of time). The accuracy in determined transport parameters depends on selection of model concept and how well the model fit the measured data.

## 4 Execution

The measurements were performed according to AP PS 400-07-026 (SKB internal controlling document) in compliance with the methodology descriptions for the borehole dilution probe equipment – SKB MD 350.001, Metodbeskrivning för grundvattenflödesmätning, and the measurement system description for SWIW test – SKB MD 353.069, MSB; Systemöversikt – SWIW-test utrustning – (SKB internal controlling documents), Table 1-1.

### 4.1 Preparations

The preparations included calibration of the fluorometer and the electric conductivity meter before arriving at the site. Briefly, this was performed by adding certain amounts of the tracer to a known test volume while registering the measured A/D-levels. From this, calibration constants were calculated and saved for future use by using the measurement application. The other sensors had been calibrated previously and were only calibrated as an additional check.

Extensive functionality checks were made prior to transport to the site and limited function checks were performed at the site. The equipment was cleaned to comply with SKB cleaning level 1 before lowering it into the borehole. All preparations were performed according to SKB Internal controlling documents, cf. Table 1-1.

### 4.2 Procedure

#### 4.2.1 Groundwater flow measurement

A total of six groundwater flow measurements were carried out, Table 4-1.

Each measurement was performed according to the following procedure. The equipment was lowered to the correct borehole length where background values of tracer concentration and supporting parameters, pressure and temperature, were measured and logged. Then, after inflating the packers and the pressure had stabilized, tracer was injected in the test section. The tracer concentration and supporting parameters were measured and logged continuously until the tracer had been diluted to such a degree that the groundwater flow rate could be calculated.

**Table 4-1. Performed dilution (flow) measurements.**

Borehole	Test section (m)*	Number of flowing fractures*	T (m <sup>2</sup> /s)*	Tracer	Test period (yymmdd–yymmdd)
KLX11A	167.8–170.8 (148–151)	2	1.78E–05	Uranine	070710–070712
KLX11A	306.0–309.0 (269–271)	3	1.04E–05	Uranine	070712–070713
KLX11A	439.0–442.0 (382–385)	3	6.21E–08	Uranine	070713–070717
KLX11A	516.5–519.5 (447–450)	2	3.39E–06	Uranine	070403–070405
KLX11A	579.0–584.0 (499–502)	5	5.76E–06	Uranine	070322–070326
KLX11A	598.0–599.0 (514–515)	2	1.35E–07	Uranine	070424–070502

\* /Väisäsvaara et al. 2007/.

\* Test section vertical depth (m b s l) is given within brackets.

## 4.2.2 SWIW tests

Two SWIW tests were performed, Table 4-2. BIPS images of the test sections are shown in Appendix C. To conduct a SWIW test requires that the SWIW equipment is connected to the borehole dilution probe, Figures 3-1 and 3-2.

The SWIW tests were carried out according to the following procedure. The equipment was lowered to the correct borehole length where background values of Uranine and supporting parameters, pressure and temperature, were measured and logged. Then, after inflating the packers and the pressure had stabilized, the circulation pump in the dilution probe was used to pump groundwater from the test section to the airtight vessel at the ground surface. Water samples were also taken for analysis of background concentration of Uranine, cesium and rubidium. When pressure had recovered after the pumping in the test section, the injection phases started with pre-injection of the native groundwater to reach steady state flow conditions. Thereafter groundwater spiked with the tracers Uranine, cesium and rubidium was injected. Finally, injection of native groundwater to push the tracers out into the fracture/fracture zone was performed. The withdrawal phase started by pumping water to the ground surface. An automatic sampler at ground surface was used to take water samples for analysis of Uranine, cesium and rubidium in the withdrawn water.

## 4.3 Data handling

During groundwater flow measurement with the dilution probe, data are automatically transferred from the measurement application to a SQL database. Data relevant for analysis and interpretation are then automatically transferred from SQL to Excel via an MSSQL (ODBC) data link, set up by the operator. After each measurement the Excel data file is copied to a CD.

The water samples from the SWIW test were analysed for Uranine tracer content at the Geosigma Laboratory in Uppsala. Cesium and rubidium contents were analysed at the Analytica laboratory in Luleå.

## 4.4 Analyses and interpretation

### 4.4.1 The dilution method – general principles

The dilution method is an excellent tool for in situ determination of flow rates in fractures and fracture zones.

In the dilution method a tracer is introduced and homogeneously distributed into a borehole test section. The tracer is subsequently diluted by the ambient groundwater flow through the borehole test section. The dilution of the tracer is proportional to the water flow through the borehole section, Figure 4-1.

**Table 4-2. Performed SWIW tests.**

Borehole	Test section (m)*	Number of flowing fractures*	T (m <sup>2</sup> /s)*	Tracers	Test period (yymmdd–yymmdd)
KLX11A	516.5–519.5 (447–450)	2	3.39E–06	Uranine/cesium/rubidium	070724–070731
KLX11A	598.0–599.0 (514–515)	2	1.35E–07	Uranine/cesium/rubidium	070626–070709

\* /Väisäsvaara et al. 2007/.

\* Test section vertical depth (m b s l) is given within brackets.

### Principle of flow determination

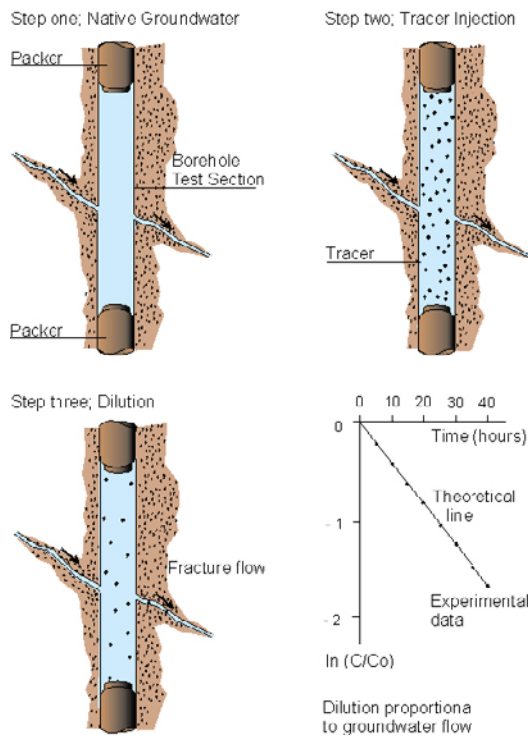


**Figure 4-1.** General principles of dilution and flow determination.

The dilution in a well-mixed borehole section, starting at time  $t = 0$ , is given by:

$$\ln(C/C_0) = -\frac{Q_w}{V} \cdot t \quad (\text{Equation 4-1})$$

where  $C$  is the concentration at time  $t$  (s),  $C_0$  is the initial concentration,  $V$  is the water volume ( $\text{m}^3$ ) in the test section and  $Q_w$  is the volumetric flow rate ( $\text{m}^3/\text{s}$ ). Since  $V$  is known, the flow rate may then be determined from the slope of the line in a plot of  $\ln(C/C_0)$ , or  $\ln C$ , versus  $t$ .

An important interpretation issue is to relate the measured groundwater flow rate through the borehole test section to the rate of groundwater flow in the fracture/fracture zone straddled by the packers. The flow-field distortion must be taken into consideration, i.e. the degree to which the groundwater flow converges and diverges in the vicinity of the borehole test section. With a correction factor,  $\alpha$ , which accounts for the distortion of the flow lines due to the presence of the borehole, it is possible to determine the cross-sectional area perpendicular to groundwater flow by:

$$A = 2 \cdot r \cdot L \cdot \alpha \quad (\text{Equation 4-2})$$

where  $A$  is the cross-sectional area ( $\text{m}^2$ ) perpendicular to groundwater flow,  $r$  is borehole radius (m),  $L$  is the length (m) of the borehole test section and  $\alpha$  is the correction factor. Figure 4-2 schematically shows the cross-sectional area,  $A$ , and how flow lines converge and diverge in the vicinity of the borehole test section.

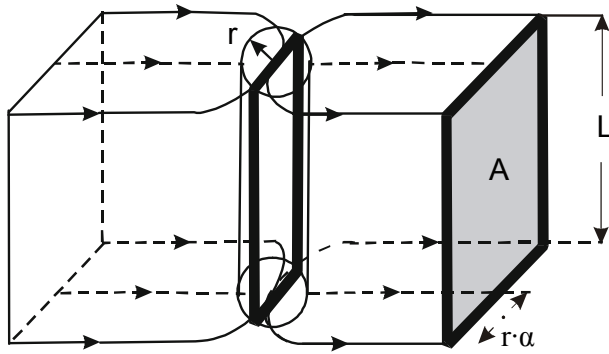


**Figure 4-2.** Diversion and conversion of flow lines in the vicinity of a borehole test section.

Assuming laminar flow in a plane parallel fissure or a homogeneous porous medium, the correction factor  $\alpha$  is calculated according to Equation (4-3), which often is called the formula of Ogilvi /Halevy et al. 1967/. Here it is assumed that the disturbed zone, created by the presence of the borehole, has an axis-symmetrical and circular form.

$$\alpha = \frac{4}{1 + (r/r_d) + (K_2/K_1)(1 - (r/r_d)^2)} \quad \text{(Equation 4-3)}$$

where  $r_d$  is the outer radius (m) of the disturbed zone,  $K_1$  is the hydraulic conductivity (m/s) of the disturbed zone, and  $K_2$  is the hydraulic conductivity of the aquifer. If the drilling has not caused any disturbances outside the borehole radius, then  $K_1 = K_2$  and  $r_d = r$  which will result in  $\alpha = 2$ . With  $\alpha = 2$ , the groundwater flow within twice the borehole radius will converge through the borehole test section, as illustrated in Figures 4-2 and 4-3.

If there is a disturbed zone around the borehole the correction factor  $\alpha$  is given by the radial extent and hydraulic conductivity of the disturbed zone. If the drilling has caused a zone with a lower hydraulic conductivity in the vicinity of the borehole than in the fracture zone, e.g. positive skin due to drilling debris and clogging, the correction factor  $\alpha$  will decrease. A zone of higher hydraulic conductivity around the borehole will increase  $\alpha$ . Rock stress redistribution, when new boundary conditions are created by the drilling of the borehole, may also change the hydraulic conductivity around the borehole and thus affect  $\alpha$ . In Figure 4-3, the correction factor,  $\alpha$ , is given as a function of  $K_2/K_1$  at different normalized radial extents of the disturbed zone ( $r/r_d$ ). If the fracture/fracture zone and groundwater flow are not perpendicular to the borehole axis, this also has to be accounted for. At a 45 degree angle to the borehole axis the value of  $\alpha$  will be about 41% larger than in the case of perpendicular flow. This is further discussed in /Gustafsson 2002, Rhén et al. 1991/.

In order to obtain the Darcy velocity in the undisturbed rock the calculated groundwater flow,  $Q_w$  is divided by A, Equation 4-4.

$$v = Q_w / A \quad \text{(Equation 4-4)}$$

The hydraulic gradient is then calculated as

$$I = v/K \quad \text{(Equation 4-5)}$$

where K is the hydraulic conductivity.

#### 4.4.2 The dilution method – evaluation and analysis

The first step of evaluation included studying a graph of the measured concentration versus time data. Then background concentration, i.e. any tracer concentration in the groundwater before tracer injection, was subtracted from the measured concentrations. Thereafter  $\ln(C/C_0)$  was plotted versus time. In most cases the relationship was linear and the proportionality constant was then calculated by performing a linear regression. In the cases where the relationship between  $\ln(C/C_0)$  and time was non-linear, a sub-interval was chosen in which the relationship was linear.



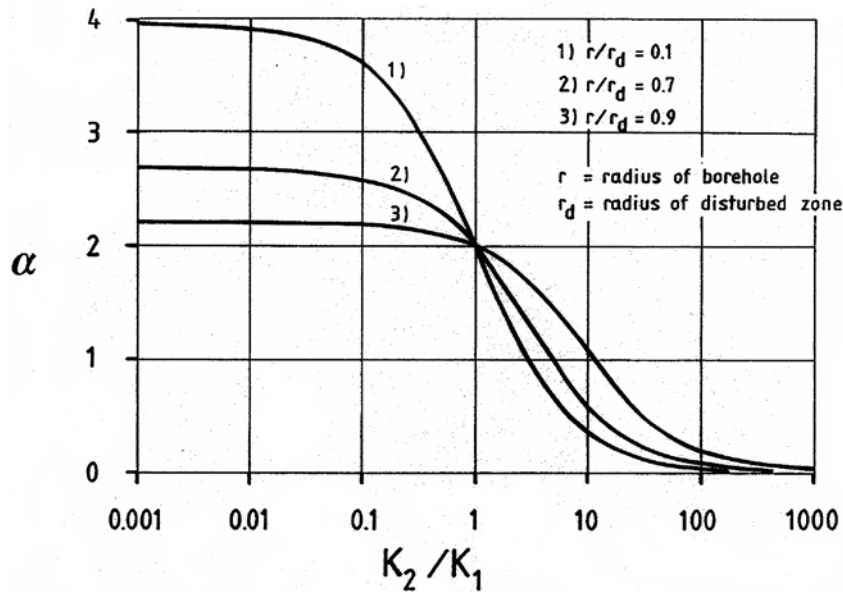


**Figure 4-3.** The correction factor,  $\alpha$ , as a function of  $K_2/K_1$  at different radial extent ( $r/r_d$ ) of the disturbed zone (skin zone) around the borehole.

The value of the slope obtained from the linear regression was then used to calculate  $Q_w$  according to Equation (4-1).

The hydraulic gradient,  $I$ , was calculated by combining Equations (4-2), (4-4) and (4-5), and choosing  $\alpha = 2$ . The hydraulic conductivity,  $K$ , in Equation (4-5) was obtained from previously performed Posiva Flow Log measurements (PFL) /Väisäsvaara et al. 2007/.

#### 4.4.3 SWIW test – basic outline

A Single Well Injection Withdrawal (SWIW) test may consist of all or some of the following phases:

1. filling pressure vessel with groundwater from the selected fracture,
2. injection of water to establish steady-state hydraulic conditions (pre-injection),
3. injection of one or more tracers,
4. injection of groundwater (chaser fluid) after tracer injection is stopped,
5. waiting phase,
6. withdrawal (recovery) phase.

The tracer breakthrough data used for evaluation are obtained from the withdrawal phase. The injection of chaser fluid, i.e. groundwater from the pressure vessel, has the effect of pushing the tracer out as a “ring” in the formation surrounding the tested section. This is generally a benefit, because when the tracer is pumped back, both ascending and descending parts are obtained in the recovery breakthrough curve. During the waiting phase there is no injection or withdrawal of fluid. The purpose of this phase is to increase the time available for time-dependent transport-processes so that these may be more easily evaluated from the resulting breakthrough curve. A schematic example of a resulting breakthrough curve during a SWIW test is shown in Figure 4-4.

The design of a successful SWIW test requires prior determination of injection and withdrawal flow rates, duration of tracer injection, duration of the various injections, waiting and pumping phases, selection of tracers, tracer injection concentrations, etc.

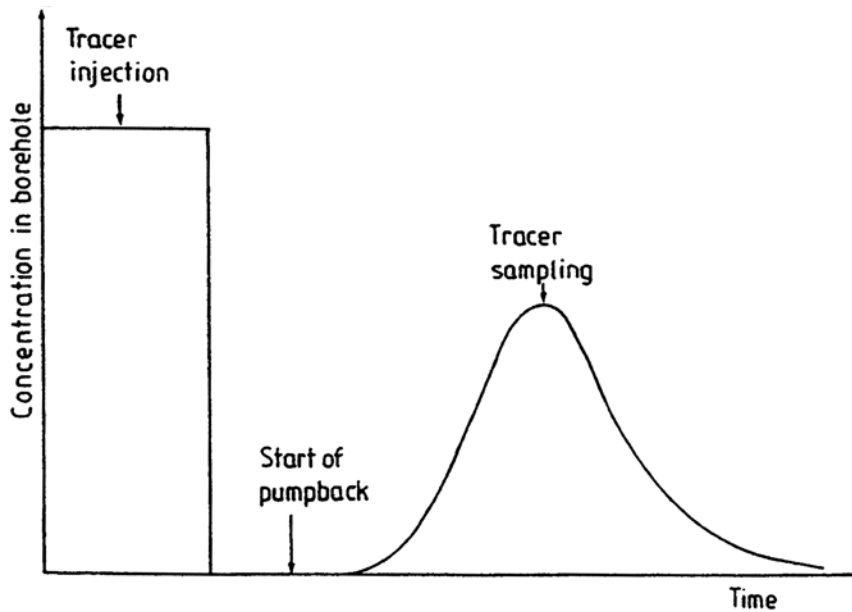


Figure 4-4. Schematic tracer concentration sequence during a SWIW test /Andersson 1995/.

#### 4.4.4 SWIW test – evaluation and analysis

The model evaluation of the experimental results was carried out assuming homogenous conditions. Model simulations were made using the model code SUTRA /Voss 1984/ and the experiments were simulated without a background hydraulic gradient. It was assumed that flow and transport occur within a planar fracture zone of some thickness. The volume available for flow was represented by assigning a porosity value to the assumed zone. Modelled transport processes include advection, dispersion and linear equilibrium sorption.

The sequence of the different injection phases was modelled as accurately as possible based on supporting data for flows and tracer injection concentration. Generally, experimental flows and times may vary from one phase to another, and the flow may also vary within phases. The specific experimental sequences for the borehole sections are listed below.

In the simulation model, tracer injection was simulated as a function accounting for mixing in the borehole section and sorption (for cesium and rubidium) on the borehole walls. The function assumes a completely mixed borehole section and linear equilibrium surface sorption:

$$C = (C_0 - C_{in}) e^{-\left(\frac{Q}{V_{bh} + K_a A_{bh}}\right)t} + C_{in} \quad (\text{Equation 4-6})$$

where  $C$  is concentration in water leaving the borehole section and entering the formation ( $\text{kg/m}^3$ ),  $V_{bh}$  is the borehole volume including circulation tubes ( $\text{m}^3$ ),  $A_{bh}$  is area of borehole walls ( $\text{m}^2$ ),  $Q$  is flow rate ( $\text{m}^3/\text{s}$ ),  $C_{in}$  is concentration in the water entering the borehole section ( $\text{kg/m}^3$ ),  $C_0$  is initial concentration in the borehole section ( $\text{kg/m}^3$ ),  $K_a$  is surface sorption coefficient (m) and  $t$  is elapsed time (s).

Based on in situ experiments /Andersson et al. 2002/ and laboratory measurements on samples of crystalline rock /Byegård and Tullborg 2005/ the sorption coefficient  $K_a$  was assigned a value of  $10^{-2}$  m in all simulations. An example of the tracer injection input function is given in Figure 4-5, showing a 50 minutes long tracer injection phase followed by a chaser phase.

Non-linear regression was used to fit the simulation model to experimental data. The estimation strategy was generally to estimate the dispersivity ( $\alpha_r$ ) and a retardation factor ( $R$ ), while setting the porosity (i.e. the available volume for flow) to a fixed value. Simultaneous fitting of both of the tracer breakthrough curves (Uranine and cesium in the example), and calculation of fitting statistics, was carried out using the approach described in /Nordqvist and Gustafsson 2004/. Tracer breakthrough curves for Uranine and rubidium are related and calculated in the same way.

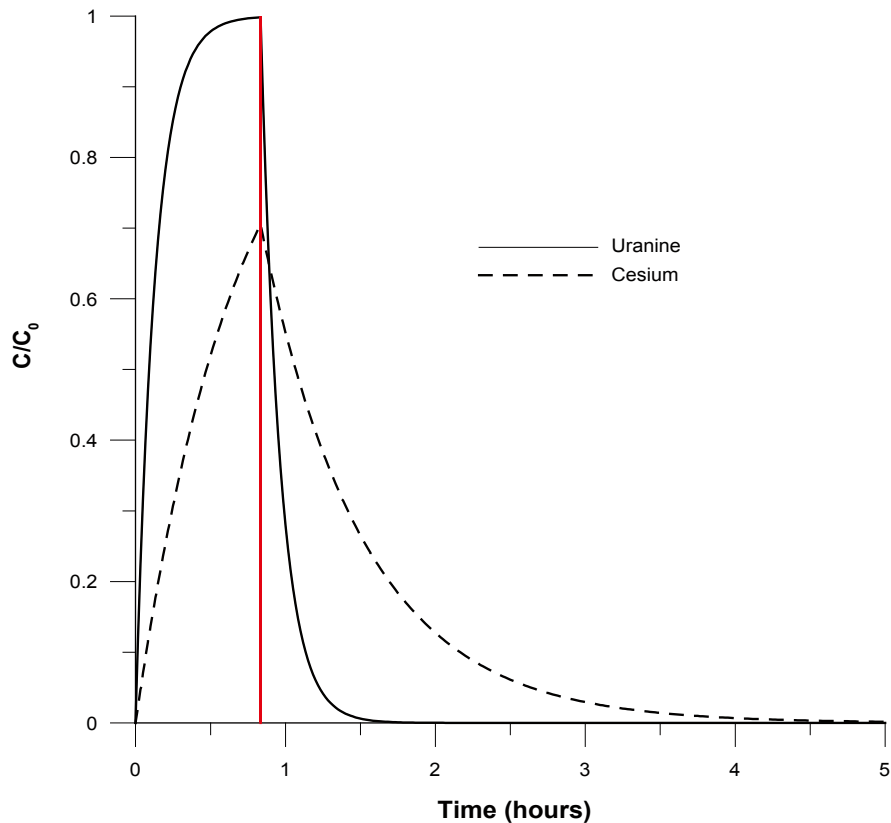


**Figure 4-5.** Example of simulated tracer injection functions for a tracer injection phase (ending at 50 minutes shown by the vertical red line) immediately followed by a chaser phase.

## 4.5 Nonconformities

The activity was performed according to the activity plan and the method description with the exception that sections 107.3–108.3 m and 265.4–266.4 m was not measured as a consequence of delays in the measurement programme. These delays were caused by the following:

- Interruption in the data transfer was a recurring problem. This was caused by potential drops in the electric power supply due to a broken electrical (canbus) circuit or unexplainable interruptions in communication with the probe.
- An abrupt stop when lowering the probe occurred at c. 505 m. A dummy was lowered to clear the passage.
- A problem occurred when hoisting the borehole probe past the transition cone between the upper percussion-drilled and the lower core-drilled part of the borehole. The probe got stuck in a gap between the transition cone and the lower core-drilled part of the borehole, caused by a pressure gauge that was left behind before the cone was installed. The probe was lifted together with the transition cone. Service of the probe and reinstallation of the transition cone caused further delay.

For the dilution measurement at c. 516 and at c. 579 m the pressure gauge shows incorrect values. Although there is a bias, with too high absolute pressures, the relative changes from the biased level is considered reasonable and used to determine if pressure was stable during dilution measurement.

For the dilution measurement at c. 168, 306, 439 and at c. 598 m the temperature gauge shows incorrect values. Although there is a bias, with too high temperatures (3–5°C), the relative changes from the biased level is considered reasonable and used to determine if temperature was stable during dilution measurement.

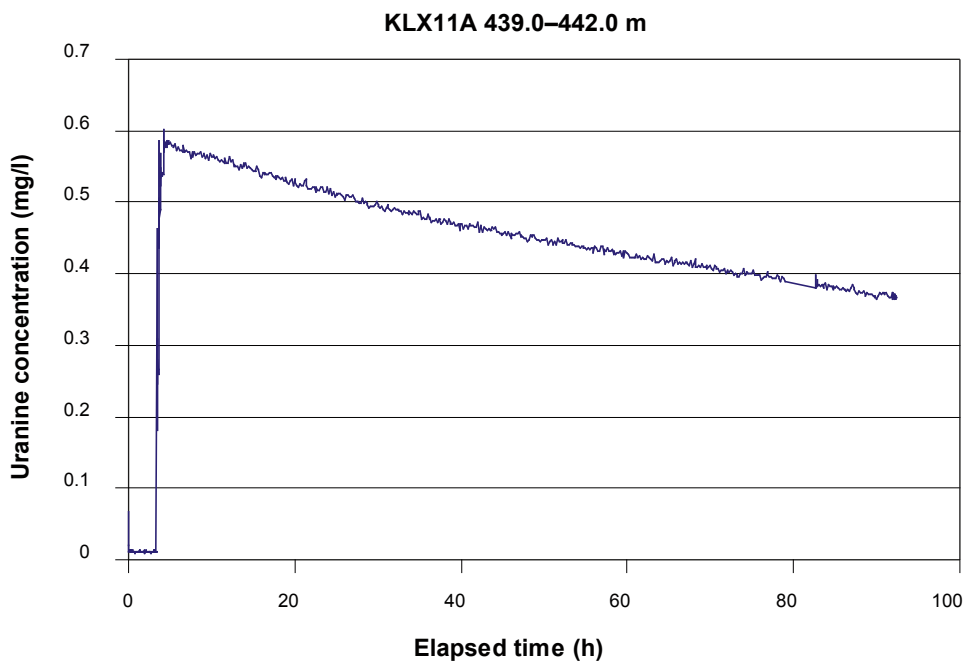
## 5 Results

Original data from the reported activity are stored in the primary database Sicada, where they are traceable by the Activity Plan number (AP PS 400-07-026). Only data in SKB's databases are accepted for further interpretation and modelling. The data presented in this report are regarded as copies of the original data. Data in the databases may be revised, if needed. Such revisions will not necessarily result in a revision of the P-report, although the normal procedure is that major data revisions entail a revision of the P-report. Minor data revisions are normally presented as supplements, available at [www.skb.se](http://www.skb.se).

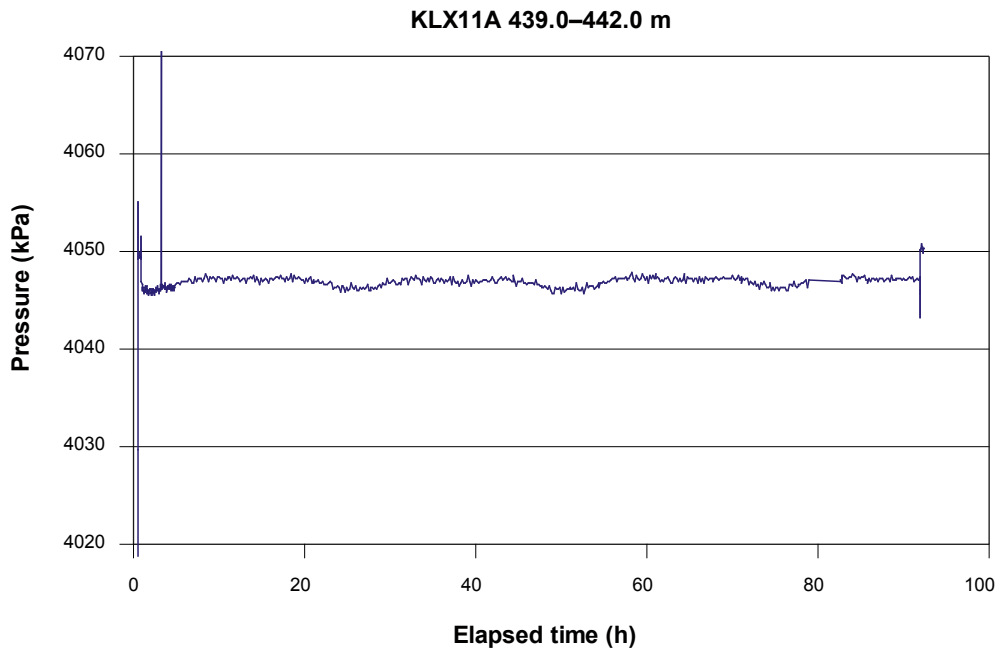
### 5.1 Dilution measurements

Figure 5-1 exemplifies a typical dilution curve in a fracture zone straddled by the test section at 439.0–442.0 m borehole length (382–385 m vertical depth) in borehole KLX11A. In the first phase, the background value is recorded. The packers are inflated and background recorded further for about 15 minutes. In phase two, Uranine tracer is injected, and after mixing an initial concentration ( $C_0$ ) of about 0.58 mg/l is achieved. In phase three, the dilution is measured for about 85 hours. Thereafter the packers are deflated and the remaining tracer flows out of the test section. Figure 5-2 shows the measured pressure during the dilution measurement. Since the pressure gauge is positioned about seven metres from the top of test section there is a bias in the pressure that is not corrected for, as only changes and trends relative to the initial value are of importance for the dilution measurement. Figure 5-3 is a plot of  $\ln(C/C_0)$  versus time and a linear regression best fit to data showing a good fit with correlation  $R^2 = 0.9903$ . The standard deviation, STDAV, shows the mean divergence of the values from the best fit line and is calculated from

$$\text{STDAV} = \sqrt{\frac{n \sum x^2 - (\sum x)^2}{n(n-1)}} \quad (\text{Equation 5})$$



**Figure 5-1.** Dilution measurement in borehole KLX11A, section 439.0–442.0 m. Uranine concentration versus time.



*Figure 5-2. Measured pressure during dilution measurement in borehole KLX11A, section 439.0–442.0 m.*

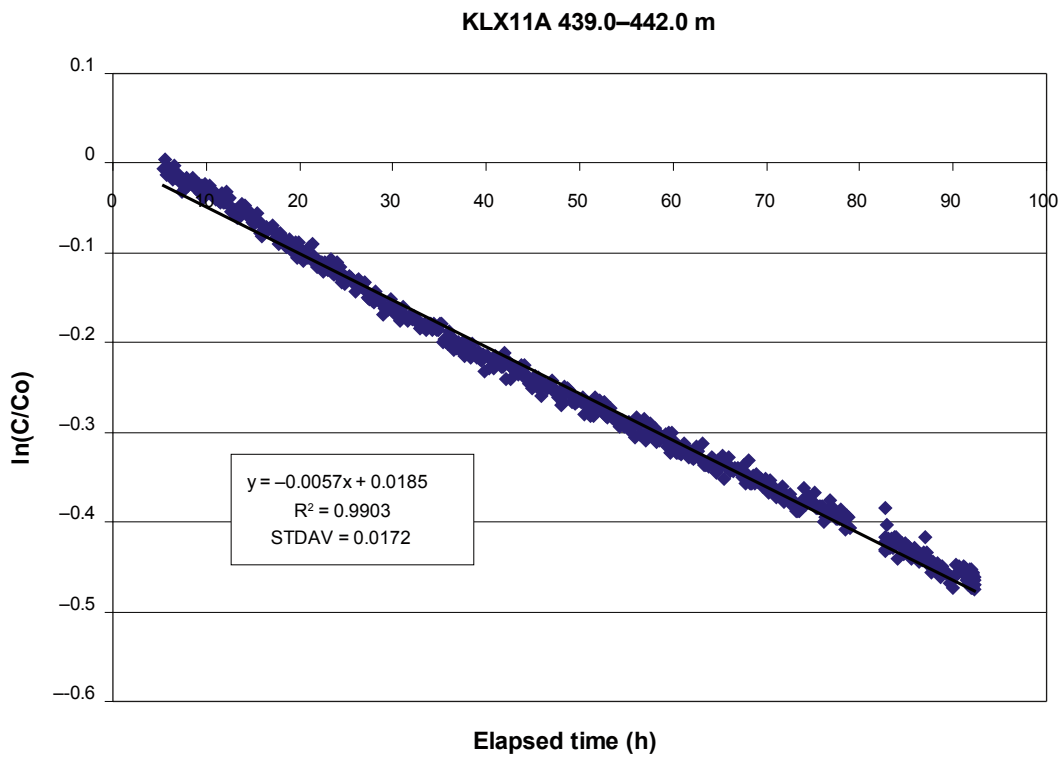


*Figure 5-3. Linear regression best fit to data from dilution measurement in borehole KLX11A, section 439.0–442.0 m.*

The calculated groundwater flow rate, Darcy velocity and hydraulic gradient are presented in Table 5-1 together with the results from all other dilution measurements carried out in borehole KLX11A.

The dilution measurements were carried out with the dye tracer Uranine. Uranine normally has a low background concentration and the tracer can be injected and measured in concentrations far above the background value, which gives a large dynamic range and accurate flow determinations.

Details of all dilution measurements, with diagrams of dilution versus time and the supporting parameters pressure, temperature and circulation flow rate are presented in Appendix B1–B6.

### 5.1.1 KLX11A, section 167.8–170.8 m

This dilution measurement was carried out with the dye tracer Uranine in a test section with two flowing fractures. The complete test procedure can be followed in Figure 5-4. The background concentration (0.01 mg/l) is measured for about 15 minutes with inflated packers. Thereafter the Uranine tracer is injected in four steps, and after mixing it finally reaches an initial concentration of 0.78 mg/l above background. Dilution is measured for about 40 hours. The packers are then deflated. The hydraulic pressure is stable (Appendix B1). The final evaluation was made on the 25 to 64 hours part of the dilution curve. The regression line fits well to the slope of the dilution with a correlation coefficient of  $R^2 = 0.9930$  for the best fit line (Figure 5-5). The groundwater flow rate, calculated from the best fit line, is 0.25 ml/min. Calculated hydraulic gradient is 0.002 and Darcy velocity  $9.2 \cdot 10^{-9}$  m/s.

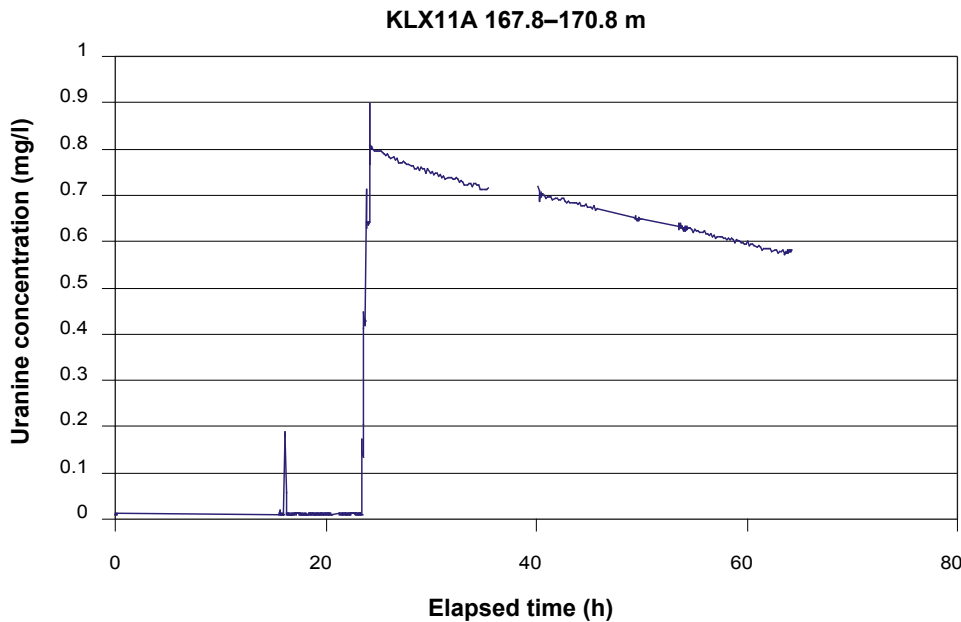


**Figure 5-4.** Dilution measurement in borehole KLX11A, section 167.8–170.8 m. Uranine concentration versus time.

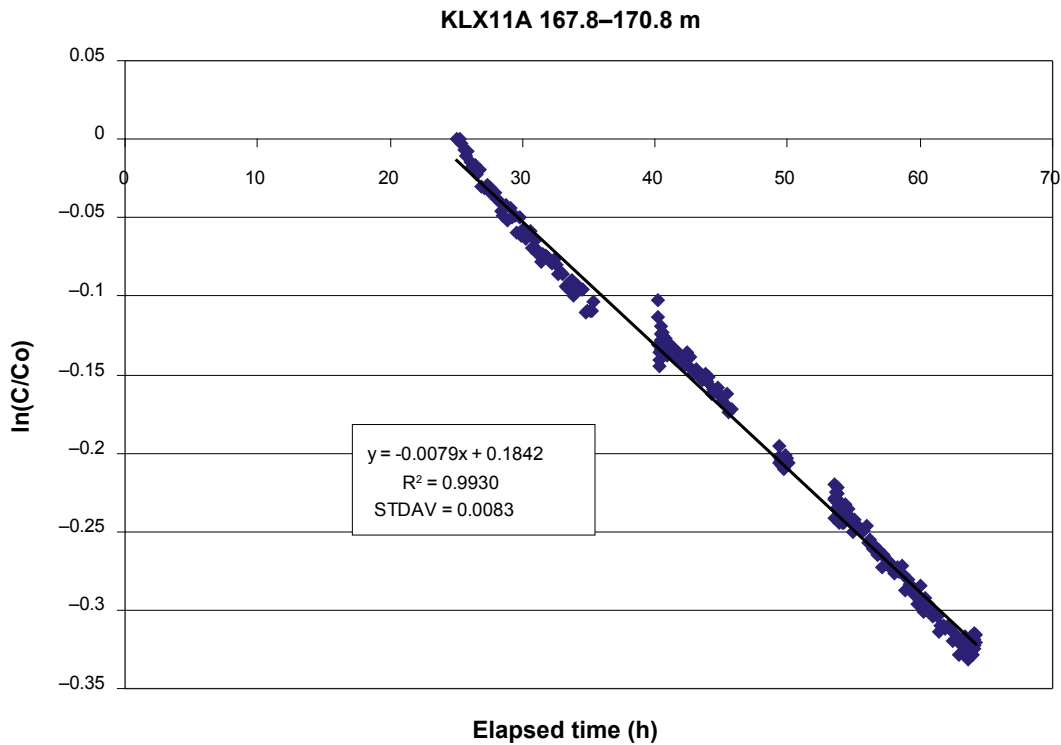


**Figure 5-5.** Linear regression best fit to data from dilution measurement in borehole KLX11A , section 167.8–170.8 m.

### 5.1.2 KLX11A, section 306.0–309.0 m

This dilution measurement was carried out with the dye tracer Uranine in a test section with three flowing fractures. The background measurement, tracer injection and dilution can be followed in Figure 5-6. Background concentration (0.01 mg/l) is measured for about 15 minutes with inflated packers. The Uranine tracer is injected in three steps and after mixing it reaches an initial concentration of 0.53 mg/l above background. Dilution is measured for about 25 hours, thereafter the packers are deflated and the remaining tracer flows out of the test section. Hydraulic pressure is stable (Appendix B2). Groundwater flow is determined from the 6–27 hours part of the dilution measurement. The correlation coefficient of the best fit line is  $R^2 = 0.9946$  (Figure 5-7), and the groundwater flow rate, calculated from the best fit line, is 0.38 ml/min. The calculated hydraulic gradient is 0.004 and Darcy velocity  $1.4 \cdot 10^{-8}$  m/s.

### 5.1.3 KLX11A, section 439.0–442.0 m

This dilution measurement was carried out in a test section with three flowing fractures. The background measurement, tracer injection and dilution can be followed in Figure 5-8. Background concentration (0.01 mg/l) is measured for about 15 minutes with inflated packers. The Uranine tracer is injected in four steps and after mixing it reaches an initial concentration of 0.57 mg/l above background. Dilution is measured for about 85 hours. Thereafter the packers are deflated. The hydraulic pressure shows small diurnal pressure variations due to earth tidal effects (Appendix B3). The final evaluation was made from 5 to 92 hours of elapsed time. The regression line fit well to the slope of the dilution, and the correlation coefficient for the best fit line is good,  $R^2 = 0.9903$  (Figure 5-9). The groundwater flow rate, calculated from the best fit line, is 0.18 ml/min. The calculated hydraulic gradient is 0.320 and Darcy velocity  $6.6 \cdot 10^{-9}$  m/s. The hydraulic gradient is large and may be caused by local effects, where the measured fracture constitutes a hydraulic conductor between other fractures with different hydraulic heads. Or the large gradient may be due to wrong estimates of the correction factor,  $\alpha$ , and/or the hydraulic conductivity of the fracture.

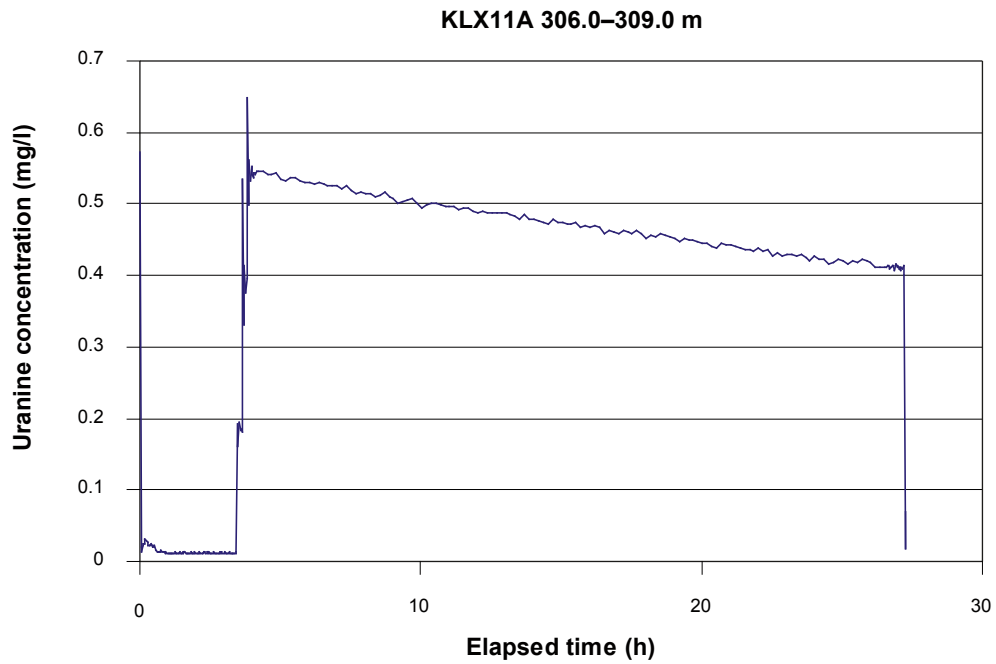


*Figure 5-6. Dilution measurement in borehole KLX11A, section 306.0–309.0 m. Uranine concentration versus time.*

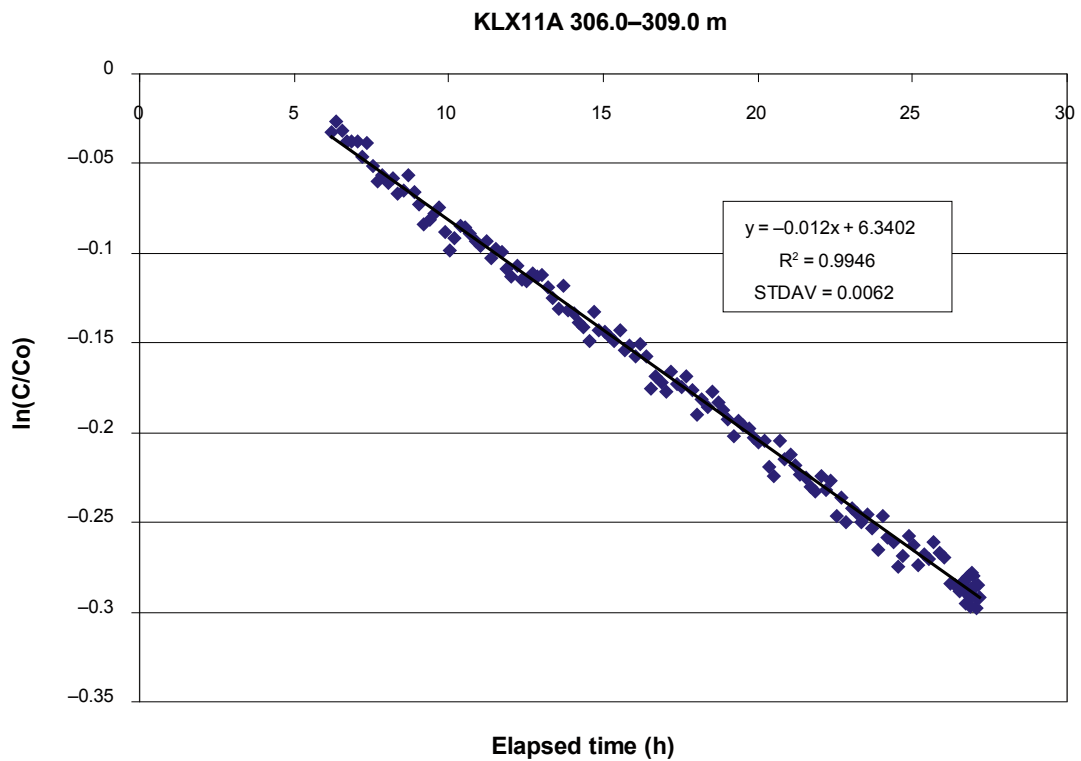


*Figure 5-7. Linear regression best fit to data from dilution measurement in borehole KLX11A, section 306.0–309.0 m.*



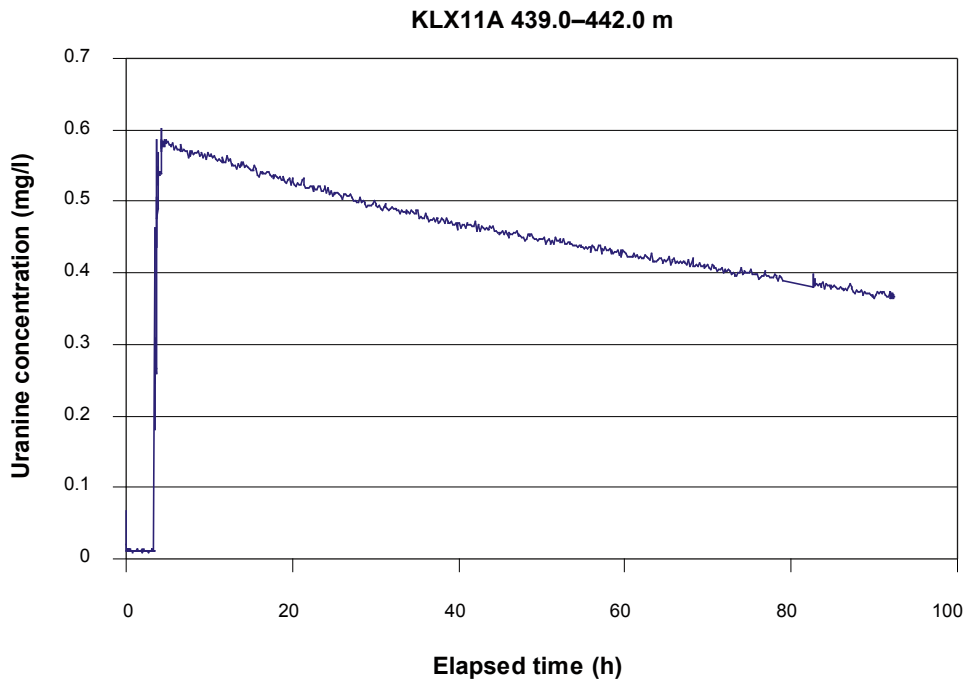


*Figure 5-8. Dilution measurement in borehole KLX11A, section 439.0–442.0 m. Uranine concentration versus time.*

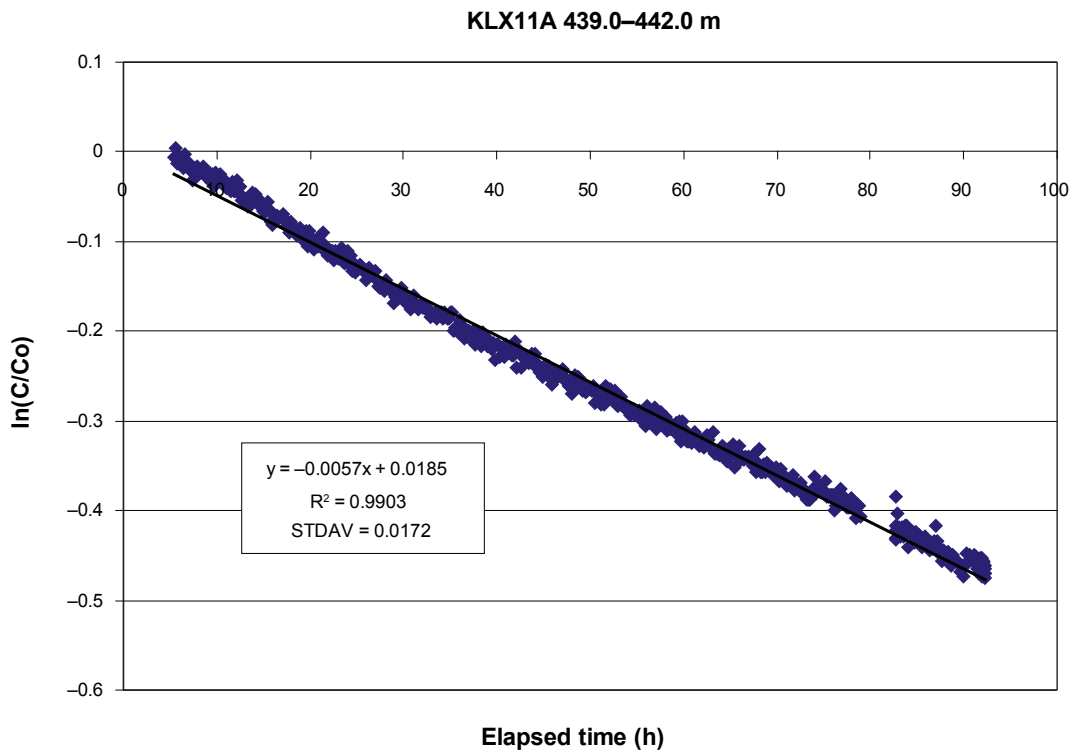


*Figure 5-9. Linear regression best fit to data from dilution measurement in borehole KLX11A, section 439.0–442.0 m.*

#### 5.1.4 KLX11A, section 516.5–519.5 m

This dilution measurement was carried out with the dye tracer Uranine in a test section with two flowing fractures. The background measurement, tracer injection and dilution can be followed in Figure 5-10. Background concentration (0.01 mg/l) is measured for about 30 minutes with inflated packers. Thereafter the Uranine tracer is injected in two steps and after mixing it finally reaches an initial concentration of 0.84 mg/l above background. Dilution is measured for about 35 hours. Thereafter the packers are deflated. The hydraulic pressure shows values of incorrect magnitude but with relative changes in an acceptable range (Appendix B4). The groundwater flow is determined from the 23–48 hours part of the dilution measurement. The correlation coefficient of the best fit line is  $R^2 = 0.9863$  (Figure 5-11), and the groundwater flow rate, calculated from the best fit line, is 0.52 ml/min. The calculated hydraulic gradient is 0.017 and Darcy velocity  $1.9 \cdot 10^{-8}$  m/s.

#### 5.1.5 KLX11A, section 579.0–584.0 m

This dilution measurement was carried out with the dye tracer Uranine in a test section with five flowing fractures. The background measurement, tracer injection and dilution can be followed in Figure 5-12. Background concentration (0.01 mg/l) is measured for about 20 minutes with inflated packers. Thereafter the Uranine tracer is injected in two steps and after mixing it finally reaches an initial concentration of 0.79 mg/l above background. Dilution is measured for about 50 hours. Thereafter pumping starts for chemical characterisation sampling. The hydraulic pressure shows incorrect values but with relative changes in an acceptable range (Appendix B5). The groundwater flow is determined from the 67–105 hours part of the dilution measurement where the pressure is fairly stable. The correlation coefficient of the best fit line is  $R^2 = 0.9927$  (Figure 5-13), and the groundwater flow rate, calculated from the best fit line, is 2.88 ml/min. The calculated hydraulic gradient is 0.055 and Darcy velocity  $6.3 \cdot 10^{-8}$  m/s.

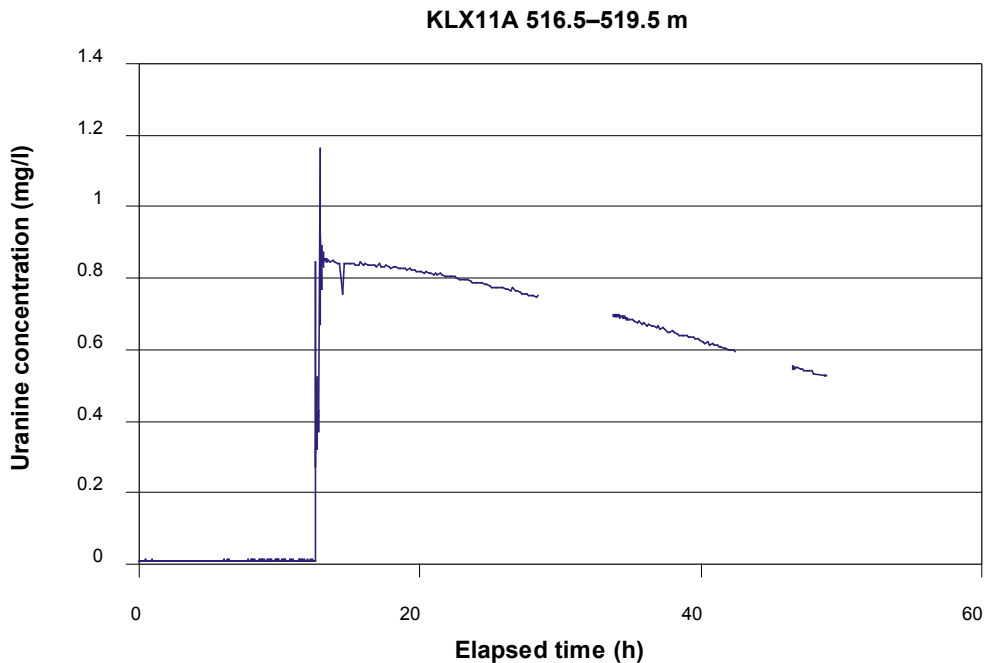


**Figure 5-10.** Dilution measurement in borehole KLX11A, section 516.5–519.5 m. Uranine concentration versus time.

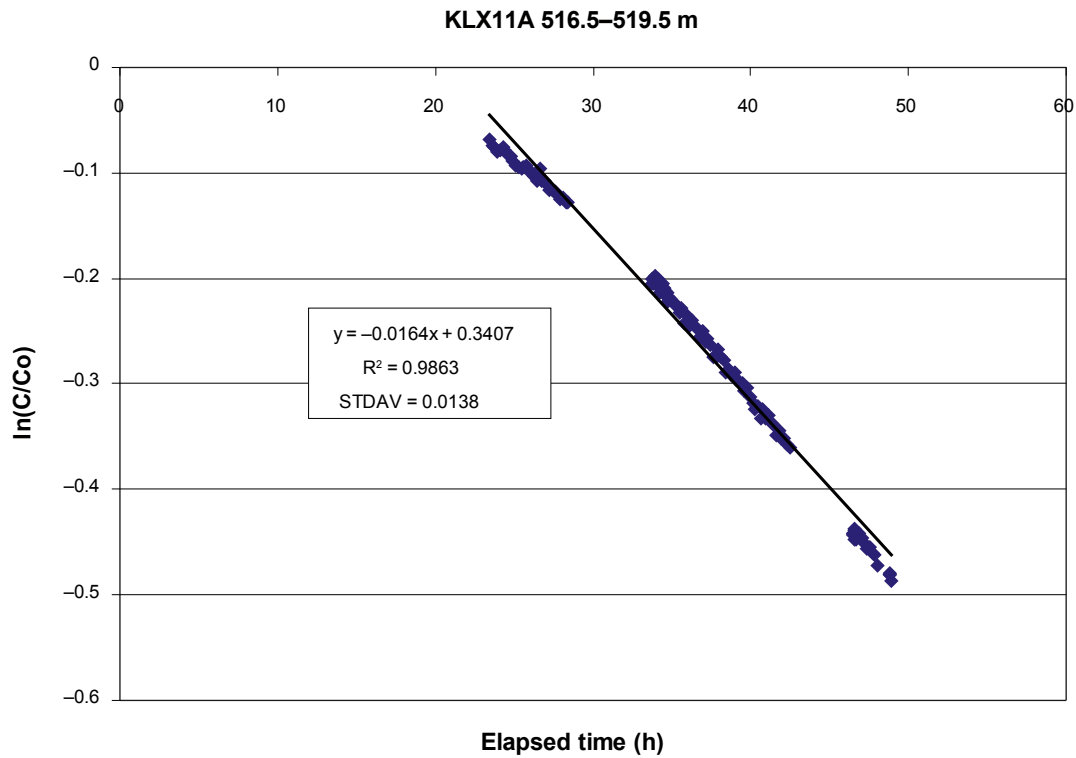


*Figure 5-11. Linear regression best fit to data from dilution measurement in borehole KLX11A, section 516.5–519.5 m.*

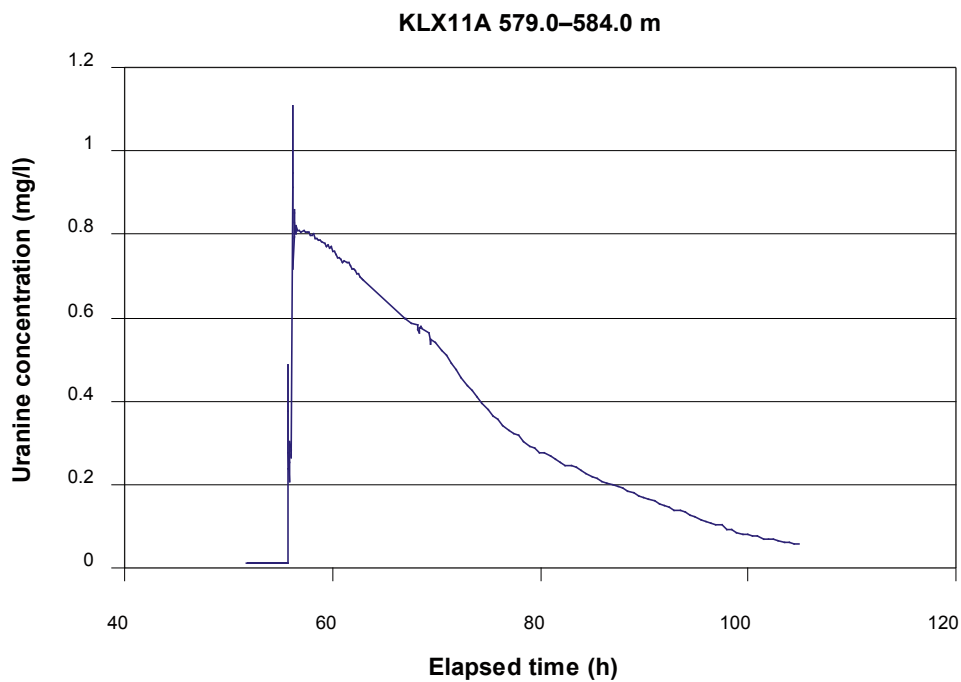


*Figure 5-12. Dilution measurement in borehole KLX11A, section 579.0–584.0 m. Uranine concentration versus time.*

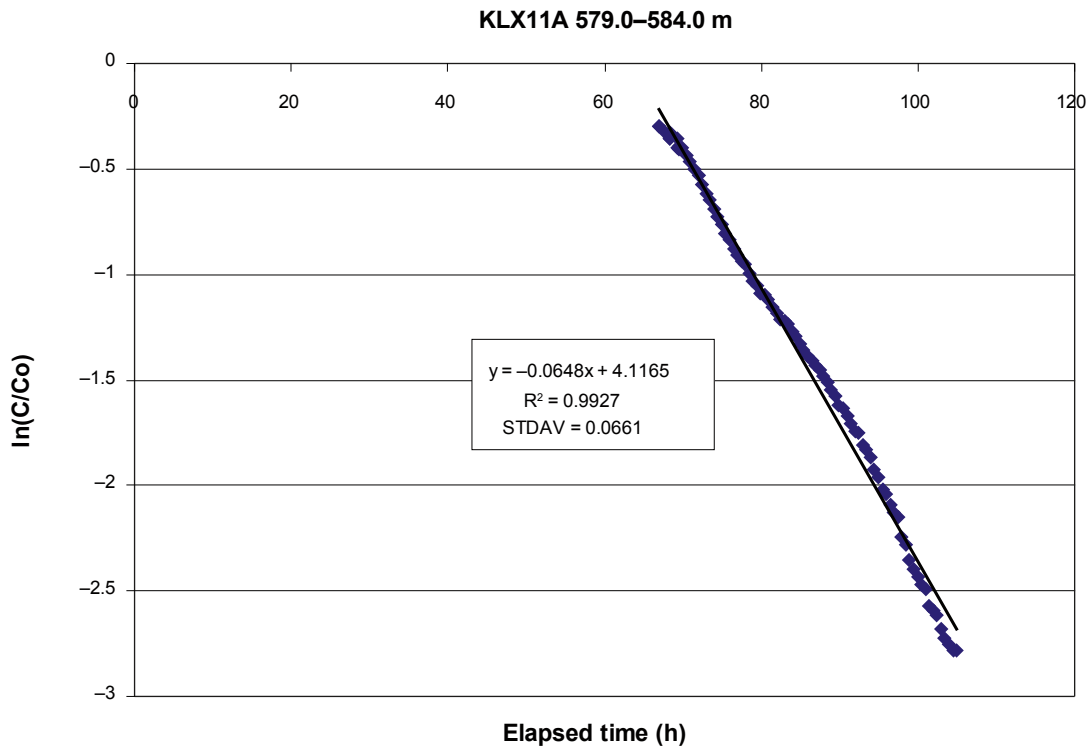


**Figure 5-13.** Linear regression best fit to data from dilution measurement in borehole KLX11A, section 579.0–584.0 m.

### 5.1.6 KLX11A, section 598.0–599.0 m

This dilution measurement was carried out with the dye tracer Uranine in a test section with two flowing fractures. The background measurement, tracer injection and dilution can be followed in Figure 5-14. Background concentration (0.01 mg/l) is measured for about 20 minutes with inflated packers. First the injection is executed at the erroneous borehole length. After adjusted position a new injection of Uranine is made. The background is assumed to be the same. The Uranine tracer is injected in three steps and after mixing it finally reaches an initial concentration of 0.98 mg/l above background. Dilution is measured for about 180 hours, thereafter pumping for water sampling for chemical analyses start. Hydraulic pressure is stable (Appendix B6). The groundwater flow is determined from the 235–355 hours part of the dilution measurement. The correlation coefficient of the best fit line is  $R^2 = 0.9911$  (Figure 5-15), and the groundwater flow rate, calculated from the best fit line, is 0.017 ml/min. The calculated hydraulic gradient is 0.014 and Darcy velocity  $1.9 \cdot 10^{-9}$  m/s.

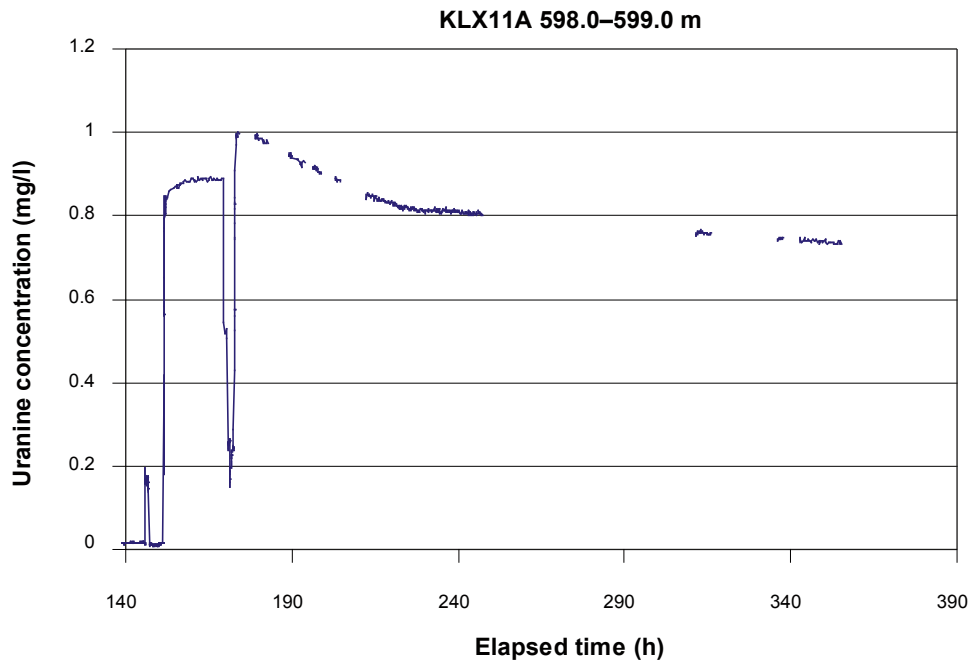


*Figure 5-14. Dilution measurement in borehole KLX11A, section 598.0–599.0 m. Uranine concentration versus time.*

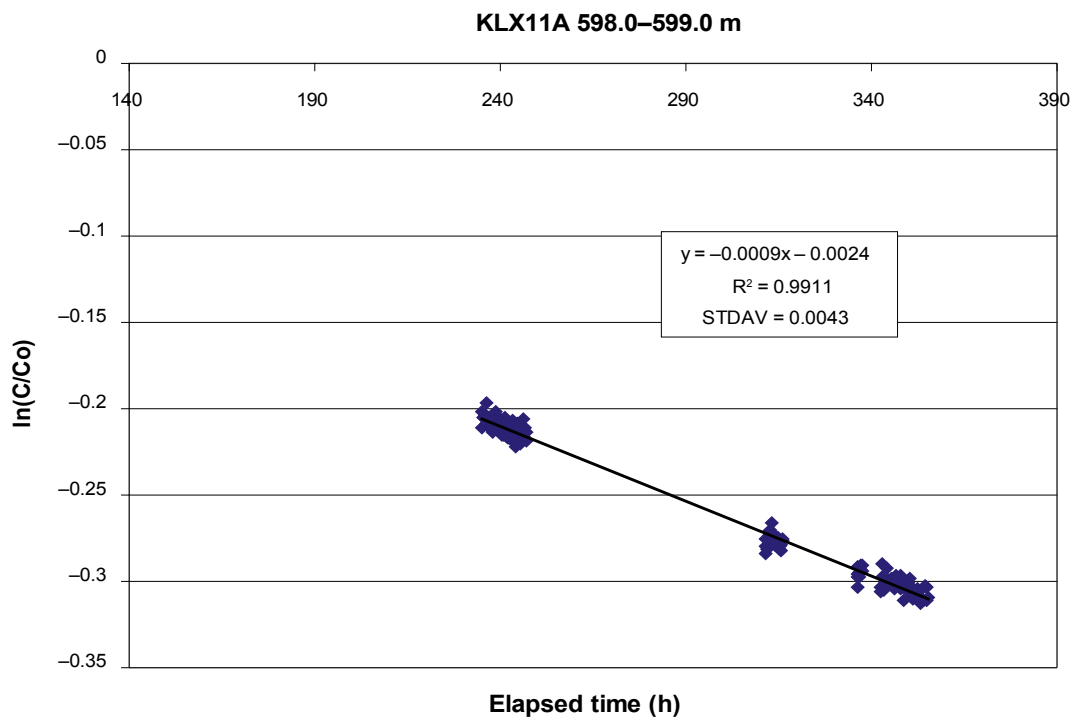


*Figure 5-15. Linear regression best fit to data from dilution measurement in borehole KLX11A, section 598.0–599.0 m.*

### 5.1.7 Summary of dilution results

Calculated groundwater flow rates, Darcy velocities and hydraulic gradients from all dilution measurements carried out in borehole KLX11A are presented in Table 5-1.

The results show that the groundwater flow varies during natural, i.e. undisturbed, conditions, with flow rates from 0.017 to 2.9 ml/min and Darcy velocities from  $1.9 \cdot 10^{-9}$  to  $6.3 \cdot 10^{-8}$  m/s. In this study no correlation were found between depth and flow rates or Darcy velocities. Both the highest and the lowest flow rate and Darcy velocity were measured in the deepest sections of the borehole. The highest at c. 579 m in deformation zone DZ13 and the lowest at c. 598 m in deformation zone DZ14 see Figures 5-16 and 5-17.

A correlation between flow rate and transmissivity is indicated in Figure 5-19, with the highest flow rates at high transmissivity. An exception is section 439.0–442.0 m (382–385 m vertical depth) where the flow rate is higher than the transmissivity indicates. Hydraulic gradients, calculated according to the Darcy concept, are large in the section at c. 439 m borehole length where no deformation zone is intersecting, see Figure 5-18. The transmissivity in this section is at the lower limit of the measurement range for the dilution probe which may decrease the accuracy of the determined groundwater flow rate, and thus also the calculated hydraulic gradient. The results from the Pipe String System at c. 439 m show no hydraulic connection to adjacent zones /Enachescu et al. 2006/. In the other measured sections the hydraulic gradient is within the expected range.

**Table 5-1. Groundwater flow rates, Darcy velocities and hydraulic gradients for all measured sections in borehole KLX11A.**

Borehole	Test section (m) <sup>*</sup>	Number of flowing fractures <sup>*</sup>	T (m <sup>2</sup> /s) <sup>*</sup>	Q (ml/min)	Q (m <sup>3</sup> /s)	Darcy velocity (m/s)	Hydraulic gradient
KLX11A	167.8–170.8 (148–151)	2	1.78E–05	0.25	4.2E–09	9.2E–09	0.002
KLX11A	306.0–309.0 (269–271)	3	1.04E–05	0.38	6.4E–09	1.4E–08	0.004
KLX11A	439.0–442.0 (382–385)	3	6.21E–08	0.18	3.0E–09	6.6E–09	0.320
KLX11A	516.5–519.5 (447–450)	2	3.39E–06	0.52	8.7E–09	1.9E–08	0.017
KLX11A	579.0–584.0 (499–502)	5	5.76E–06	2.88	4.8E–08	6.3E–08	0.055
KLX11A	598.0–599.0 (514–515)	2	1.35E–07	0.02	2.9E–10	1.9E–09	0.014

<sup>\*</sup> /Väisäsvaara et al. 2007/.

<sup>\*</sup> Test section vertical depth (m b s l) is given within brackets.

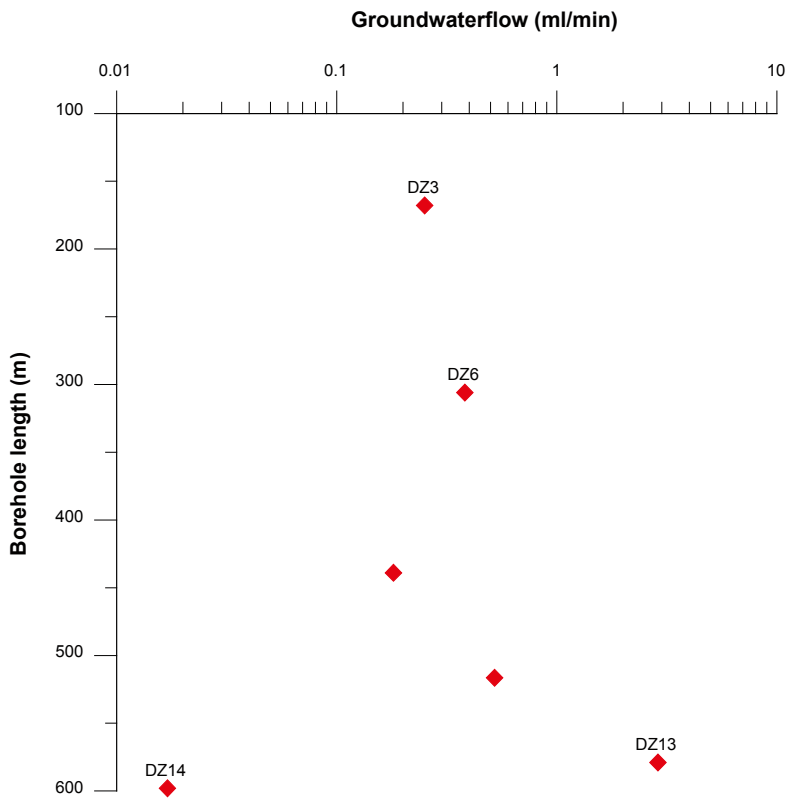


**Figure 5-16.** Groundwater flow rate versus borehole length during natural hydraulic gradient conditions. Results from dilution measurements in fracture zones in borehole KLX11A. Labels DZ3, DZ6, DZ13 and DZ14 refer to minor fracture zone notation /Carlsten et al. 2006/.

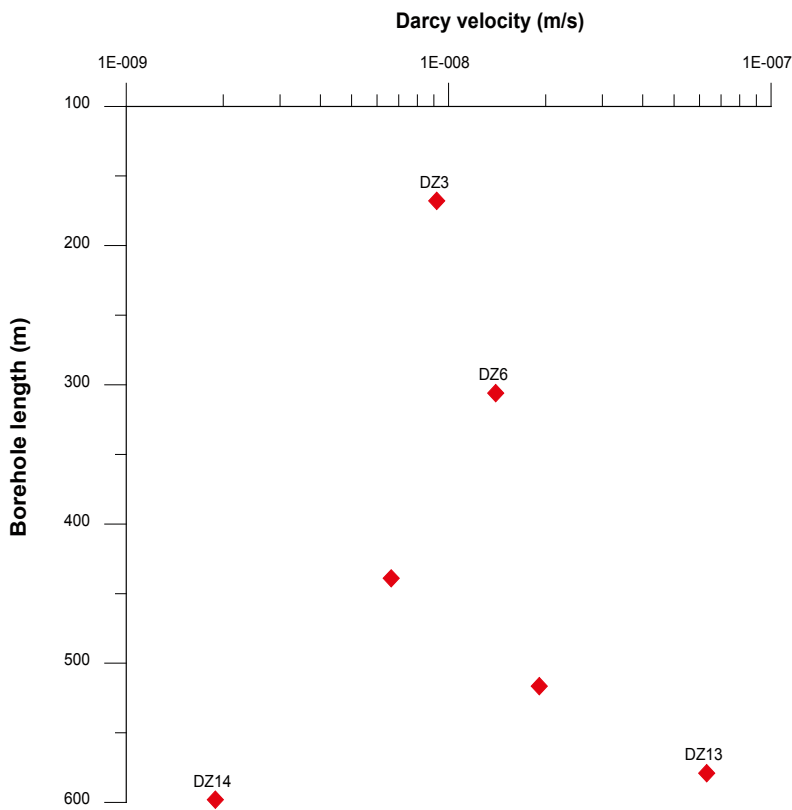


**Figure 5-17.** Darcy velocity versus borehole length during natural hydraulic gradient conditions. Results from dilution measurements in fracture zones in borehole KLX11A. Labels DZ3, DZ6, DZ13 and DZ14 refer to minor fracture zone notation /Carlsten et al. 2006/.

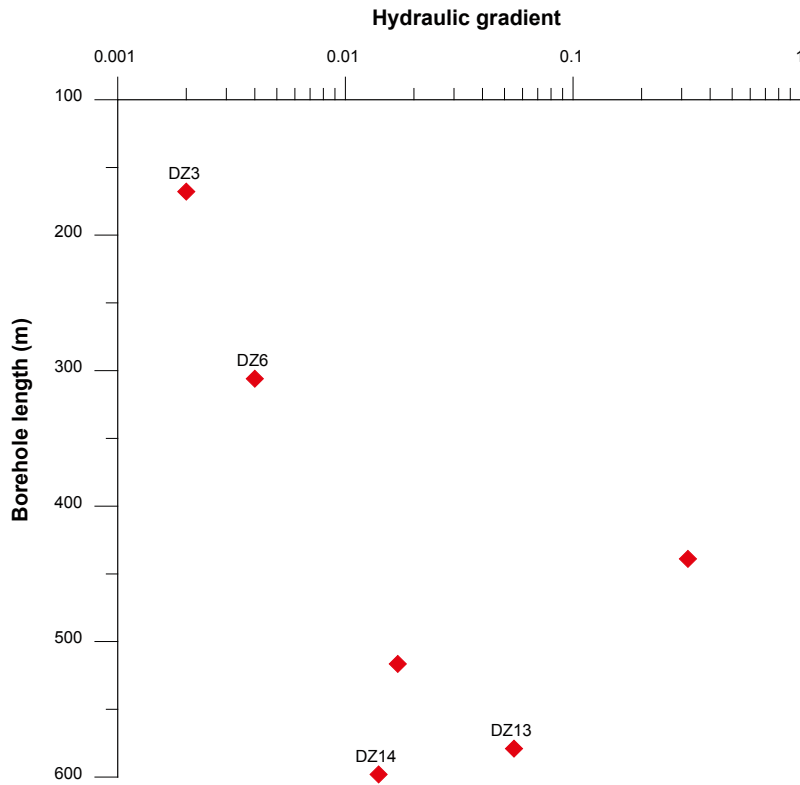


**Figure 5-18.** Hydraulic gradient versus borehole length during natural hydraulic gradient conditions, Results from dilution measurements in fracture zones in borehole KLX11A. Labels DZ3, DZ6, DZ13 and DZ14 refer to minor fracture zone notation /Carlsten et al. 2006/.

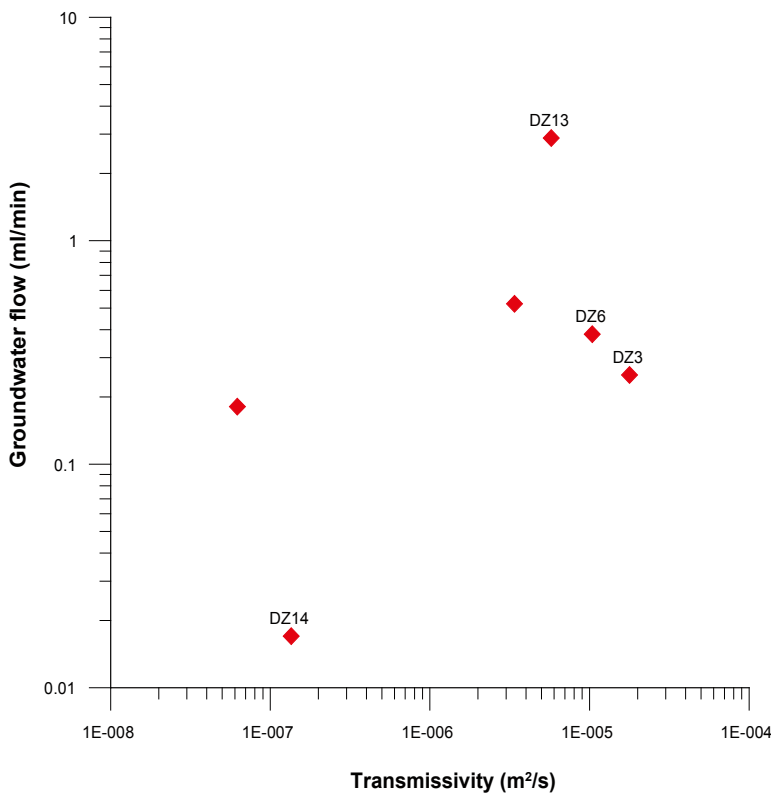


**Figure 5-19.** Groundwater flow rate versus transmissivity during undisturbed, i.e. natural hydraulic gradient conditions. Results from dilution measurements in fracture zones in borehole KLX11A. Labels DZ3, DZ6, DZ13 and DZ14 refer to minor fracture zone notation /Carlsten et al. 2006/.



## 5.2 SWIW tests

### 5.2.1 Treatment of experimental data

The experimental data presented in this section have been corrected for background concentrations. Sampling times have been adjusted to account for residence times in injection and sampling tubing. Thus, time zero in all plots refers to when the fluid containing the tracer mixture begins to enter the tested borehole section.

### 5.2.2 Tracer recovery breakthrough in KLX11A, 516.5–519.5 m

Durations and flows for the various experimental phases are summarised in Table 5-2. Injected mass and initial concentration in the section for the three tracers are given in Table 5-3. Initial concentration,  $C_0$  is the tracer-concentration at the beginning of the dilution, the injected concentration minus the background in the section.

The experimental breakthrough curves from the recovery phase for Uranine, cesium and rubidium respectively, are shown in Figures 5-20a to 5-20c. The time coordinates are corrected for residence time in the tubing, as described above, and concentrations are normalised through division by the total injected tracer mass.

Normalised breakthrough curves (concentration divided by total injected tracer mass) for all three tracers are plotted in Figure 5-21. The figure shows that the tracers behave in different ways, presumably caused by different sorption properties. The breakthrough curves approximately conform to what would be expected from a SWIW test using tracers of different sorption properties. The considerable difference between Uranine and the two other curves may also be seen as an indication of a strong sorption effect for cesium and rubidium. The figure indicates similar tracer behaviour as in previously performed SWIW tests within the site investigation programmes, /Gustafsson and Nordqvist 2005, Gustafsson et al. 2005, 2006ab, Thur et al. 2006, 2007/.

Tracer recovery based on available experimental data result in values of 98% for Uranine, 45% for cesium and 43% for rubidium. These estimates are based on the average pumping flow rate during the recovery phase. Plausible visual extrapolations of the curves do not clearly indicate incomplete recovery and that the tracer recovery would be different among the three tracers. Thus, for the subsequent model evaluation, it is assumed that tracer recovery is the same for all of the tracers.

**Table 5-2. Durations (h) and fluid flows (L/h) during various experimental phases for section 516.5–519.5 m in borehole KLX11A. All times have been corrected for tubing residence time such that time zero refers to the time when the tracer mixture begins to enter the borehole section.**

Phase	Start (h)	Stop (h)	Volume (L)	Average flow (L/h)	Cumulative injected volume (L)
Pre-injection	-1.36	0.00	24.8	18.2	24.8
Tracer injection	0.00	0.86	16.0	18.6	40.8
Chaser injection	0.86	5.45	82.5	18.0	123.3
Recovery	5.45	163.14	2,834	18.2	

**Table 5-3. Injected mass (mg) and initial concentration (mg/l) for section 516.5–519.5 m in borehole KLX11A.**

Tracer	Injected mass (mg)	Initial concentration (mg/l)
Uranine	950	61.3
Cesium	639	41.3
Rubidium	1,515	97.7

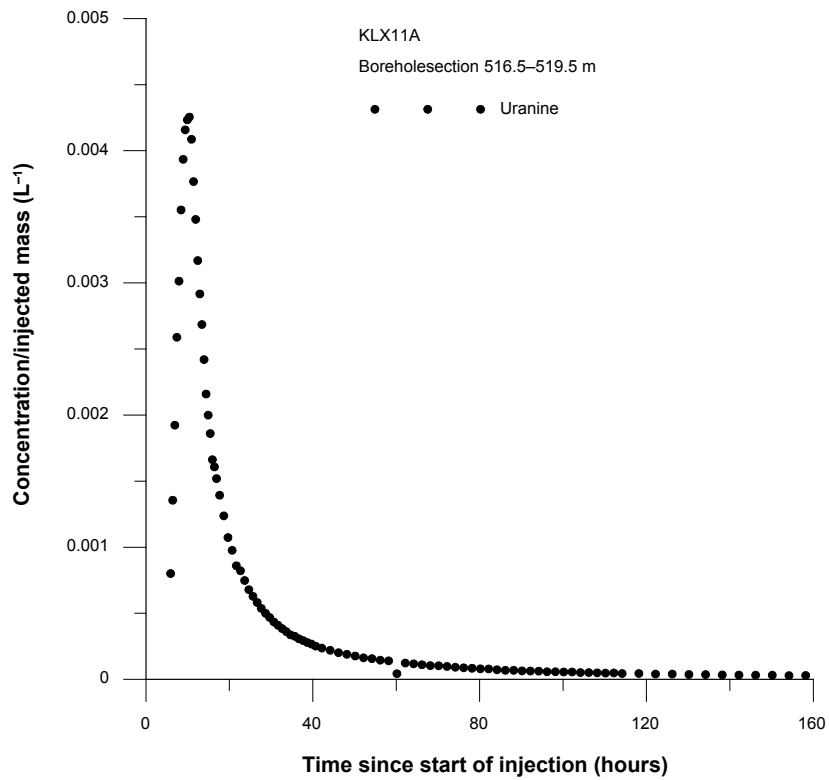


Figure 5-20a. Normalised withdrawal (recovery) phase breakthrough curve for Uranine in section 516.5–519.5 m in borehole KLX11A.

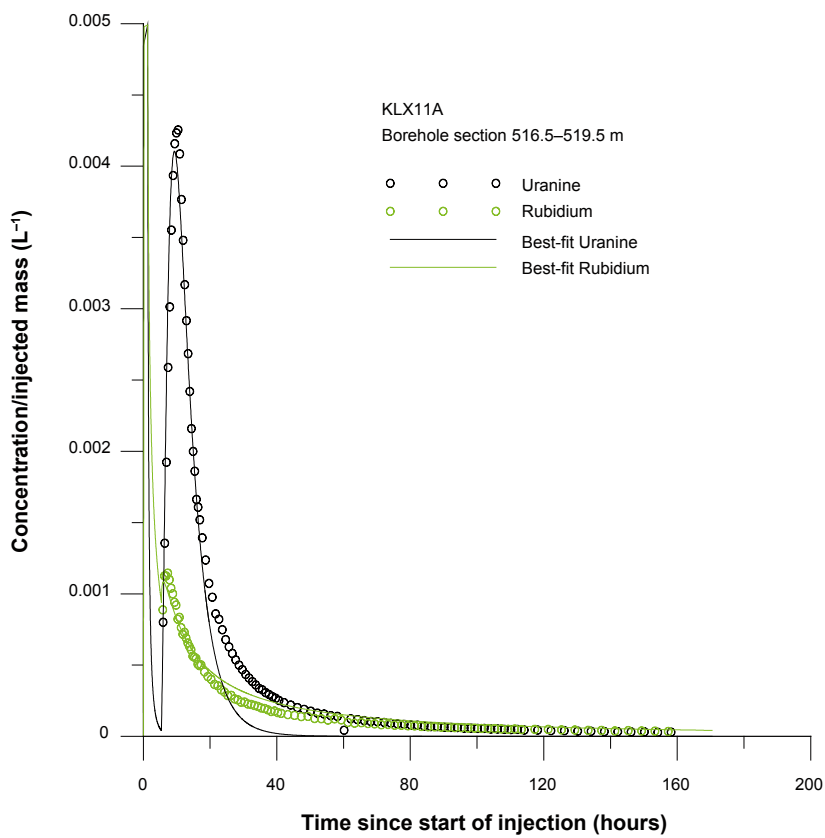
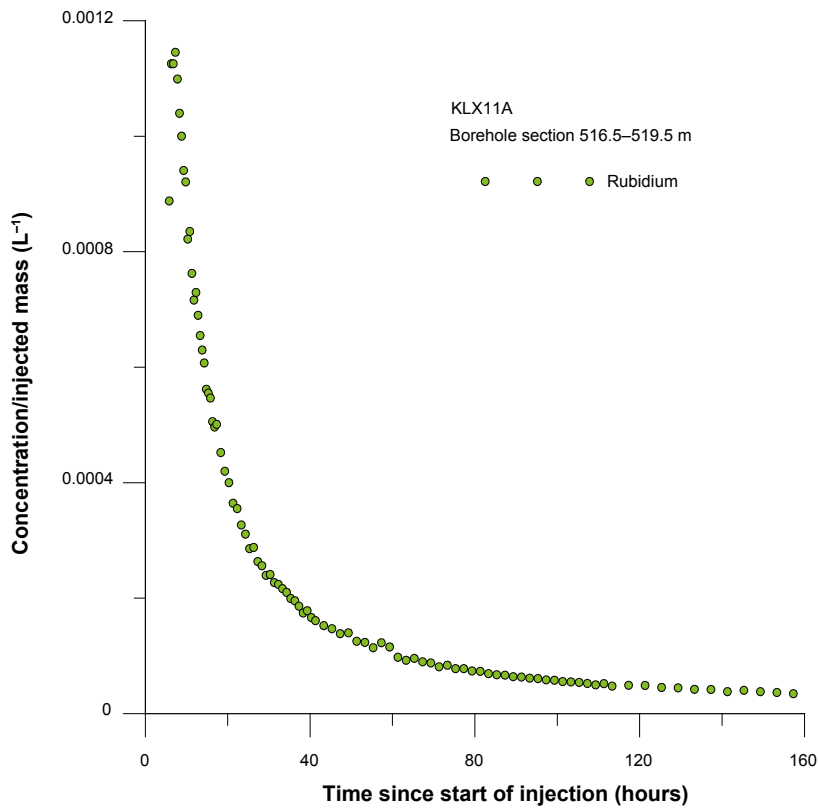
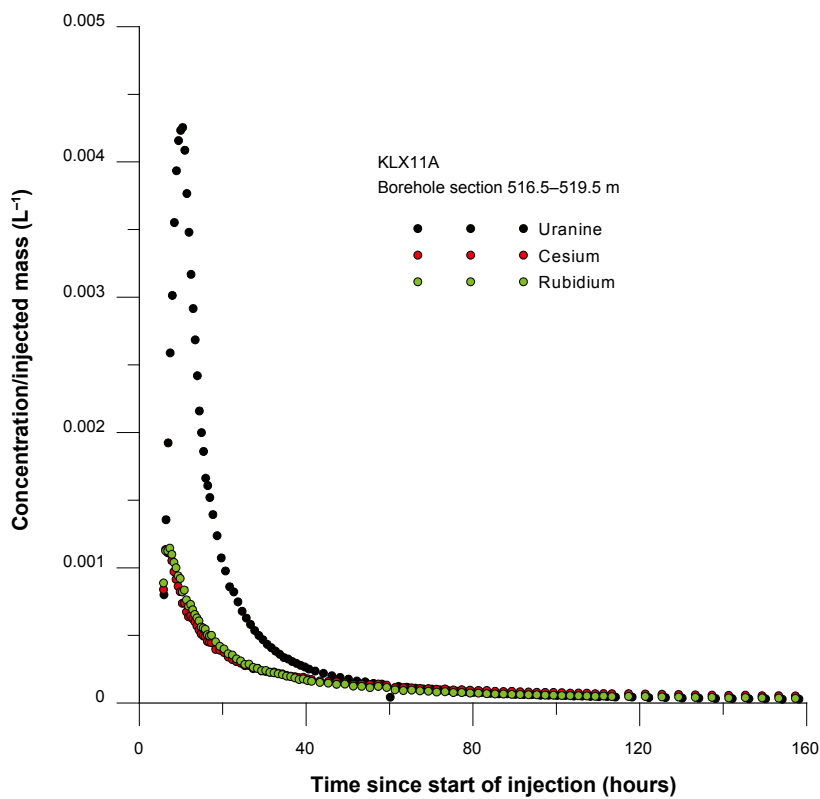


Figure 5-20b. Normalised withdrawal (recovery) phase breakthrough curve for cesium in section 516.5–519.5 m in borehole KLX11A.



*Figure 5-20c. Normalised withdrawal (recovery) phase breakthrough curve for rubidium in section 516.5–519.5 m in borehole KLX11A.*



*Figure 5-21. Normalised withdrawal (recovery) phase breakthrough curves for Uranine, cesium and rubidium in section 516.5–519.5 m.*

### 5.2.3 Model evaluation KLX11A, 516.5–519.5 m

The model simulations were carried out assuming negligible hydraulic background gradient, i.e. radial flow. From the dilution measurements, the ambient flow through the borehole section was estimated at about 0.52 ml/min, see Table 5-1. The simulated times and flows for the various experimental phases are given in Table 5-2. This borehole section is interpreted to consist of two flowing fractures, see Table 5-1. In the simulation model, the flow zone is approximated by a 0.1 m thick fracture zone.

The experimental evaluation was carried out by simultaneous model fitting of Uranine and a sorbing tracer as outlined in Section 4.4. Separate regression analyses were carried out for simultaneous fitting of Uranine/cesium and Uranine/rubidium, respectively.

For a given regression run, estimation parameters were longitudinal dispersivity ( $\alpha_L$ ) and a linear retardation factor (R), while the porosity is given a fixed value. Regression was carried out for five different values of porosity: 0.002, 0.005, 0.01, 0.02 and 0.05. For all cases, the fits between model and experimental data are similar. Example of model fits are shown in Figure 5-22a and Figure 5-22b.

The model fits to the experimental breakthrough curves are generally fairly good, especially for the sorbing tracers cesium and rubidium, respectively. The main discrepancy is observed for the tailing part of the Uranine curve, where the simulated curve levels out to background values faster than the experimental curve.

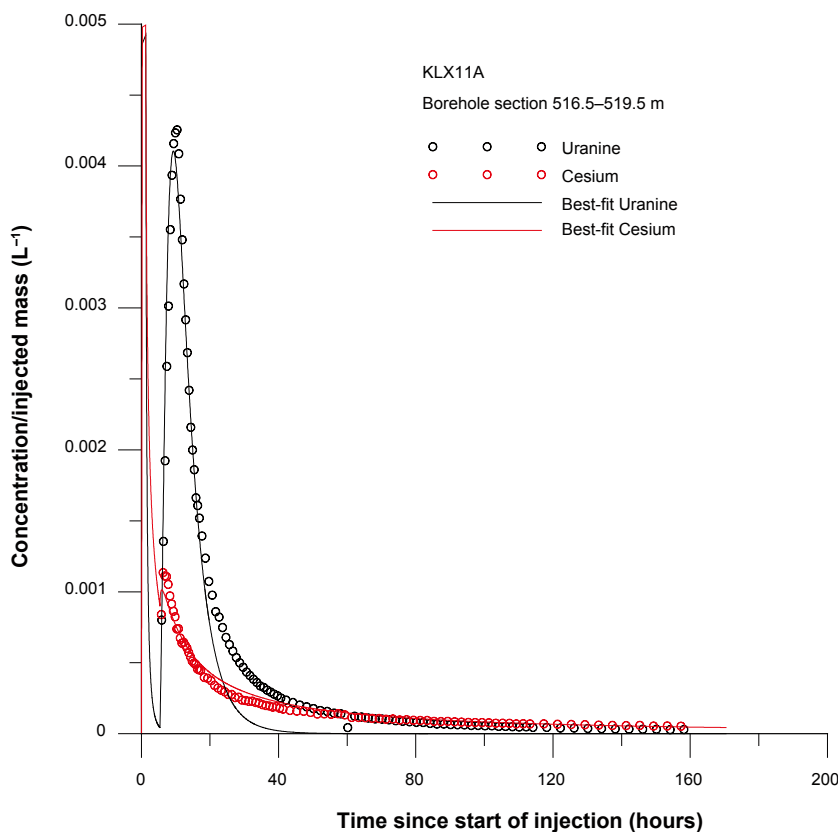


*Figure 5-22a. Example of simultaneous fitting of Uranine and cesium for section 516.5–519.5 m in borehole KLX11A. All observation data are given equal regression weights.*

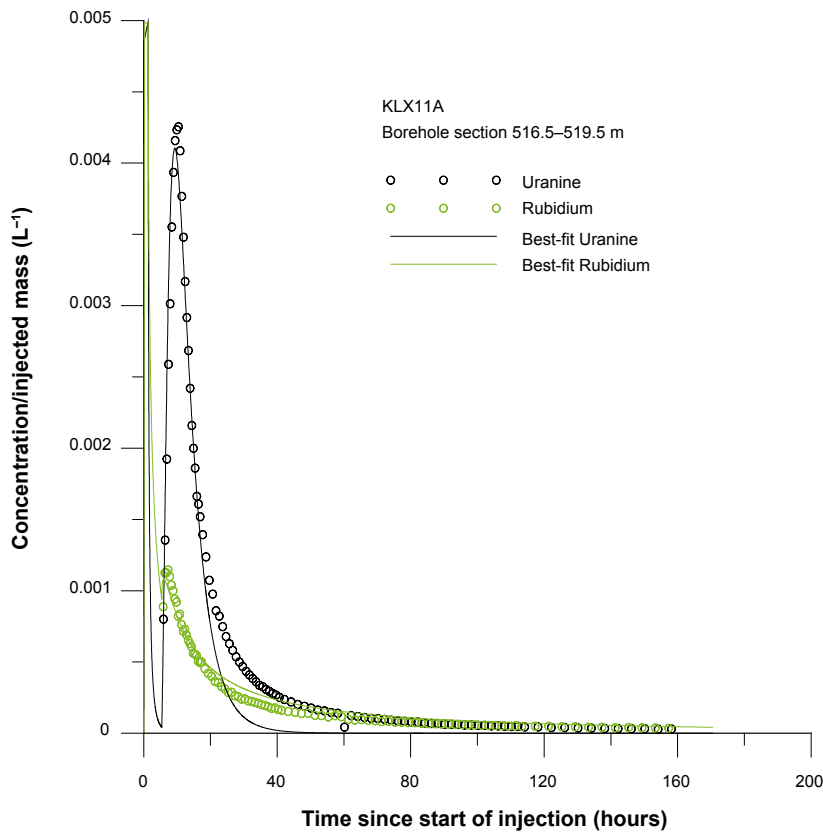


**Figure 5-22b.** Example of simultaneous fitting of Uranine and rubidium for section 516.5–519.5 m in borehole KLX11A. All observation data are given equal regression weights.

All of the regression runs (Tables 5-4a and 5-4b) resulted in similar values of the retardation coefficient for each sorbing tracer, while the estimated values of the longitudinal dispersivity are strongly dependent on the assumed porosity value. Both of these observations are consistent with prior expectations of the relationships between parameters in a SWIW test /Nordqvist and Gustafsson 2002/.

The estimated values of R for cesium (765–820) and rubidium (594–630) indicate very strong sorption effects which, agrees approximately with values from previous SWIW tests as well as earlier cross-hole tests. Estimated values of R for rubidium are lower than for cesium, although one may consider the values being of similar magnitudes.

**Table 5-4a. Results of simultaneous fitting of Uranine and cesium for section 516.5–519.5 m in borehole KLX11A. Approximate values of the coefficient of variation (estimation standard error divided by the estimated value) are given within parenthesis.**

Porosity (fixed)	$a_L$ (estimated)	R (estimated)
0.002	1.48 (0.04)	820 (0.16)
0.005	0.94 (0.04)	815 (0.16)
0.01	0.66 (0.04)	808 (0.16)
0.02	0.47 (0.04)	796 (0.16)
0.05	0.30 (0.04)	765 (0.15)

**Table 5-4b. Results of simultaneous fitting of Uranine and rubidium for section 516.5–519.5 m in borehole KLX11A. Approximate values of the coefficient of variation (estimation standard error divided by the estimated value) are given within parenthesis.**

Porosity (fixed)	$a_L$ (estimated)	R (estimated)
0.002	1.48 (0.04)	630 (0.15)
0.005	0.94 (0.04)	627 (0.15)
0.01	0.66 (0.04)	622 (0.15)
0.02	0.47 (0.04)	614 (0.15)
0.05	0.30 (0.04)	594 (0.15)

#### 5.2.4 Tracer recovery breakthrough in KLX11A, 598.0–599.0 m

Durations and flows for the various experimental phases are summarised in Table 5-5. Injected mass and initial concentration in the section for the three tracers are given in Table 5-6. Initial concentration,  $C_0$  is the tracer-concentration at the beginning of the dilution, the injected concentration minus the background in the section.

The experimental breakthrough curves from the recovery phase for Uranine, cesium and rubidium respectively, are shown in Figures 5-23a to 5-23c. The time coordinates are corrected for residence time in the tubing, as described above, and concentrations are normalised through division by the total injected tracer mass.

Normalised breakthrough curves (concentration divided by total injected tracer mass) for all three tracers are plotted in Figure 5-24. The considerable difference between Uranine and the two other curves may be seen as an indication of a relatively strong retardation effect for cesium and rubidium. The breakthrough curves approximately conform to what would be expected from a SWIW test using tracers of different sorption properties. The figure indicates similar tracer behaviour as in previously performed SWIW tests within the site investigation programmes, /Gustafsson and Nordqvist 2005, Gustafsson et al. 2005, 2006ab, Thur et al. 2006, 2007/.

**Table 5-5. Durations (h) and fluid flows (L/h) during various experimental phases for section 598.0–599.0 m in borehole KLX11A. All times have been corrected for tubing residence time such that time zero refers to the time when the tracer mixture begins to enter the borehole section.**

Phase	Start (h)	Stop (h)	Volume (L)	Average flow (L/h)	Cumulative injected volume (L)
Pre-injection	-6.76	0.00	17.9	2.6	17.9
Tracer injection	0.00	0.80	7.4	9.2	25.3
Chaser injection	0.80	9.90	87.9	9.7	113.2
Recovery	11.73	277.71	2,403	9.4	

**Table 5-6. Injected mass (mg) and initial concentration (mg/l) for section 598.0–599.0 m in borehole KLX11A.**

Tracer	Injected mass (mg)	Initial concentration (mg/l)
Uranine	942	122.3
Cesium	697	90.5
Rubidium	1,610	209.1

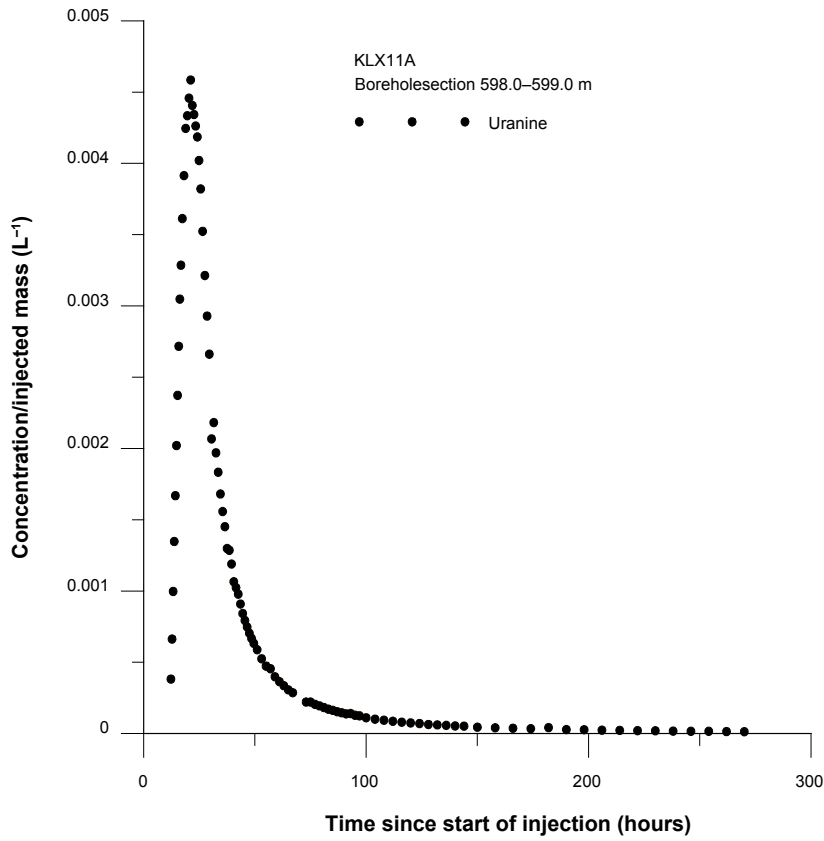


**Figure 5-23a.** Normalised withdrawal (recovery) phase breakthrough curve for Uranine in section 598.0–599.0 m in borehole KLX11A.

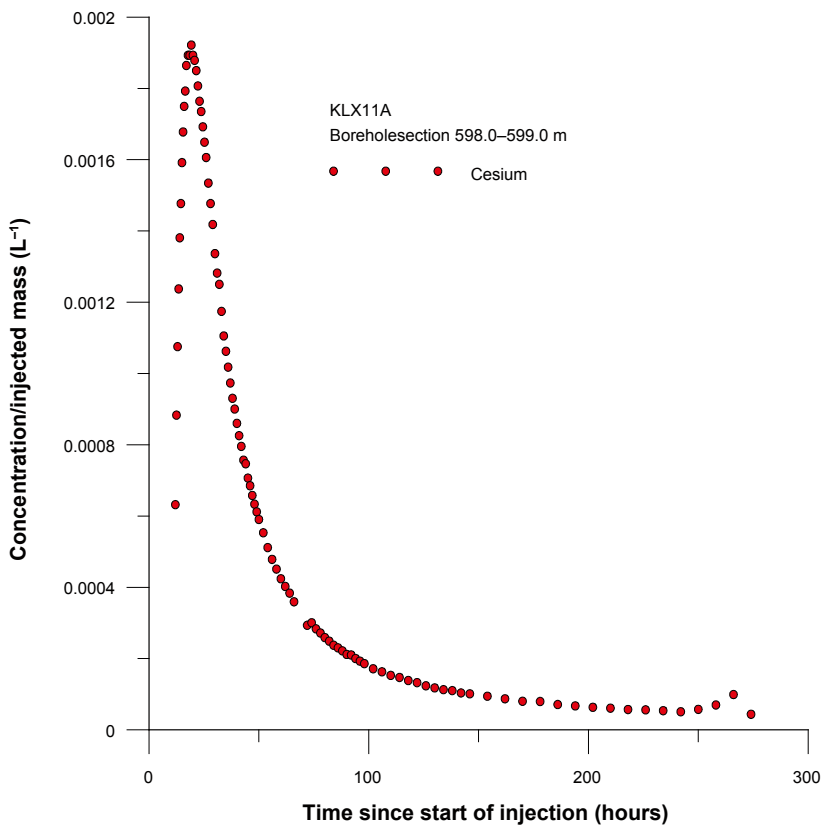


**Figure 5-23b.** Normalised withdrawal (recovery) phase breakthrough curve for cesium in section 598.0–599.0 m in borehole KLX11A.

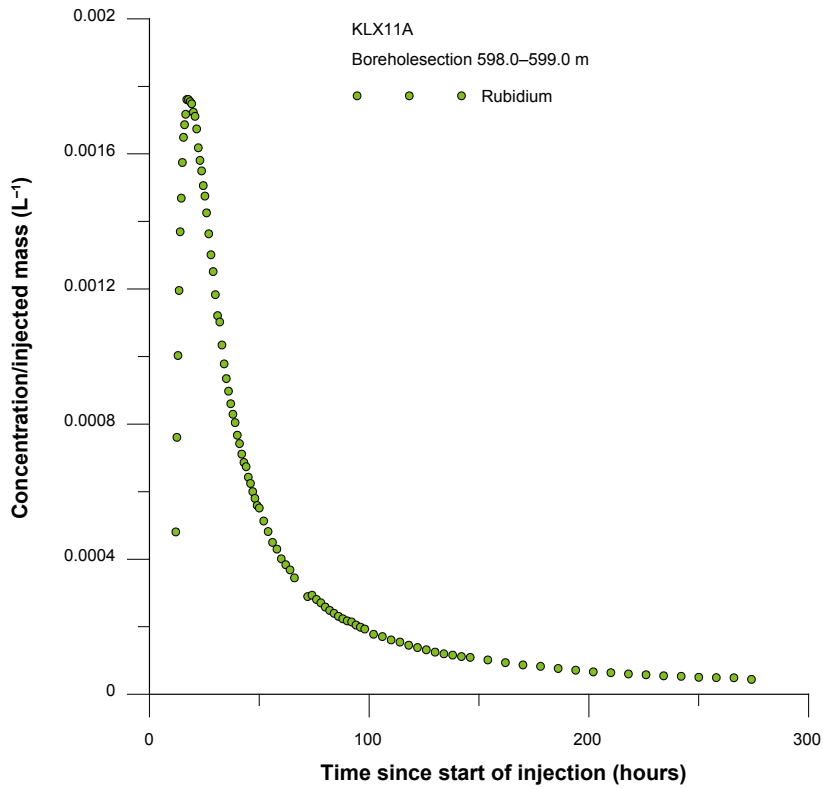


**Figure 5-23c.** Normalised withdrawal (recovery) phase breakthrough curve for rubidium in section 598.0–599.0 m in borehole KLX11A.

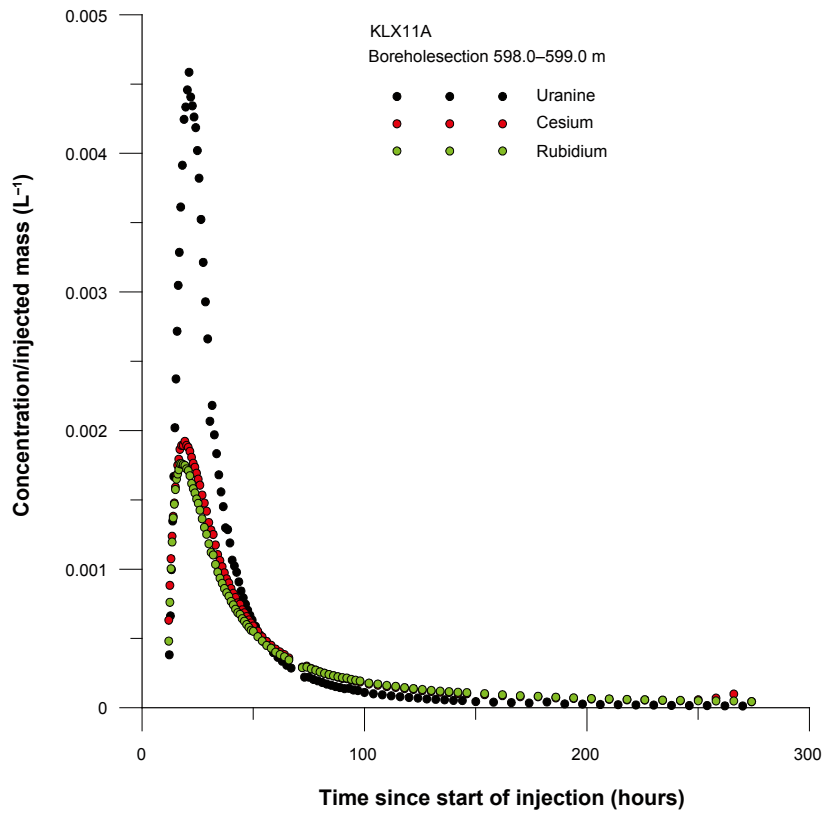


**Figure 5-24.** Normalised withdrawal (recovery) phase breakthrough curves for Uranine, cesium and rubidium in section 598.0–599.05 m.



Tracer recovery based on available experimental data result in values of 95% for Uranine, 72% for cesium and 68% for rubidium. These estimates are based on the average pumping flow rate during the recovery phase. Plausible visual extrapolations of the curves do not clearly indicate incomplete recovery and that the tracer recovery would be different among the three tracers. Thus, for the subsequent model evaluation, it is assumed that tracer recovery is the same for all of the tracers.

### 5.2.5 Model evaluation KLX11A, 598.0–599.0 m

The model simulations were carried out assuming negligible hydraulic background gradient, i.e. radial flow. From the dilution measurements, the ambient flow through the borehole section was estimated at about 0.017 ml/min, see Table 5-1. The simulated times and flows for the various experimental phases are given in Table 5-5. This borehole section is interpreted to consist of two flowing fractures, see Table 5-1. In the simulation model, the flow zone is approximated by a 0.1 m thick fracture zone.

The experimental evaluation was carried out by simultaneous model fitting of Uranine and a sorbing tracer as outlined in Section 4.4. Separate regression analyses were carried out for simultaneous fitting of Uranine/cesium and Uranine/rubidium, respectively.

For a given regression run, estimation parameters were longitudinal dispersivity ( $\alpha_L$ ) and a linear retardation factor (R), while the porosity is given a fixed value. Regression was carried out for five different values of porosity: 0.002, 0.005, 0.01, 0.02 and 0.05. For all cases, the fits between model and experimental data are similar. Example of model fits are shown in Figure 5-25a and Figure 5-25b.

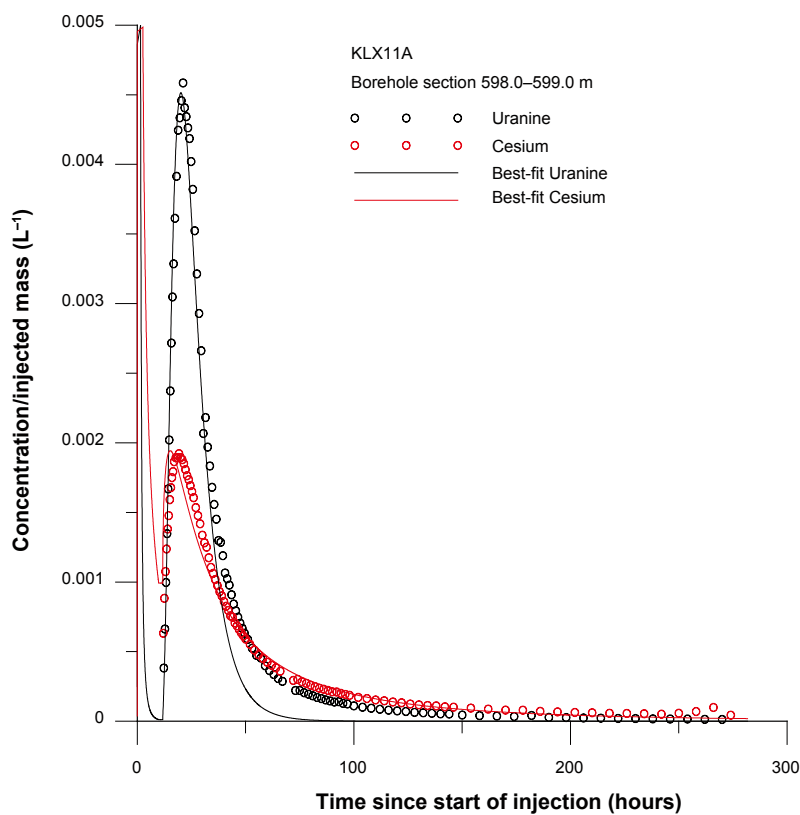


**Figure 5-25a.** Example of simultaneous fitting of Uranine and cesium for section 598.0–599.0 m in borehole KLX11A. All observation data are given equal regression weights.

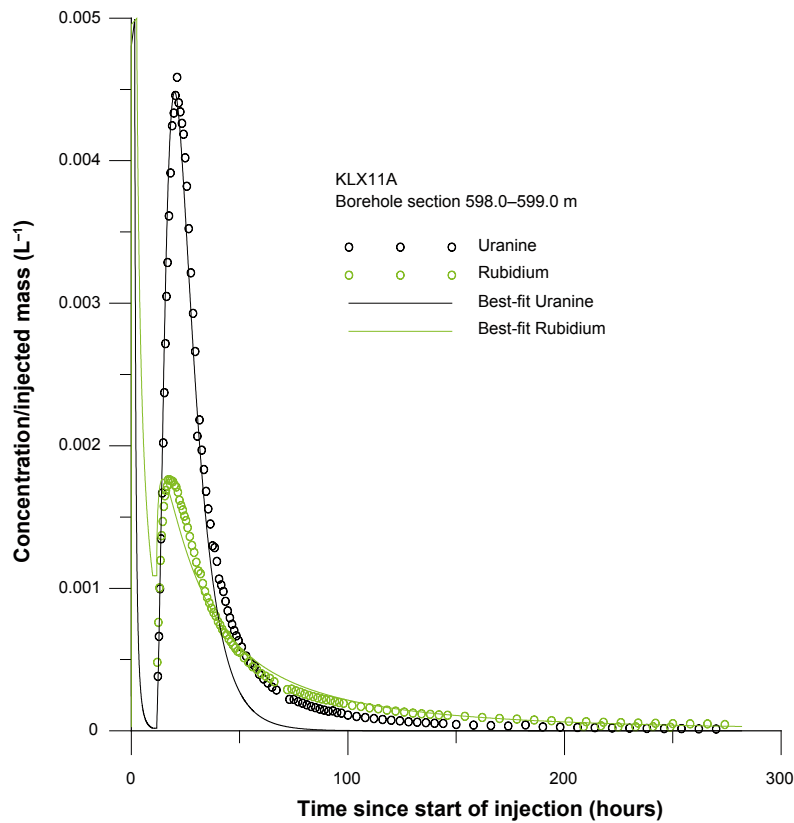


**Figure 5-25b.** Example of simultaneous fitting of Uranine and rubidium for section 598.0–599.0 m in borehole KLX11A. All observation data are given equal regression weights.

The model fits to the experimental breakthrough curves are generally fairly good, especially for the sorbing tracers cesium and rubidium, respectively. The main discrepancy is observed for the tailing part of the Uranine curve, where the simulated curve levels out to background values faster than the experimental curve.

All of the regression runs (Tables 5-7a and 5-7b) resulted in similar values of the retardation coefficient for each sorbing tracer, while the estimated values of the longitudinal dispersivity are strongly dependent on the assumed porosity value. Both of these observations are consistent with prior expectations of the relationships between parameters in a SWIW test /Nordqvist and Gustafsson 2002/.

The estimated values of  $R$  for cesium (65–66) and rubidium (103–105) indicate strong sorption effects, and agrees approximately with values from cross-hole tests, obtained using similar transport models (advection-dispersion and linear sorption). However, in this test estimated values of  $R$  for both cesium and rubidium are lower than in previous SWIW tests in the area. As a comparison, the mean values of  $R$  in KLX03 are 235 for cesium and 391 for rubidium, /Gustafsson et al. 2006a/ and in KLX18A 529 for cesium and 2,661 for rubidium /Thur et al. 2006/.

**Table 5-7a. Results of simultaneous fitting of Uranine and cesium for section 598.0–599.0 m in borehole KLX11A. Approximate values of the coefficient of variation (estimation standard error divided by the estimated value) are given within parenthesis.**

<b>Porosity (fixed)</b>	<b>a<sub>L</sub> (estimated)</b>	<b>R (estimated)</b>
0.002	1.25 (0.04)	66 (0.13)
0.005	0.79 (0.04)	66 (0.13)
0.01	0.56 (0.04)	66 (0.13)
0.02	0.40 (0.04)	66 (0.13)
0.05	0.25 (0.04)	65 (0.13)

**Table 5-7b. Results of simultaneous fitting of Uranine and rubidium for section 598.0–599.0 m in borehole KLX11A. Approximate values of the coefficient of variation (estimation standard error divided by the estimated value) are given within parenthesis.**

<b>Porosity (fixed)</b>	<b>a<sub>L</sub> (estimated)</b>	<b>R (estimated)</b>
0.002	1.26 (0.04)	105 (0.13)
0.005	0.80 (0.04)	105 (0.13)
0.01	0.56 (0.04)	105 (0.13)
0.02	0.40 (0.04)	104 (0.13)
0.05	0.25 (0.04)	103 (0.13)

## 6 Discussion and conclusions

The dilution measurements were carried out in selected fracture zones in borehole KLX11A at levels from c. 168 to 598 m borehole length (148 to 514 m vertical depth), where hydraulic transmissivity ranged within  $T = 6.2 \cdot 10^{-8}$ – $1.8 \cdot 10^{-5}$  m<sup>2</sup>/s. The borehole intersects some minor local deformation zones that are identified by SKB's single hole interpretation (SHI) of cored boreholes as seen in Table 6-1 /Carlsten et al. 2006/. The borehole is totally dominated by quartz monzodiorite, denoted RU1.

The results of the dilution measurements in borehole KLX11A show that the groundwater flow varies considerably during natural conditions, with flow rates from 0.02 to 2.88 ml/min and Darcy velocities from  $1.9 \cdot 10^{-9}$  to  $6.3 \cdot 10^{-8}$  m/s ( $1.6 \cdot 10^{-4}$ – $5.4 \cdot 10^{-3}$  m/d). These results are in accordance with previous dilution measurements carried out in boreholes KSH02, KLX02, KLX03 and KLX18A. In these boreholes hydraulic transmissivity in the test sections was within  $T = 1.3 \cdot 10^{-8}$ – $1.3 \cdot 10^{-5}$  m<sup>2</sup>/s and flow rate ranged from 0.02–4.2 ml/min and Darcy velocity from  $9.3 \cdot 10^{-10}$  till  $1.2 \cdot 10^{-7}$  m/s ( $8.0 \cdot 10^{-5}$ – $1.0 \cdot 10^{-2}$  m/d) /Gustafsson and Nordqvist 2005, Gustafsson et al. 2006a, Thur et al. 2006/.

Groundwater flow rates and Darcy velocities calculated from dilution measurements in borehole KLX11A are also within the range that can be expected based on experience from previously preformed dilution measurements under natural gradient conditions at other sites in Swedish crystalline rock /Gustafsson and Andersson 1991, Gustafsson and Morosini 2002, Gustafsson and Nordqvist 2005, Gustafsson et al. 2005, 2006ab, Thur et al. 2006, 2007/.

**Table 6-1. Intersected zones, groundwater flow rates, Darcy velocities and hydraulic gradients for all measured sections in boreholes KLX11A.**

Borehole	Test section (m)*	Rock types and Zones**	No of flowing fractures*	T (m <sup>2</sup> /s)*	Q (ml/min)	Q (m <sup>3</sup> /s)	Darcy velocity (m/s)	Hydraulic gradient
KLX11A	167.8–170.8 (148–151)	quartz monzodiorite DZ3	2	1.78E–05	0.25	4.2E–09	9.2E–09	0.002
KLX11A	306.0–309.0 (269–271)	quartz monzodiorite DZ6	3	1.04E–05	0.38	6.4E–09	1.4E–08	0.004
KLX11A	439.0–442.0 (382–385)	quartz monzodiorite	3	6.21E–08	0.18	3.0E–09	6.6E–09	0.320
KLX11A	516.5–519.5 (447–450)	quartz monzodiorite	2	3.39E–06	0.52	8.7E–09	1.9E–08	0.017
KLX11A	579.0–584.0 (499–502)	quartz monzodiorite DZ13	5	5.76E–06	2.88	4.8E–08	6.3E–08	0.055
KLX11A	598.0–599.0 (514–515)	quartz monzodiorite DZ14	2	1.35E–07	0.02	2.9E–10	1.9E–09	0.014

\* /Väisäsvaara et al. 2007/.

\*\* /Carlsten et al. 2006/.

\* Test section vertical depth (m b s l) is given within brackets.

In KLX11A the highest and the lowest flow rate and Darcy velocity is measured in the deepest sections of the borehole. The determined groundwater flow rates are fairly proportional to the hydraulic transmissivity, although the statistical basis is weak. No correlation is notable between borehole length, i.e. depth and flow rate or Darcy velocity.

Hydraulic gradients in KLX11A, calculated according to the Darcy concept, are within the expected range (0.001–0.05) in five out of six measured test sections. In the section at c. 439 m borehole length (382 m vertical depth) the hydraulic gradient is considered to be large. Local effects where the measured fractures constitute a hydraulic conductor between other fractures with different hydraulic heads or wrong estimation of the correction factor,  $\alpha$ , and/or the hydraulic conductivity of the fracture could explain the large hydraulic gradient.

The SWIW tests in section 516.5–519.5 and 598.0–599.0 m borehole lengths resulted in high-quality tracer breakthrough data. Experimental conditions (flows, times, events, etc) are well known and documented, as well as borehole geological conditions with BIPS logging (Appendix C). Together they provide a good basis for possible further evaluation.

The results show relatively smooth breakthrough curves. The most significant result is that there is a very clear effect of retardation/sorption of cesium and rubidium.

The model evaluation was made using a radial flow model with advection, dispersion and linear equilibrium sorption as transport processes. It is important that experimental conditions (times, flows, injection concentration, etc) are incorporated accurately in the simulations. The evaluation carried out may be regarded as a typical preliminary approach for evaluation of a SWIW test where sorbing tracers are used. Background flows were in this case assumed to be insignificant. However, in sections such as the one between 516.5–519.5 m, the dilution measurements indicate relatively high natural flow in this section and it may not be excluded that the natural flow can influence the recovery breakthrough curves.

The estimated values of the retardation factor for cesium (about 800) and rubidium (about 620) in section 516.5–519.5 m indicates strong sorption. In section 598.0–599.0 the sorption is weaker, R for cesium is about 66 and for rubidium about 104. A somewhat un-expected result is that rubidium shows stronger sorption than cesium in section 598.0–599.0 m, in reverse to the theory /Andersson et al. 2002/. Rubidium was introduced as a tracer of lower sorption capacity than cesium.

It should also be pointed out that the lack of model fit in the tailing parts of the curves (most visible for Uranine) appears to be a consistent feature in the SWIW tests performed so far /Gustafsson and Nordqvist 2005, Gustafsson et al. 2005, 2006ab, Thur et al. 2006, 2007/. Thus, there seems to be some generally occurring process that has not yet been identified, but is currently believed to be an effect of the tested medium and not an experimental artefact. Studies to identify possible causes for the observed discrepancy are ongoing.

## 7 References

- Andersson P, 1995.** Compilation of tracer tests in fractured rock. SKB PR 25-95-05, Svensk Kärnbränslehantering AB.
- Andersson P, Byegård J, Winberg A, 2002.** Final report of the TRUE Block Scale project. 2. Tracer tests in the block scale. SKB TR-02-14, Svensk Kärnbränslehantering AB.
- Byegård J, Tullborg E-L, 2005.** Sorption experiments and leaching studies using fault gouge material and rim zone material from the Äspö Hard Rock Laboratory. SKB Technical Report, Svensk Kärnbränslehantering AB (in prep).
- Carlsten S, Hultgren P, Keisu M, Strähle A, Wahlgren C-H, 2006.** Oskarshamn site investigation. Geological single-hole interpretation of KLX11A. SKB P-07-69, Svensk Kärnbränslehantering AB (in prep).
- Enachescu C, Rohs S, Wolf P, 2006.** Oskarshamn site investigation. Hydraulic injection tests in borehole KLX11A. Subarea Laxemar. SKB P-06-201, Svensk Kärnbränslehantering AB.
- Gustafsson E, 2002.** Bestämning av grundvattenflödet med utspädningsteknik – Modifiering av utrustning och kompletterande mätningar. SKB R-02-31 (in Swedish), Svensk Kärnbränslehantering AB.
- Gustafsson E, Andersson P, 1991.** Groundwater flow conditions in a low-angle fracture zone in Finnsjön, Sweden. *Journal of Hydrology*, Vol 126, pp 79–111. Elsevier, Amsterdam.
- Gustafsson E, Morosini M, 2002.** In-situ groundwater flow measurements as a tool for hardrock site characterisation within the SKB programme. *Norges geologiske undersøkelse. Bulletin* 439, 33–44.
- Gustafsson E, Nordqvist R, 2005.** Oskarshamn site investigation. Groundwater flow measurements and SWIW-tests in boreholes KLX02 and KSH02. SKB P-05-28, Svensk Kärnbränslehantering AB.
- Gustafsson E, Nordqvist R, Thur P, 2005.** Forsmark site investigation. Groundwater flow measurements and SWIW tests in boreholes KFM01A, KFM02A, KFM03A and KFM03B. SKB P-05-77, Svensk Kärnbränslehantering AB.
- Gustafsson E, Nordqvist R, Thur P, 2006a.** Oskarshamn site investigation. Groundwater flow measurements and SWIW-tests in borehole KLX03. SKB P-05-246, Svensk Kärnbränslehantering AB.
- Gustafsson E, Nordqvist R, Thur P, 2006b.** Forsmark site investigation. Groundwater flow measurements and SWIW tests in borehole KFM08A. SKB P-06-90, Svensk Kärnbränslehantering AB.
- Halevy E, Moser H, Zellhofer O, Zuber A, 1967.** Borehole dilution techniques – a critical review. In: *Isotopes in Hydrology, Proceedings of a Symposium, Vienna 1967*, IAEA, Vienna, pp 530–564.
- Nordqvist R, Gustafsson E, 2002.** Single-well injection-withdrawal tests (SWIW). Literature review and scoping calculations for heterogeneous crystalline bedrock conditions. SKB R-02-34, Svensk Kärnbränslehantering AB.
- Nordqvist R, Gustafsson E, 2004.** Single-well injection-withdrawal tests (SWIW). Investigation of evaluation aspects under heterogeneous crystalline bedrock conditions. SKB R-04-57, Svensk Kärnbränslehantering AB.

**Rhén I, Oskarshamn T, Gustafson G, 1991.** Transformation of dilution rates in borehole sections to groundwater flow in the bedrock. Technical note 30. In: Liedholm M. (ed) 1991. SKB-Äspö Hard Rock Laboratory, Conceptual Modeling of Äspö, technical Notes 13–32. General Geological, Hydrogeological and Hydrochemical information. Äspö Hard Rock Laboratory Progress Report PR 25-90-16b, Svensk Kärnbränslehantering AB.

**SKB, 2001a.** Program för platsundersökning vid Oskarshamn. SKB R-01-42 (in Swedish), Svensk Kärnbränslehantering AB.

**SKB, 2001b.** Site investigations – Investigation methods and general execution programme. SKB TR-01-29, Svensk Kärnbränslehantering AB.

**Thur P, Nordqvist R, Gustafsson E, 2006.** Oskarshamn site investigation. Groundwater flow measurements and SWIW test in boreholes KLX18A. SKB P-06-287, Svensk Kärnbränslehantering AB (in prep).

**Thur P, Nordqvist R, Gustafsson E, 2007.** Forsmark site investigation. Groundwater flow measurements and SWIW test in boreholes KFM01D. SKB P-07-52, Svensk Kärnbränslehantering AB (in prep).

**Voss C I, 1984.** SUTRA – Saturated-Unsaturated Transport. A finite element simulation model for saturated-unsaturated fluid-density-dependent groundwater flow with energy transport or chemically-reactive single-species solute transport. U.S. Geological Survey Water-Resources Investigations Report 84-4369.

**Väisäsvaara J, Kristiansson S, Sokolnicki M, 2007.** Oskarshamn site investigation. Difference flow logging of borehole KLX11A. Sub-area Laxemar. SKB P-07-24, Svensk Kärnbränslehantering AB (in prep).

## Borehole data KLX11A

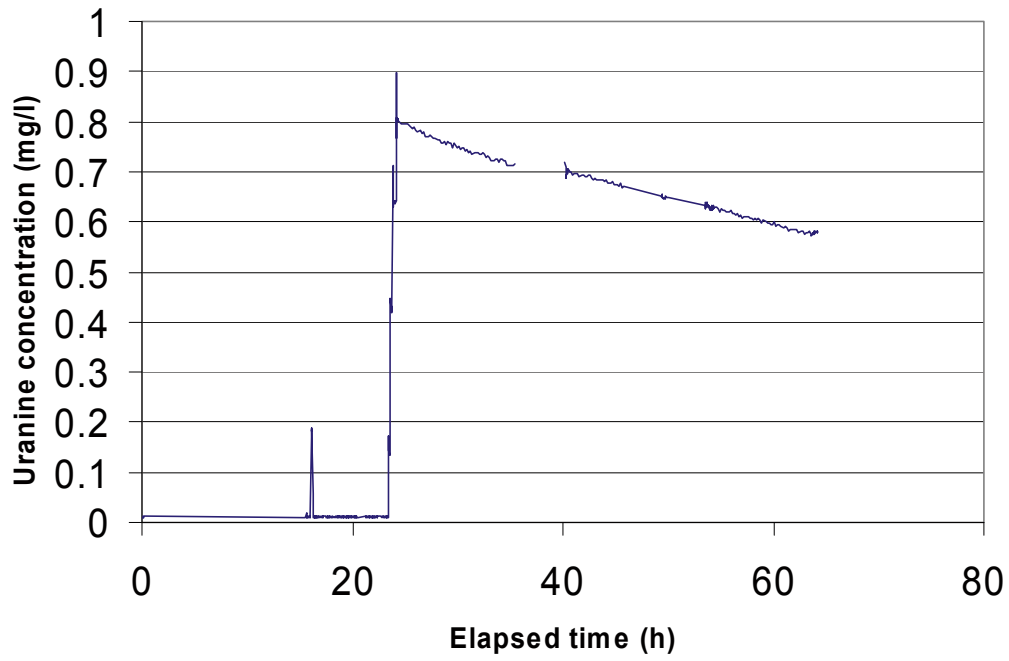
### SICADA - Information about KLX11A

<b>Title</b>	<b>Value</b>				
	Information about cored borehole KLX11A (2007-03-02).				
<b>Comment:</b>	No comment exists.				
<b>BOREHOLE LENGTH:</b>					
Signed/Approved By	Length(m)	Reference Level			
Lars-Eric Samuelsson	992.29	Top of casing (center)			
<b>DRILLING PERIODS:</b>					
Signed/Approved By	From Date	To Date	Secup(m)	Seclow(m)	Drilling Type
Lars-Eric Samuelsson	2005-11-01	2005-11-08	0.43	100.06	Percussion
Lars-Eric Samuelsson	2005-11-24	2006-03-02	100.06	992.29	Core drilling
<b>STARTING POINT COORDINATE:</b>					
Signed/Approved By	Length(m)	Northing(m)	Easting(m)	Elevation	Coord System
Gerry Johansson	0.00	6366339.72	1546608.49	27.14	RT90-RHB70
Gerry Johansson	3.00	6366339.72	1546609.19	24.23	RT90-RHB70
<b>STARTING POINT ANGLES:</b>					
Signed/Approved By	Length(m)	Bearing	Inclination (- = down)	Coord System	
Gerry Johansson	0.00	89.84	-76.43	RT90-RHB70	
<b>BOREHOLE DIAMETERS:</b>					
Signed/Approved By	Secup(m)	Seclow(m)	Hole Diam(m)		
Lars-Eric Samuelsson	0.43	9.60	0.343		
Lars-Eric Samuelsson	9.60	12.05	0.248		
Lars-Eric Samuelsson	12.05	99.96	0.195		
Lars-Eric Samuelsson	99.96	100.06	0.160		
Lars-Eric Samuelsson	100.06	101.53	0.086		
Lars-Eric Samuelsson	101.53	992.29	0.076		
<b>CORE DIAMETERS:</b>					
Signed/Approved By	Secup(m)	Seclow(m)	Core Diam(m)		
Lars-Eric Samuelsson	100.06	100.53	0.072		
Lars-Eric Samuelsson	100.53	992.29	0.050		
<b>CASING DIAMETERS:</b>					
Signed/Approved By	Secup(m)	Seclow(m)	Case In(m)	Case Out(m)	Comment
Lars-Eric Samuelsson	0.00	12.05	0.200	0.208	
Lars-Eric Samuelsson	0.43	9.60	0.310	0.323	
<b>CONE DIMENSIONS:</b>					
Signed/Approved By	Secup(m)	Seclow(m)	Cone In(m)	Cone Out(m)	
Lars-Eric Samuelsson	96.08	100.85			
<b>GROVE MILLING:</b>					
Signed/Approved By	Length(m)	Trace Detectable			
Lars-Eric Samuelsson	110.00	Yes			
Lars-Eric Samuelsson	150.00	Yes			
Lars-Eric Samuelsson	200.00	Yes			
Lars-Eric Samuelsson	250.00	Yes			
Lars-Eric Samuelsson	300.00	Yes			
Lars-Eric Samuelsson	350.00	Yes			
Lars-Eric Samuelsson	400.00	Yes			
Lars-Eric Samuelsson	450.00	Yes			
Lars-Eric Samuelsson	500.00	Yes			
Lars-Eric Samuelsson	550.00	Yes			
Lars-Eric Samuelsson	600.00	Yes			
Lars-Eric Samuelsson	650.00	Yes			
Lars-Eric Samuelsson	700.00	Yes			
Lars-Eric Samuelsson	750.00	Yes			
Lars-Eric Samuelsson	800.00	Yes			
Lars-Eric Samuelsson	850.00	Yes			
Lars-Eric Samuelsson	900.00	Yes			
Lars-Eric Samuelsson	944.00	Yes			
Lars-Eric Samuelsson	974.00	Yes			
<b>INSTALLED SECTIONS:</b>					
Signed/Approved By	Section No	Start Date	Secup(m)	Seclow(m)	
<b>SECTION INFORMATION:</b>					
Signed/Approved By	Status				

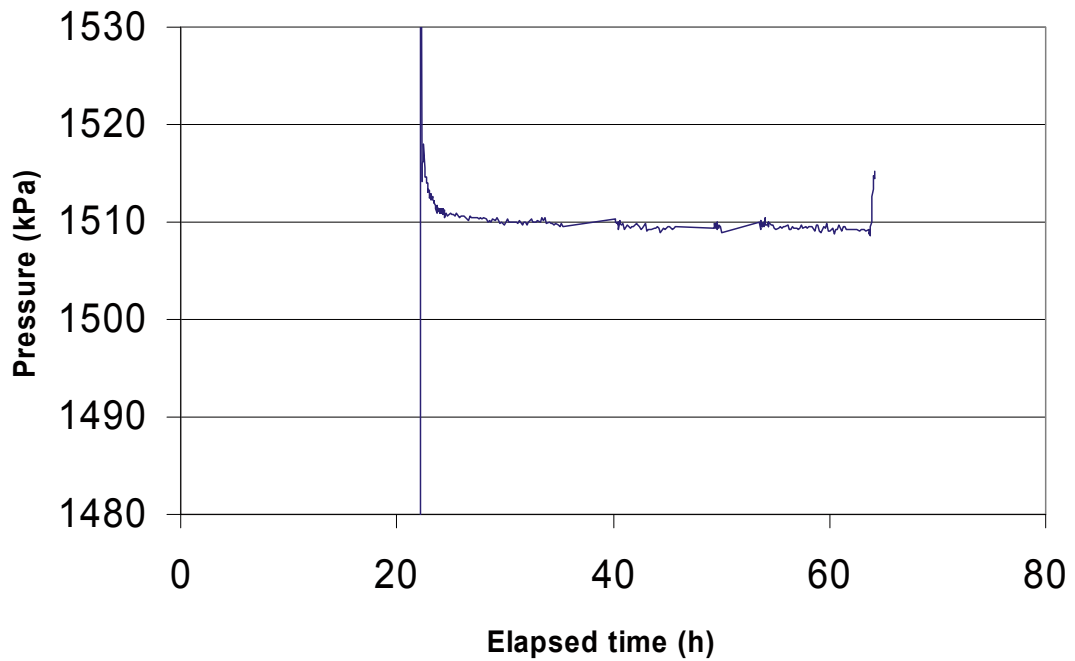


Dilution measurement KLX11A 167.8–170.8 m

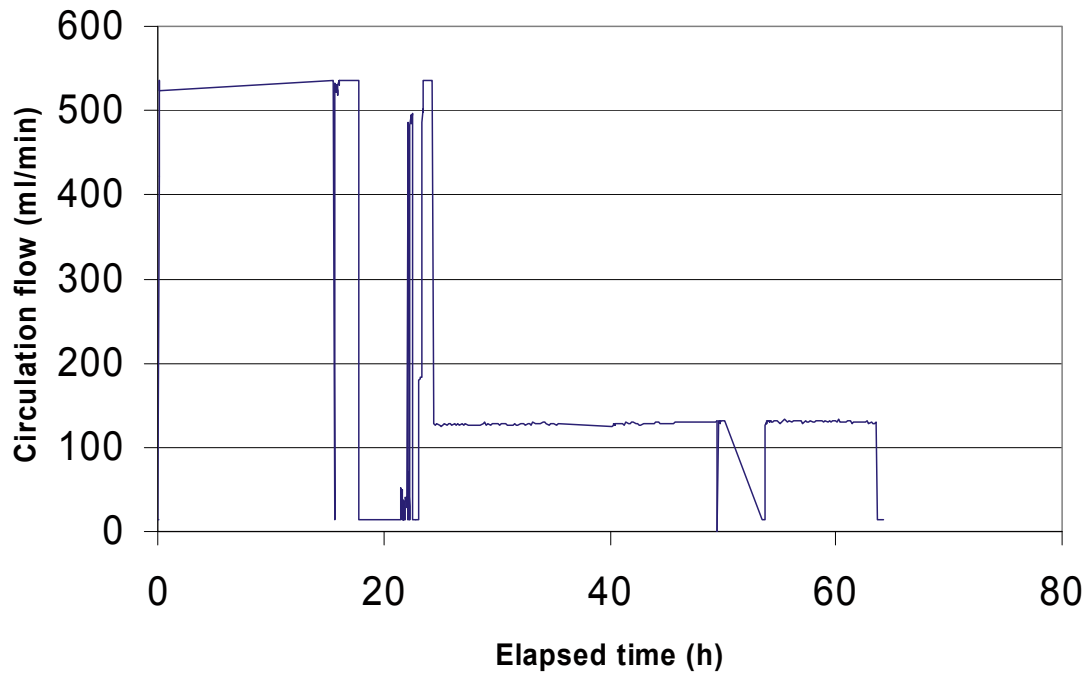
KLX11A 167.8-170.8 m



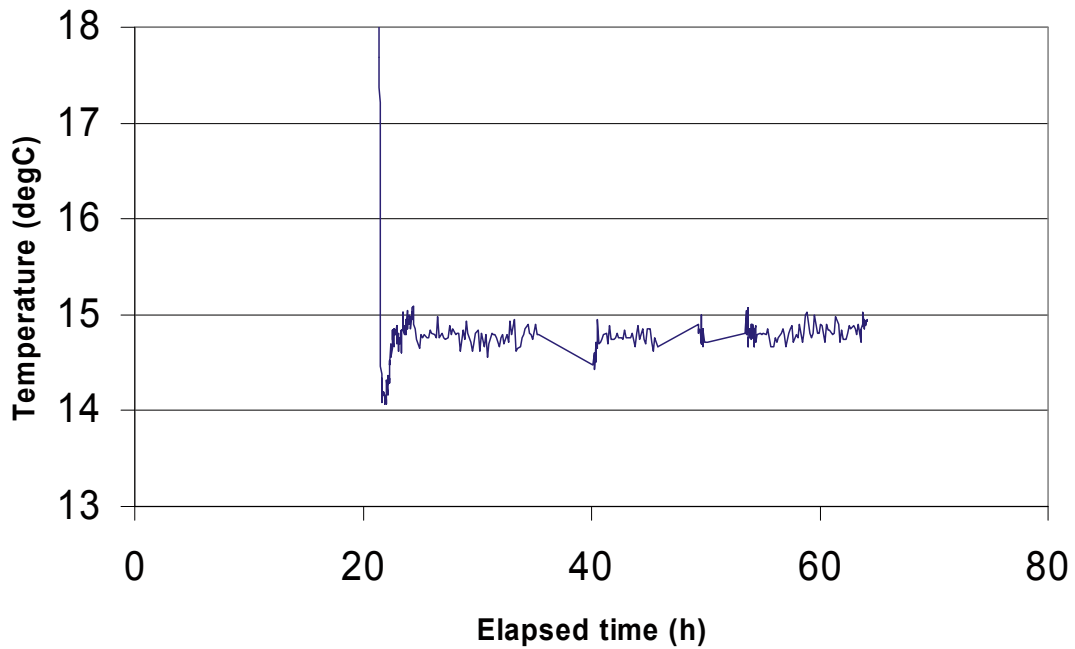
KLX11A 167.8-170.8 m



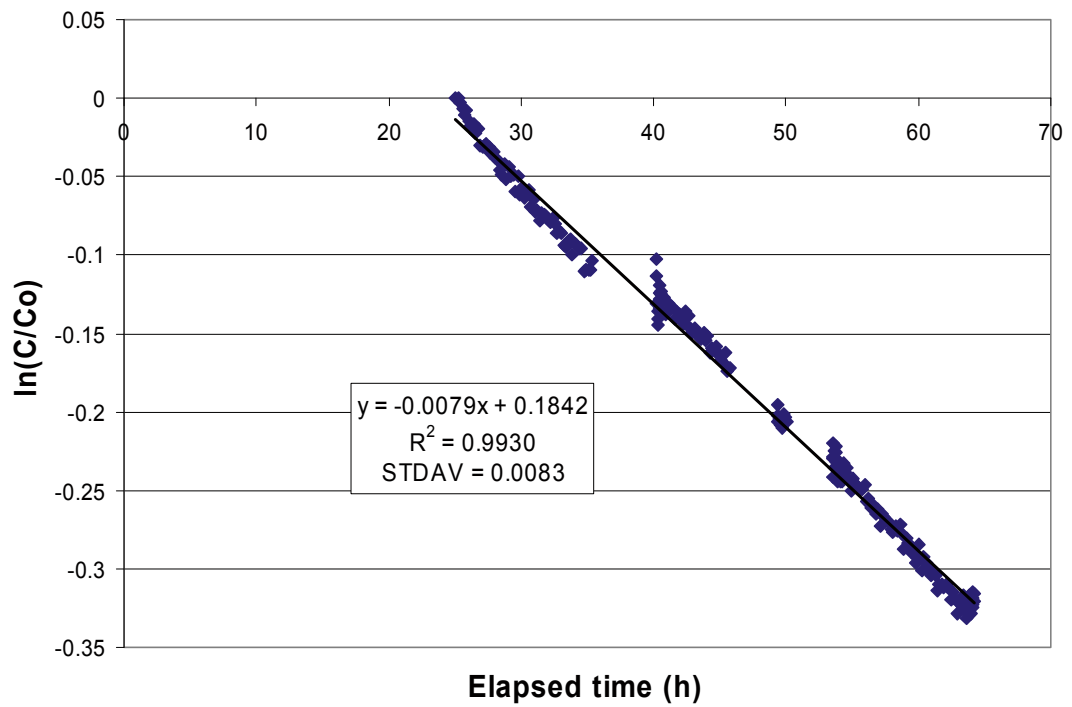
KLX11A 167.8-170.8 m



KLX11A 167.8-170.8 m



### KLX11A 167.8-170.8 m

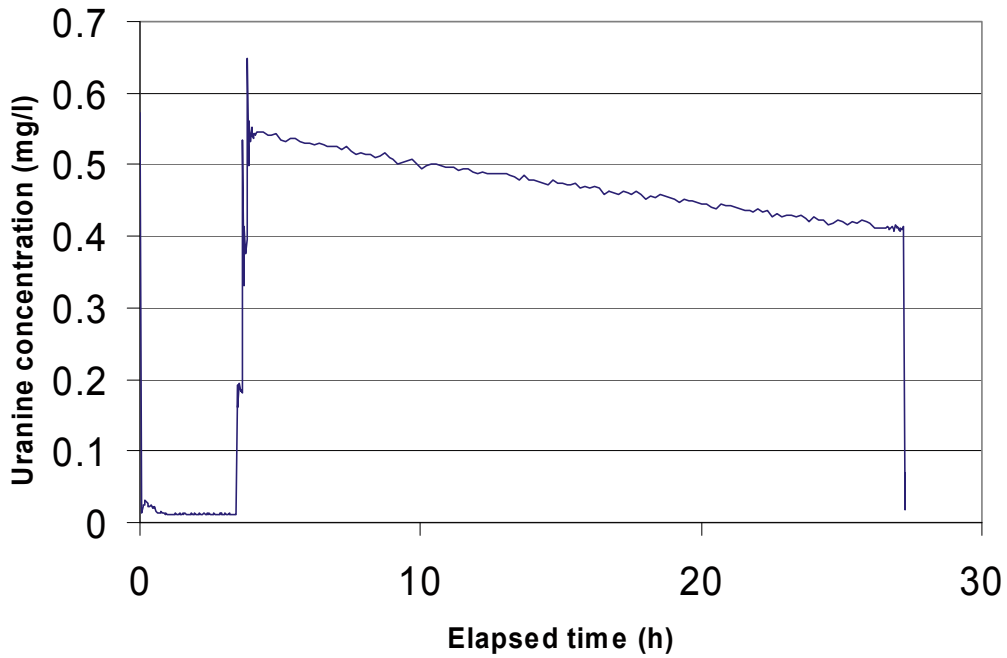


Part of dilution curve (h)	V (ml)	ln(C/Co)/t	Q (ml/h)	Q (ml/min)	Q (m3/s)	R2-value
25-64	1909	-0.0079	15.08	0.251	4.19E-09	0.9930

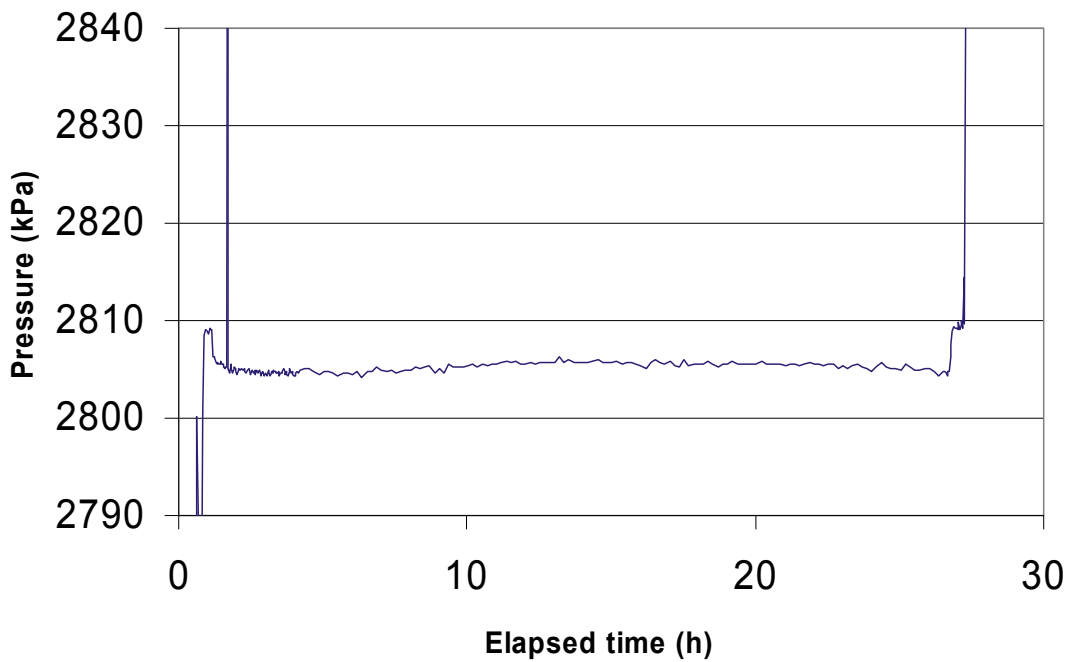
Part of dilution curve (h)	K (m/s)	Q (m3/s)	A (m2)	v(m/s)	I
25-64	5.93E-06	4.19E-09	0.456	9.19E-09	0.002

Dilution measurement KLX11A 306.0–309.0 m

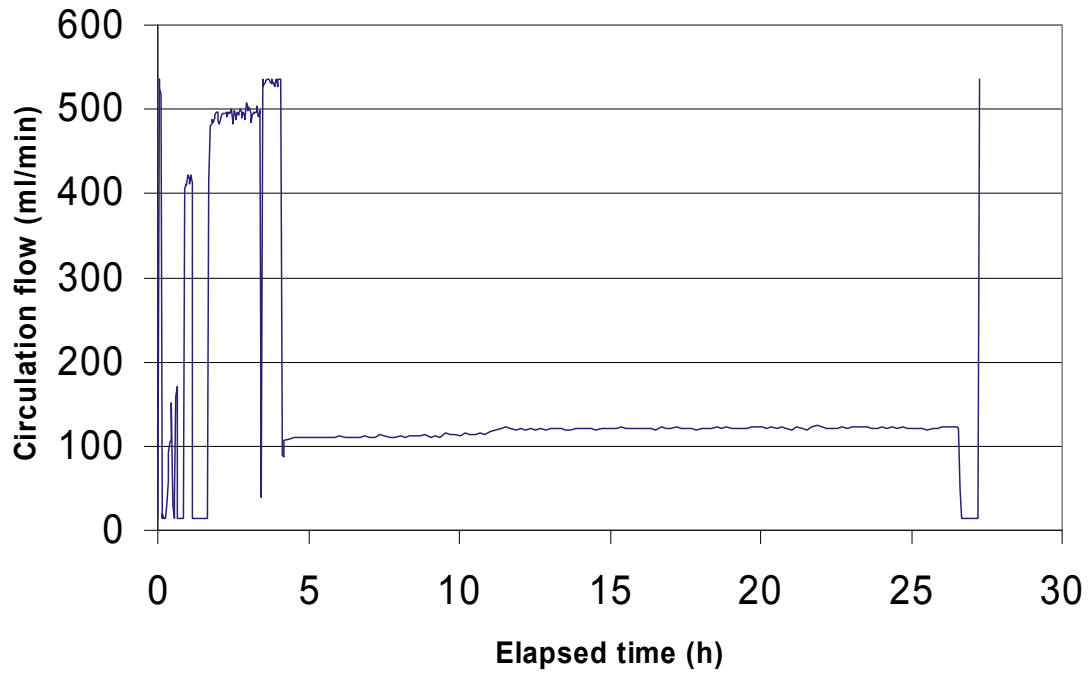
KLX11A 306.0-309.0 m



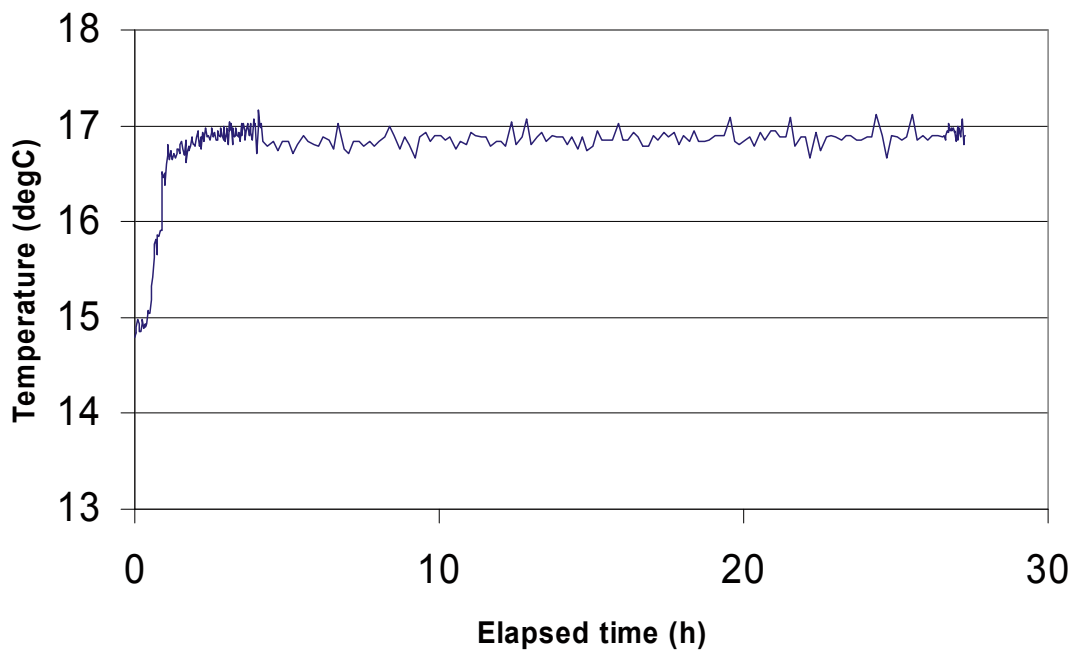
KLX11A 306.0-309.0 m



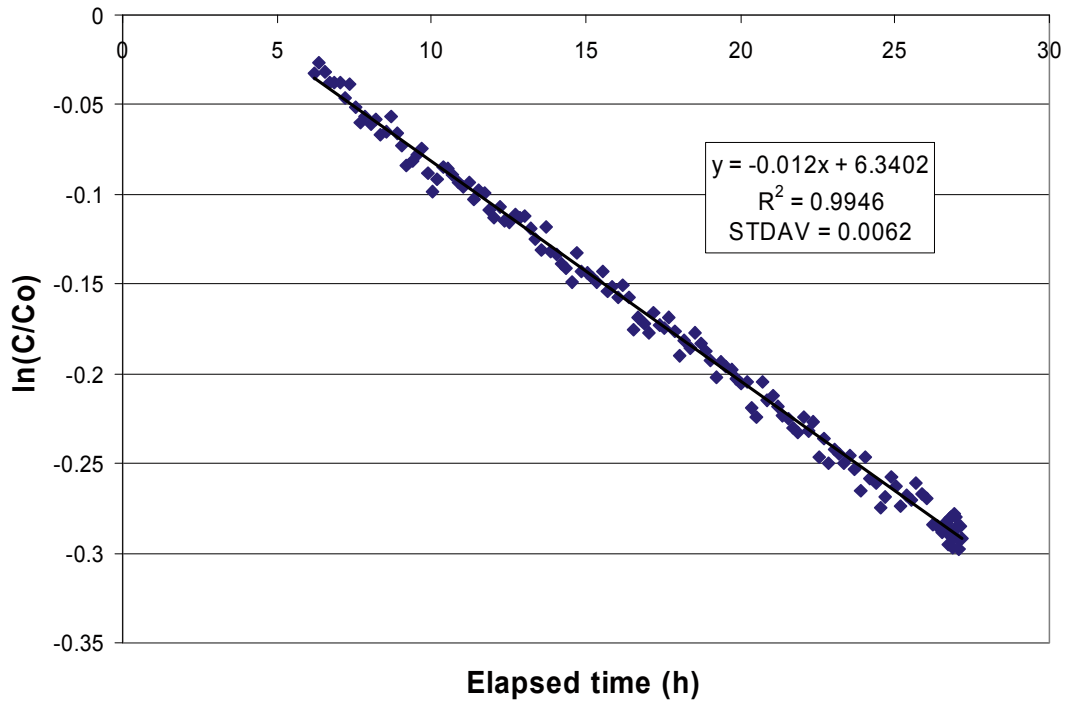
KLX11A 306.0-309.0 m



KLX11A 306.0-309.0 m



### KLX11A 306.0-309.0 m

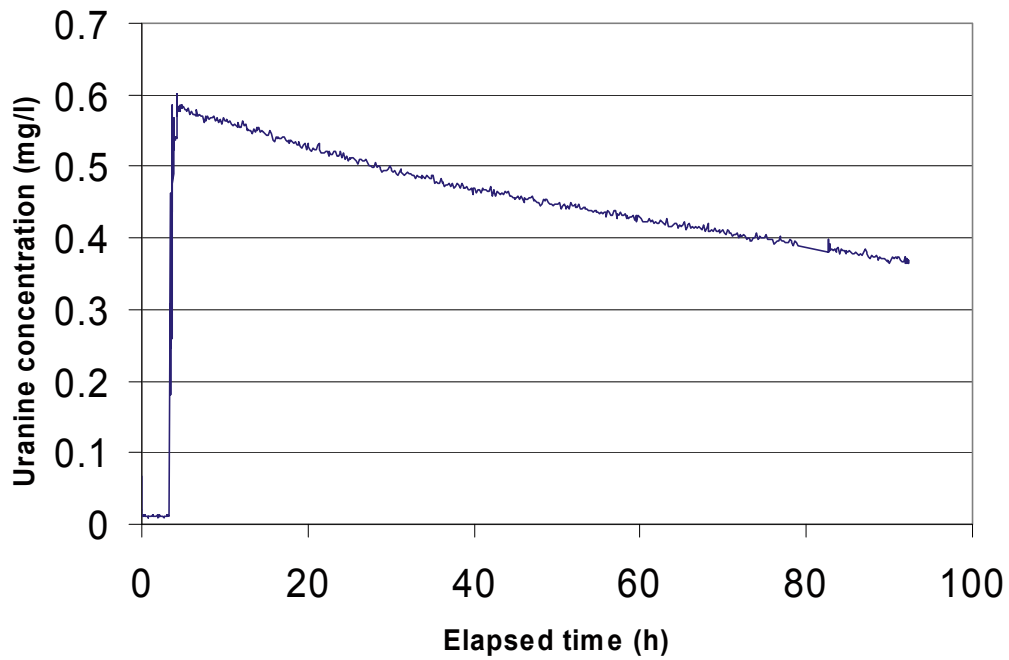


Part of dilution curve (h)	V (ml)	ln(C/Co)/t	Q (ml/h)	Q (ml/min)	Q (m3/s)	R2-value
6 ~ 27	1909	-0.012	22.91	0.382	6.36E-09	0.9946

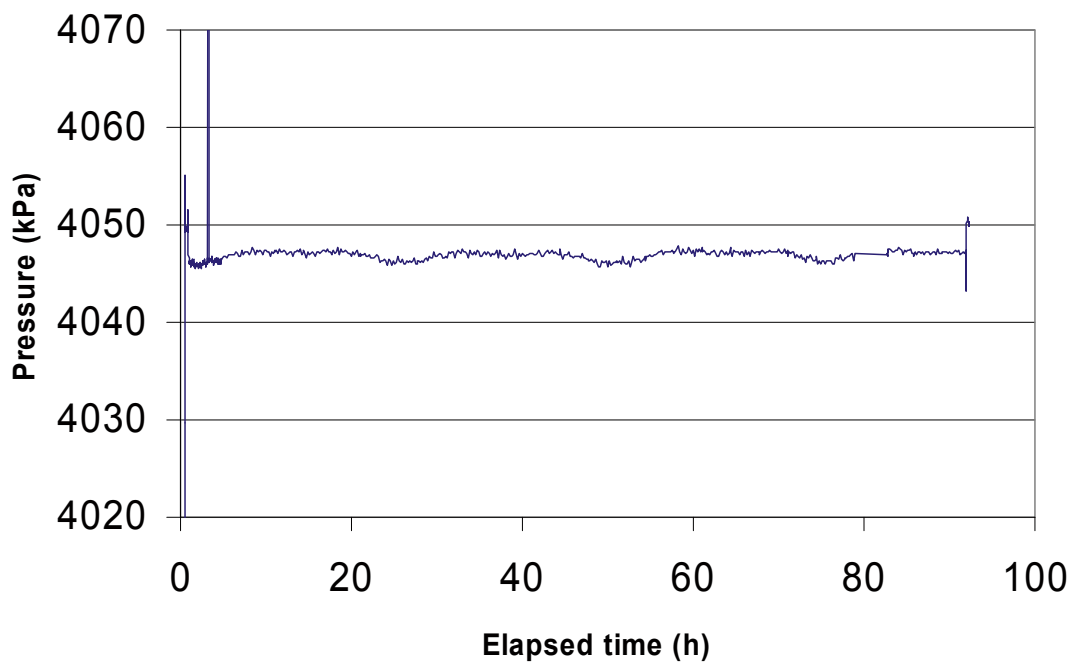
Part of dilution curve (h)	K (m/s)	Q (m3/s)	A (m2)	v(m/s)	I
6 ~ 27	3.47E-06	6.36E-09	0.456	1.40E-08	0.004

Dilution measurement KLX11A 439.0–442.0 m

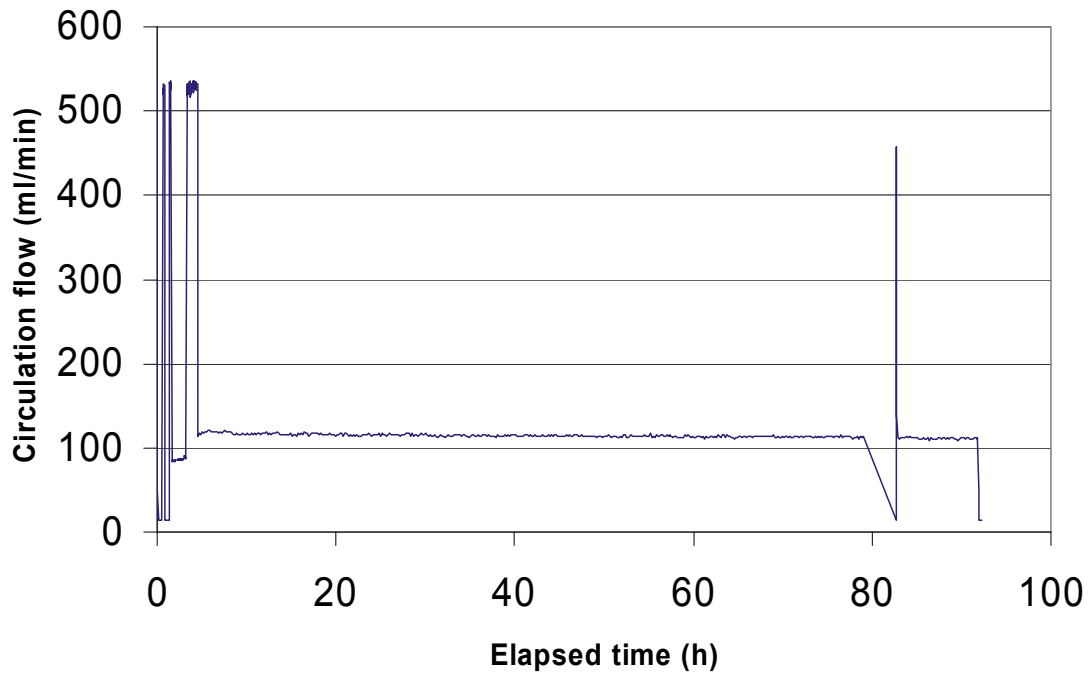
KLX11A 439.0-442.0 m



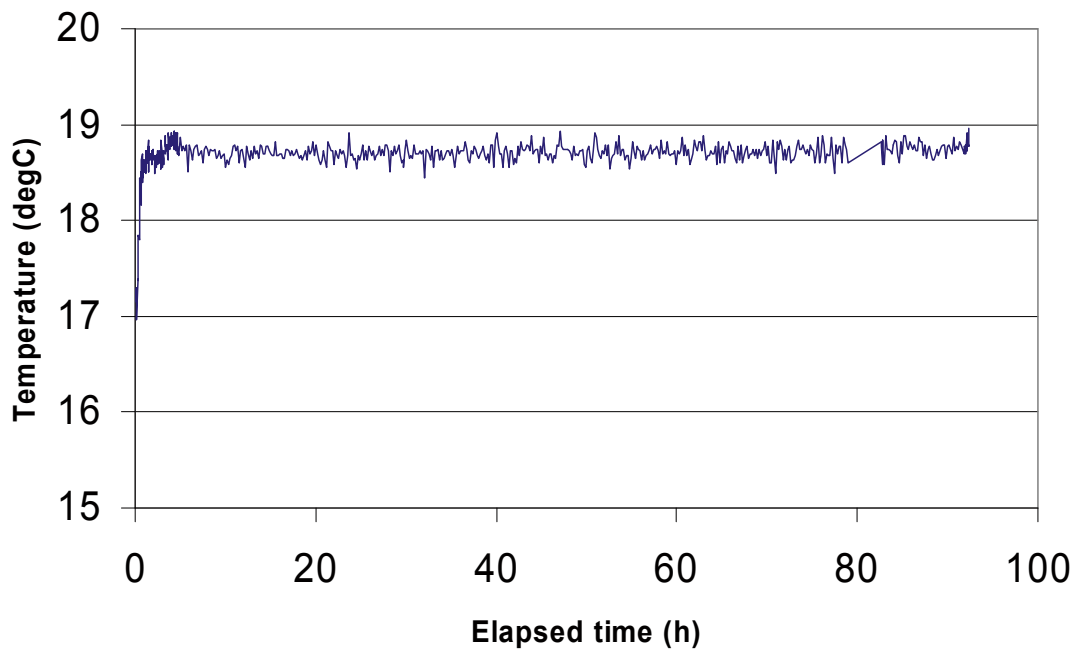
KLX11A 439.0-442.0 m



KLX11A 439.0-442.0 m

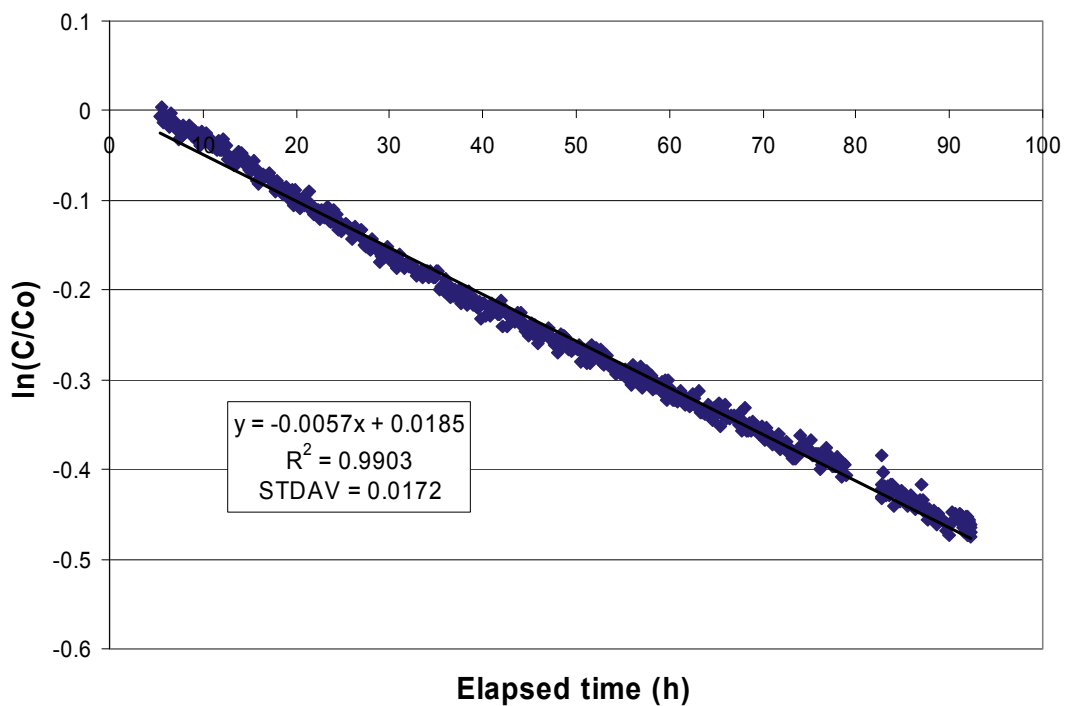


KLX11A 439.0-442.0 m





### KLX11A 439.0-442.0 m

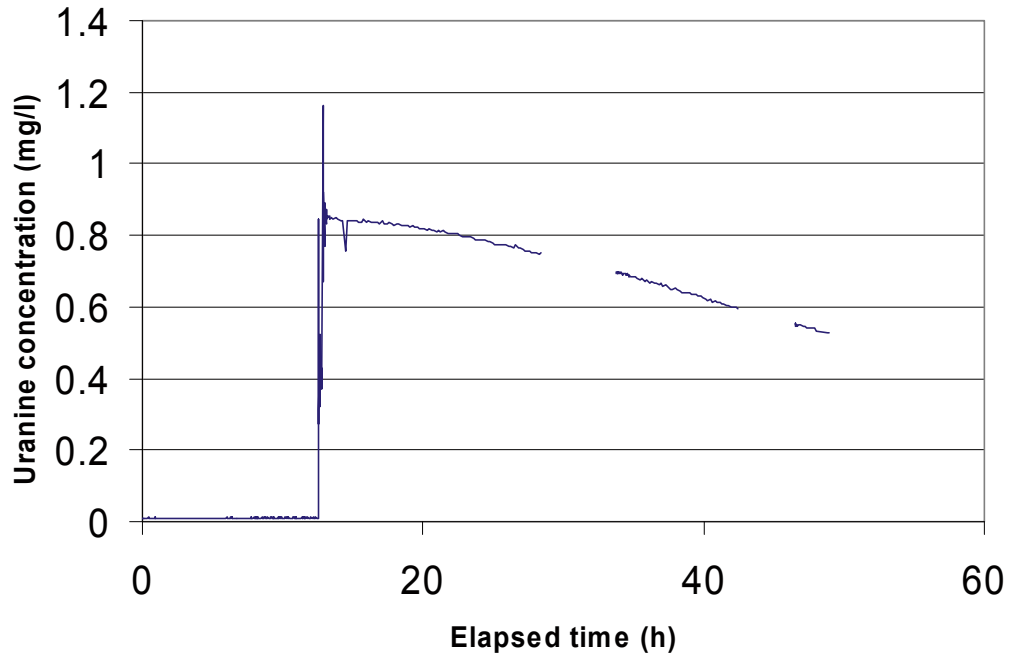


Part of dilution curve (h)	V (ml)	$\ln(C/Co)/t$	Q (ml/h)	Q (ml/min)	Q (m3/s)	R2-value
5-92	1909	-0.0057	10.88	0.181	3.02E-09	0.9903

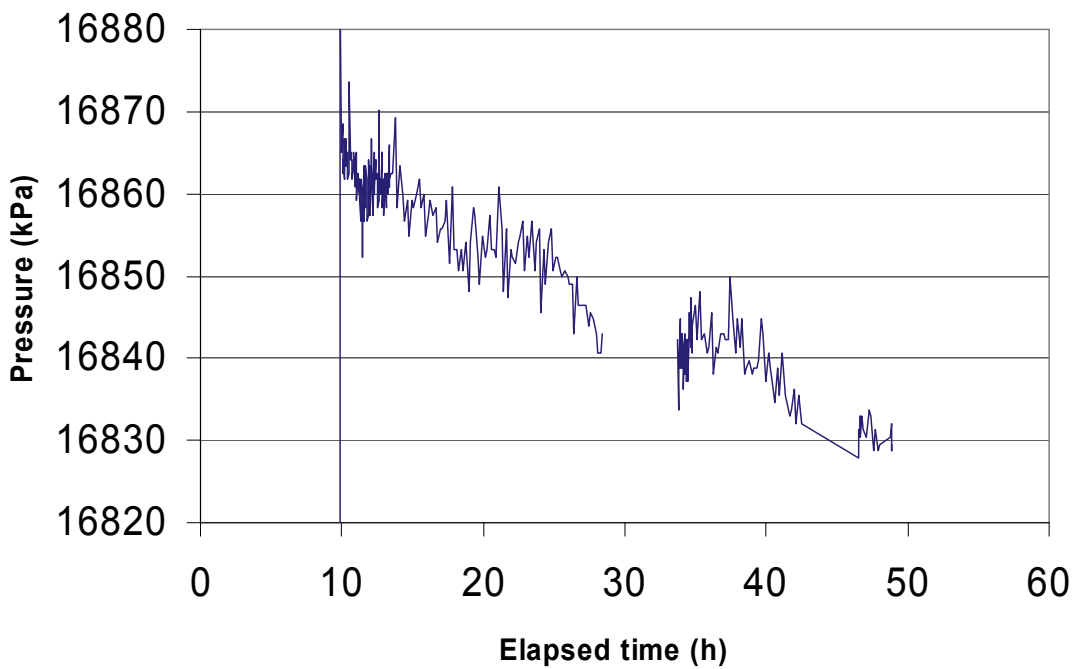
Part of dilution curve (h)	K (m/s)	Q (m3/s)	A (m2)	v(m/s)	I
5-92	2.07E-08	3.02E-09	0.456	6.63E-09	0.320

Dilution measurement KLX11A 516.5–519.5 m

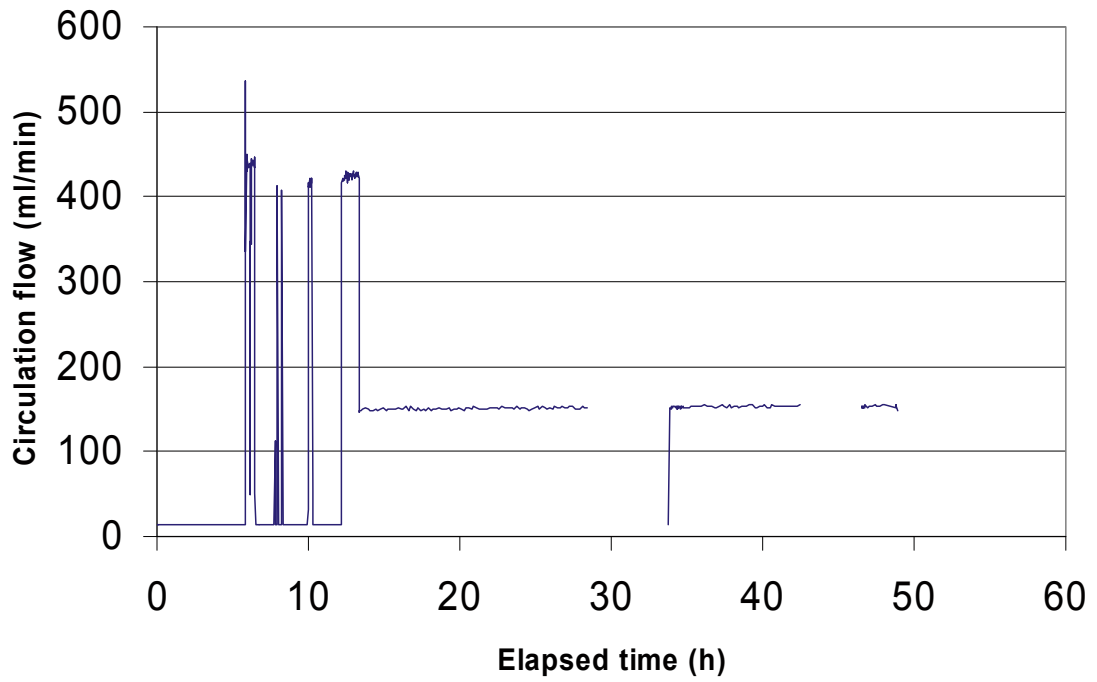
KLX11A 516.5-519.5 m



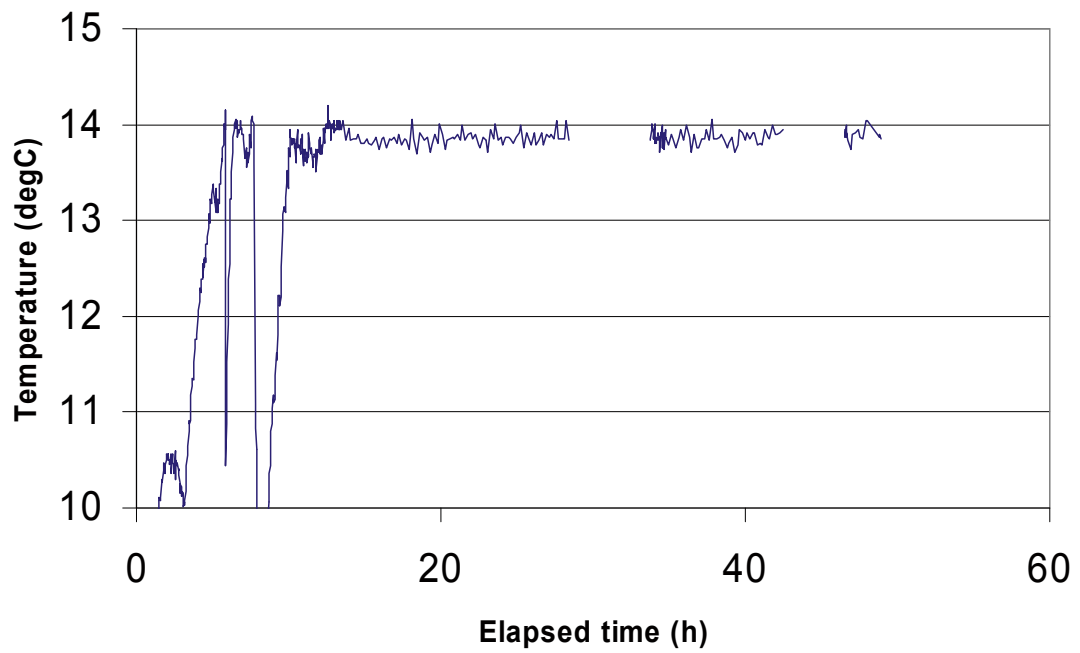
KLX11A 516.5-519.5 m



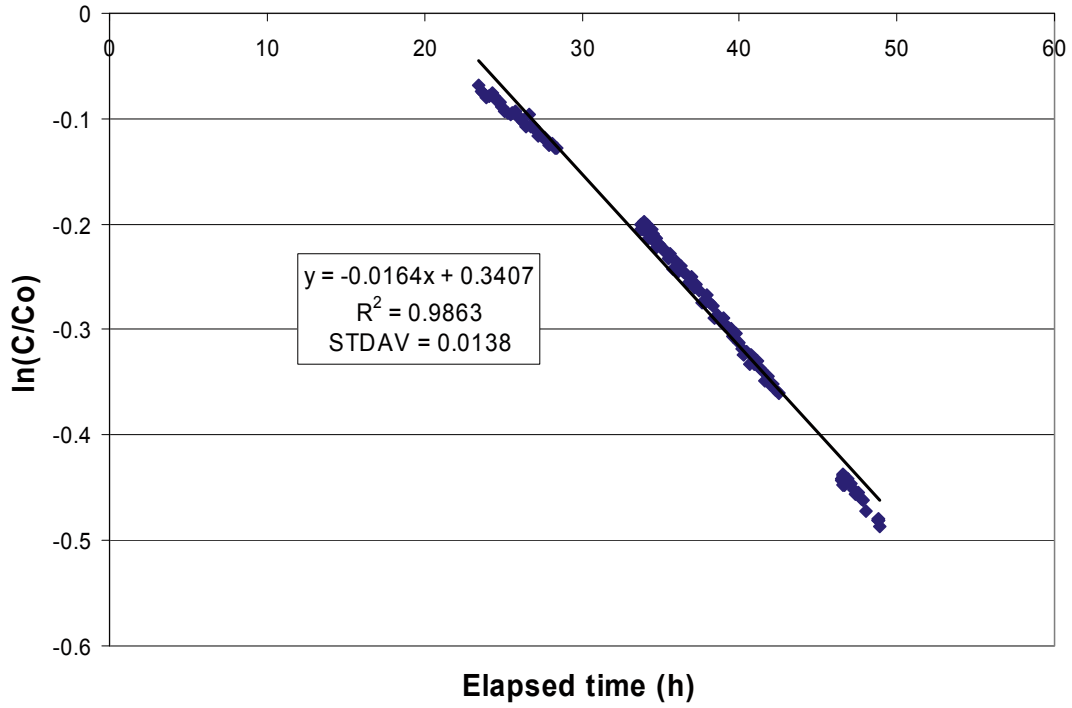
### KLX11A 516.5-519.5 m



### KLX11A 516.5-519.5 m



### KLX11A 516.5-519.5 m

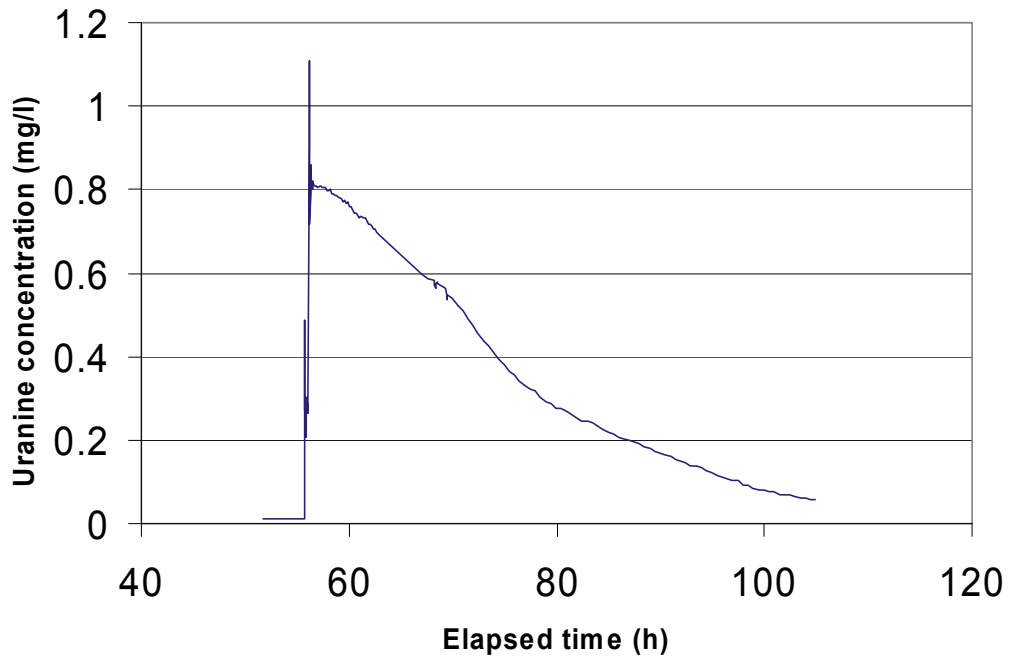


Part of dilution curve (h)	V (ml)	ln(C/Co)/t	Q (ml/h)	Q (ml/min)	Q (m3/s)	R2-value
23-48	1909	-0.0164	31.31	0.522	8.70E-09	0.9863

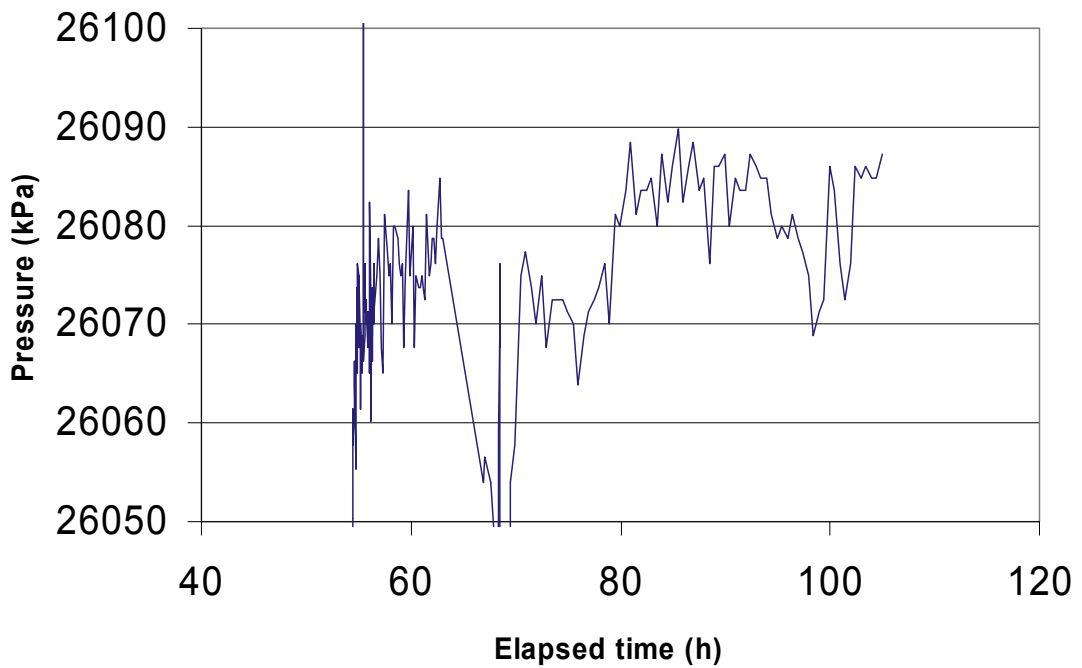
Part of dilution curve (h)	K (m/s)	Q (m3/s)	A (m2)	v(m/s)	I
23-48	1.13E-06	8.70E-09	0.456	1.91E-08	0.017

Dilution measurement KLX11A 579.0–584.0 m

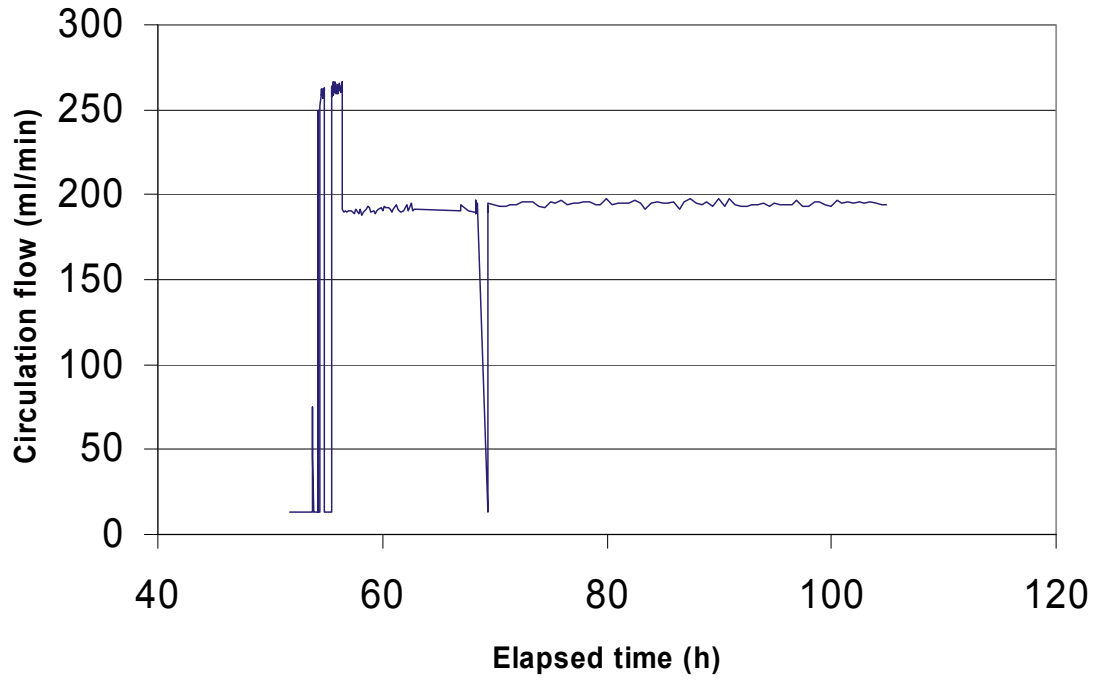
KLX11A 579.0-584.0 m



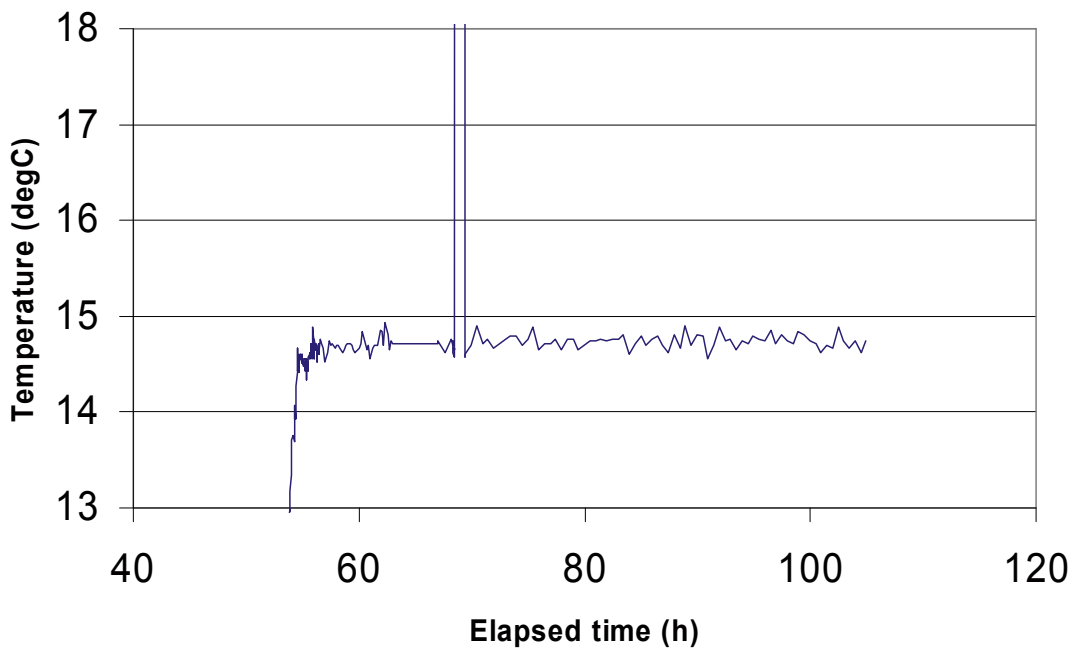
KLX11A 579.0-584.0 m



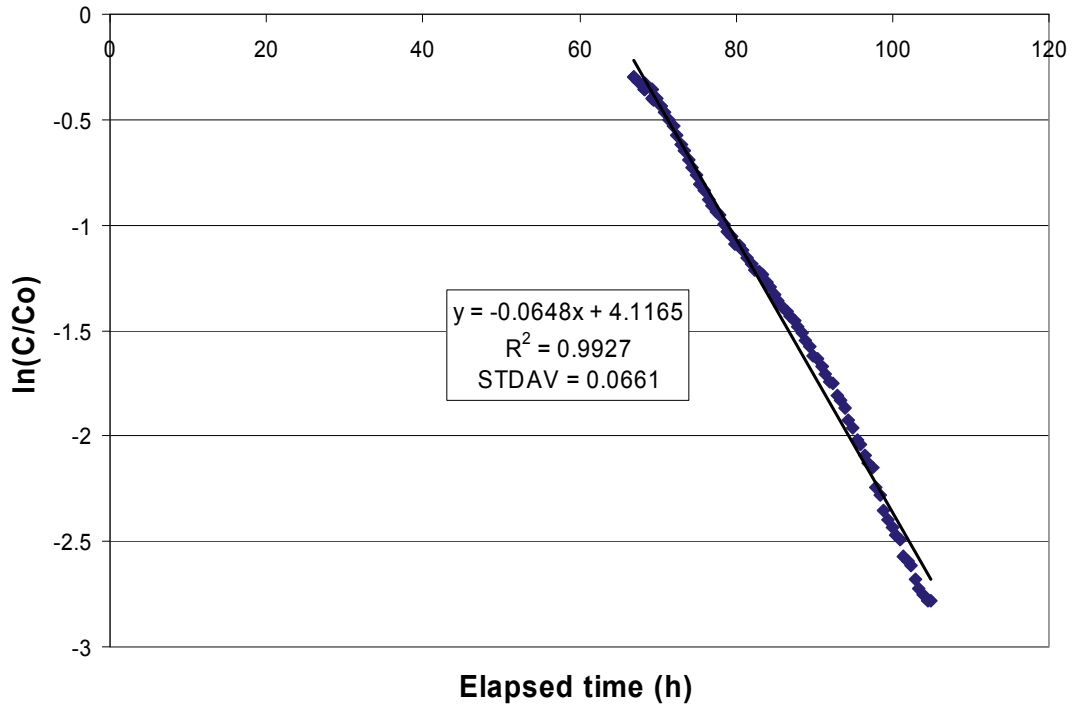
KLX11A 579.0-584.0 m



KLX11A 579.0-584.0 m



### KLX11A 579.0-584.0 m

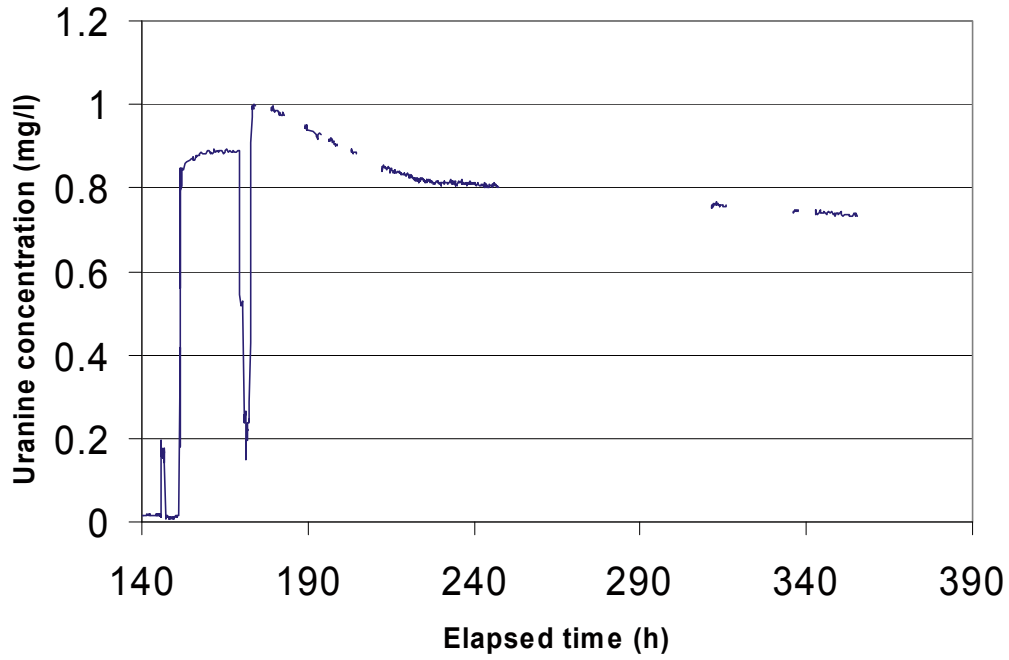


Part of dilution curve (h)	V (ml)	ln(C/Co)/t	Q (ml/h)	Q (ml/min)	Q (m3/s)	R2-value
67-105	2668	-0.0648	172.89	2.881	4.80E-08	0.9927

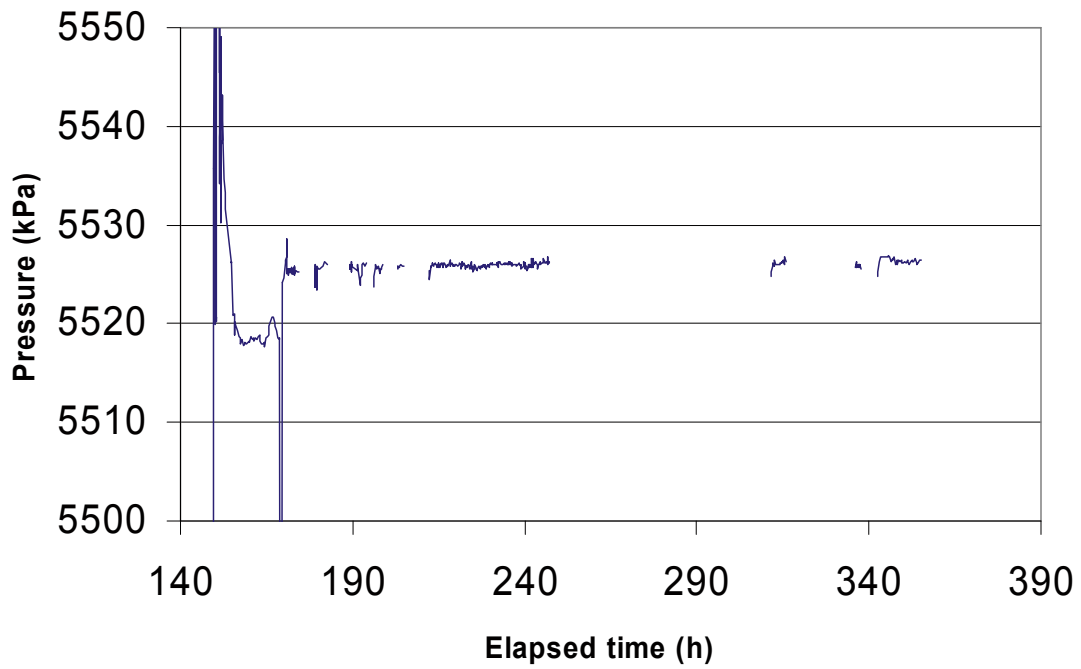
Part of dilution curve (h)	K (m/s)	Q (m3/s)	A (m2)	v(m/s)	I
67-105	1.15E-06	4.80E-08	0.7600	6.32E-08	0.055

Dilution measurement KLX11A 598.0–599.0 m

KLX11A 598.0-599.0 m

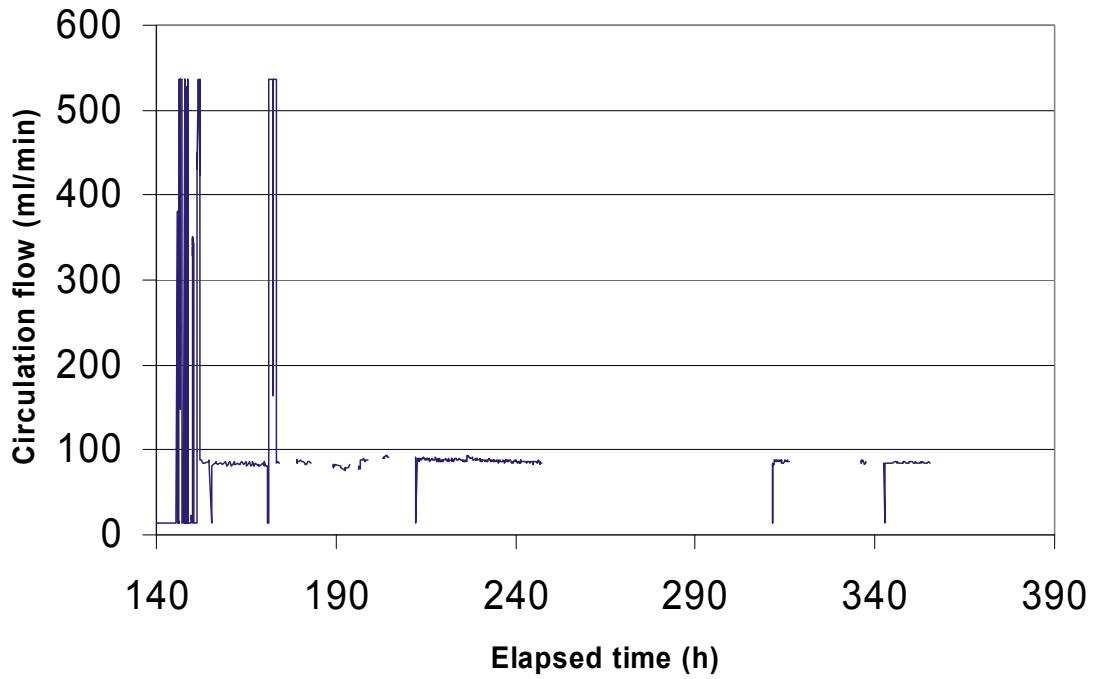


KLX11A 598.0-599.0 m

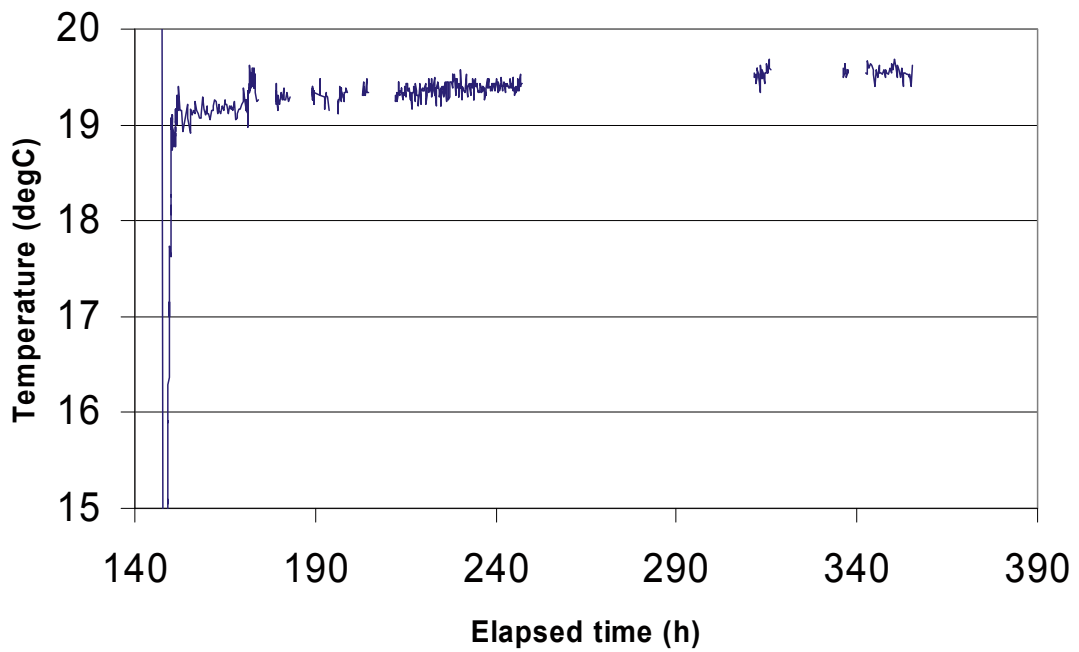




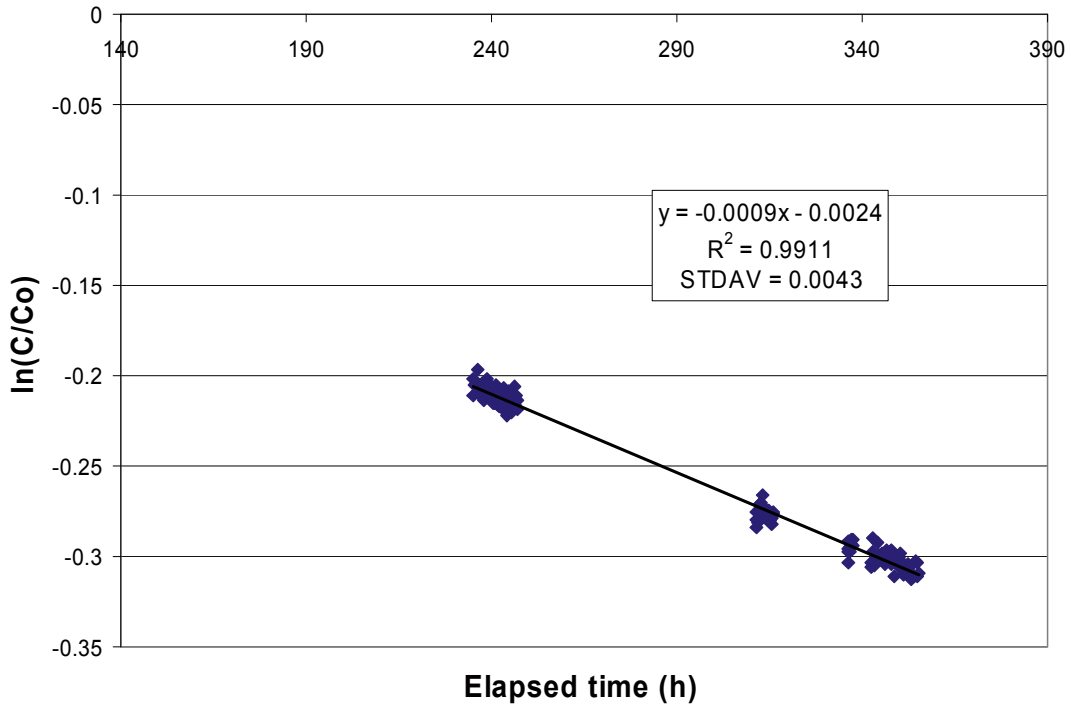
KLX11A 598.0-599.0 m



KLX11A 598.0-599.0 m



### KLX11A 598.0-599.0 m



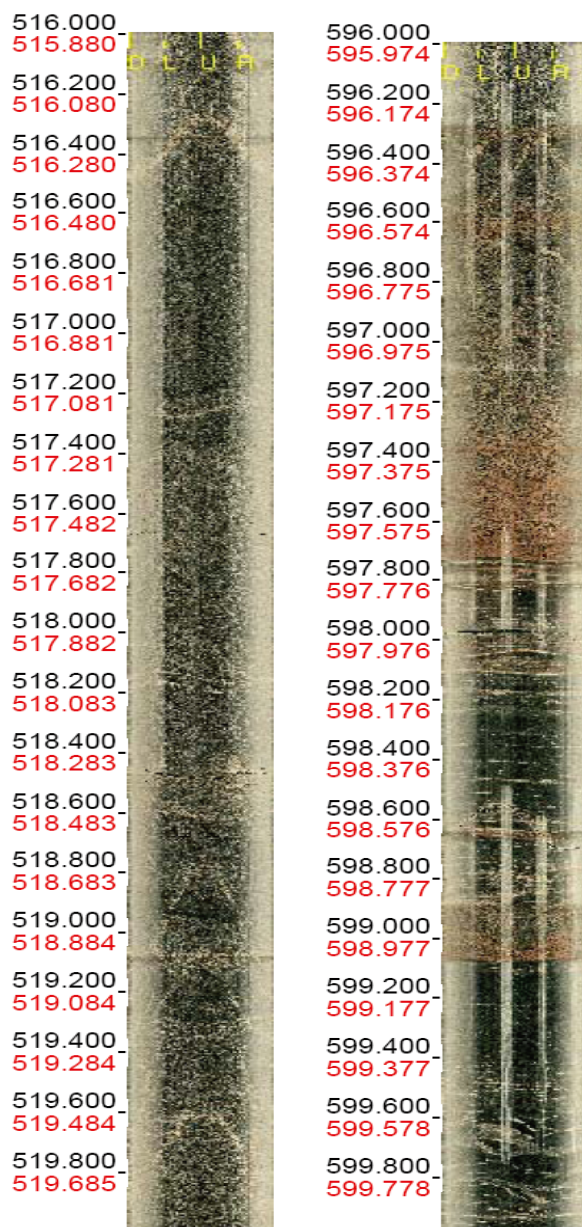
Part of dilution curve (h)	V (ml)	$\ln(C/Co)/t$	Q (ml/h)	Q (ml/min)	Q (m3/s)	R2-value
235-355	1150	-0.0009	1.04	0.017	2.88E-10	0.9911

Part of dilution curve (h)	K (m/s)	Q (m3/s)	A (m2)	v(m/s)	I
235-355	1.35E-07	2.88E-10	0.1520	1.89E-09	0.014

## BIPS logging KLX11A

### BIPS logging in KLX11A

Adjusted depth range: 515.880-519.685 m and 595.974-599.778



Black number = Recorded depth  
 Red number = Adjusted depth  
 Azimuth = 90.6  
 Inclination = -70.4